(12) LEVEL II

DNA 5372T-2

AD A102512

DTIC FILE COPY

WESCOM: A FORTRAN CODE FOR EVALUATION OF NUCLEAR WEAPON EFFECTS ON SATELLITE COMMUNICATIONS

Volume 2: Code Structure

General Electric Company
816 State Street
Santa Barbara, California 93102

31 January 1981

Topical Report for Period 2 January 1980—31 January 1981

CONTRACT No. DNA 001-80-C-0098

APPROVED FOR PUBLIC RELEASE;
DISTRIBUTION UNLIMITED.

THIS WORK SPONSORED BY THE DEFENSE NUCLEAR AGENCY
UNDER RDT&E RMSS CODE B322080464 S99QAXHE04341 H2590D.

Prepared for

Director
DEFENSE NUCLEAR AGENCY
Washington, D. C. 20305

Destroy this report when it is no longer needed. Do not return to sender.

PLEASE NOTIFY THE DEFENSE NUCLEAR AGENCY, ATTN: STTI, WASHINGTON, D.C. 20305, IF YOUR ADDRESS IS INCORRECT, IF YOU WISH TO BE DELETED FROM THE DISTRIBUTION LIST, OR IF THE ADDRESSEE IS NO LONGER EMPLOYED BY YOUR ORGANIZATION.

UNCLASSIFIED

SECURITY CLASSIFICATION OF THIS PAGE (When Data Entered)

REPORT DOCUMENTATION PAGE

READ INSTRUCTIONS BEFORE COMPLETING FORM

1. REPORT NUMBER: DNA 5372T-2	2. GOVT ACCESSION NO.: AD-A102 572
3. RECIPIENT'S CATALOG NUMBER:	
4. TITLE (and Subtitle): WESCOM - A FORTRAN CODE FOR EVALUATION OF NUCLEAR WEAPON EFFECTS ON SATELLITE COMMUNICATIONS, Volume 2, Code Structure	5. TYPE OF REPORT & PERIOD COVERED: Topical Report for Period 2 Jan 80—31 Jan 81
	6. PERFORMING ORG. REPORT NUMBER: GE80TMP-30
7. AUTHOR(s): Warren S. Knapp	8. CONTRACT OR GRANT NUMBER(s): DNA 001-80-C-0098
9. PERFORMING ORGANIZATION NAME AND ADDRESS: General Electric Company, 816 State Street, Santa Barbara, California 93102	10. PROGRAM ELEMENT, PROJECT, TASK AREA & WORK UNIT NUMBERS: Subtask S99QAXHE043-41
11. CONTROLLING OFFICE NAME AND ADDRESS: Director, Defense Nuclear Agency, Washington, D.C. 20305	12. REPORT DATE: 31 January 1981
	13. NUMBER OF PAGES: 200
14. MONITORING AGENCY NAME & ADDRESS (if different from Controlling Office)	15. SECURITY CLASS. (of this report): UNCLASSIFIED
	15a. DECLASSIFICATION/DOWNGRADING SCHEDULE

16. DISTRIBUTION STATEMENT (of this Report)

Approved for public release; distribution unlimited.

17. DISTRIBUTION STATEMENT (of the abstract entered in Block 20, if different from Report)

18. SUPPLEMENTARY NOTES

This work sponsored by the Defense Nuclear Agency under RDT&E RMSS Code B322080464 S99QAXHE04341 H2590D.

19. KEY WORDS (Continue on reverse side if necessary and identify by block number)

Satellite Communications
Nuclear Weapon Effects
Computer Code
Electromagnetic Propagation

20. ABSTRACT (Continue on reverse side if necessary and identify by block number)

The WESCOM (Weapon Effects on Satellite COMmunications) code is a computer program for use in evaluating electromagnetic propagation effects resulting from the detonation of nuclear weapons on satellite communication systems. The code is intended as a replacement for the SATL code documented in DNA 2796T, DNA 2796T-1, and DNA 3598T.

DD FORM 1 JAN 73 1473 EDITION OF NOV 65 IS OBSOLETE

346420

UNCLASSIFIED

SECURITY CLASSIFICATION OF THIS PAGE (When Data Entered)

TABLE OF CONTENTS

TABLE OF CONTENTS (Continued)

LIST OF ILLUSTRATIONS

LIST OF TABLES

SECTION 1
INTRODUCTION

The WESCOM* code is a digital computer program for use in evaluating nuclear weapon effects on satellite communications systems.† The code is intended for use in the evaluation of system performance for a variety of weapon and system parameters. The code is designed for operation on most computers used for system studies. Operational information is given in Volume 1 (User's Manual). In this volume a description of the code structure and selected routines is given for use in conjunction with FORTRAN source listings. Volume 3 provides summary descriptions of the environment, propagation, and signal processing models for users and analysts requiring an understanding of the level of modeling used in the code.

The WESCOM code consists of a main driver (control) routine and a number of subroutines and functions. The FORTRAN names and a brief description of the purpose of each routine are given in Table 1. Section 2 of this volume describes the interconnections between routines and common blocks. Intermediate level descriptions of selected routines are given in Section 3.

---

* WESCOM is an acronym for Weapon Effects on Satellite COMmunications.

† Excluding effects on system materials.

Table 1. Description of WESCOM routines.

Name of Routine	Description
Control	Main driver routine for WESCOM code
ACCUM	Integrates f(x)dx for a specified interval in x assuming either a linear or exponential variation
AM3ABS	Computes the absorption from ambient oxygen (O_2) and water vapor along a specified path
ANLYT2	Computes solution to differential equation used in deionization above 100 km
ANTND	Driver routine for antenna noise module
ARRLIM	Determines debris location and size from debris marker particle location
ATMOSF	Provides properties of the normal or heaved atmosphere above 100 km
ATMOSI	Initializes atmospheric properties for routine ATMOSU
ATMOSU	Determines properties of the undisturbed atmosphere
AZELR	Computes true azimuth, elevation, and slant range of one point relative to another point (points specified by vectors)
BALFIT	Fits a fourth order curve to ballistic equation solution
BB	Calculate maximum FM baseband frequency
BDPSK	Computes probability bit error for a binary differential psk system in a fading environment
BETAS	Computes absorption and backscatter for beta sheath

Table 1 (Continued)

Name of Routine	Description
BFIELD	Computes properties of magnetic dipole field at a point
BFZ	Computes function used in Booker interpolation
BKRIAD	Determines four point interpolation using Booker exponential formulation
BLKDTA	Defines parameters and constants for labled common blocks
BTRACE	Determines location of ionized air parcels along a geomagnetic field line
CARDIN	Reads input cards and writes card image output
CHEMD	Driver routine for D-region chemistry module
CHEMDQ	Driver routine for steady-state D-region chemistry
CHEMEF	Determines chemistry and ionization for E- and F-regions
CHEMHR	Determines chemistry and ionization for heated regions
CHEMQ	Determines steady-state ionization above 100 km
CHMION	Determines species concentrations in E- and F-regions
CHXSPC	Determines energy histogram for charge exchange particles
CLOSE	Determines location of closest point of approach between two vectors
CMDEDT	Edits burst list for bursts to be used in D-region chemistry calculations
CMFEDT	Edits burst list for bursts to be used in E- and F-region chemistry calculations
COMB	Determines number of ways of choosing I quantities from a total of M quantities without regard to order

Table 1 (Continued)

Name of Routine	Description
CONSPC	Determines energy histogram for loss-cone particles
COORDV	Determines vector coordinates from latitude, longitude, and altitude
COORDX	Transforms coordinates of a point in one coordinate system to any of the other three systems; the coordinate systems are: 1. ground range, azimuth, altitude 2. X (east), Y (north), Z (vertical) 3. slant range, azimuth, elevation 4. elevation, azimuth, altitude
CORDTF	Determines coordinate conversions for input geometry and prepares summary output
CPSK	Computes probability of bit error for an M-ary coherent psk system in a noise environment (no fading)
CROSS	Calculates cross product for two vectors
DATE	Computes Gregorian date and zone time after specified time interval
DBMHT	Determines time-dependent debris region quantities for high-altitude bursts
DBMLT	Determines time-dependent debris region quantities for low-altitude bursts
DBSTAM	Driver routine for post-stabilization debris geometry
DEBRIS	Driver routine to determine energy deposition by heavy particles
DECODE	Decodes four digit integer into elements
DEDEP	Determines delayed energy deposition rate
DELPSK	Computes probability of bit error for a coherent psk system for slow fading environment
DIFINT	Evaluates three integrals associated with diffusion ionization profile

Table 1 (Continued)

Name of Routine	Description
DISTF	Calculates exponential term in debris distribution function
DOT	Calculates vector dot product
DPSK	Computes probability of bit error for an M-ary differentially coherent psk system in a noise environment (no fading)
DQPSK	Computes probability of bit error for a differentially coherent 4-ary psk system for slow fading
DRATE	Determines reaction rate coefficients for D-region chemistry solutions
DSTINT	Determines absorption due to dust clouds
DTNEP	Computes D-region positive ion and electron concentrations due to prompt radiation
DTNEQ	Computes steady-state D-region positive ion and electron concentrations due to delayed radiation
DUSTMI	Determines time-independent quantities for dust regions
EANOM	Calculates eccentric anomaly for satellite orbit
EDEPB	Determines energy deposition rate due to beta particles
EDEPG	Determines energy deposition rate due to gamma rays
EDEPND	Determines energy deposition rate due to neutron elastic collisions and capture reactions
EIF	Calculates the exponential integral function for positive arguments
ELDEN	Driver routine for chemistry and ionization calculations

Name of Routine	Description
ENEF	Driver routine for E- and F-region chemistry module
EN2VIB	Computes the concentration of N_2 in the first vibrational state
EQCROS	Locates the air parcel in the fireball at apogee that will stop at the magnetic equator
EQLAIR	Determines equilibrium air species concentrations
EQLMTL	Determines equilibrium aluminum and uranium species concentrations
ERF	Evaluates error function
ERFC	Evaluates complement of the error function
EUVFIT	Determines total UV radiation and fraction radiated in five radiation groups
EXINTP	Provides exponential interpolation
EXPINT	Determines the integral of a quantity when the quantity is defined by a series of exponentials
F2	Evaluates function used in beta particle energy deposition routine
FAC	Computes K factorial
FBEN	Determines ionization and collision frequencies at point within fireball
FBINT	Driver routine for fireball environment and propagation effects module
FBITMD	Computes mass density and mass density scale height at bottom of high-altitude fireballs
FBMHI	Determines time-independent fireball quantities for high-altitude bursts
FBMHT	Determines time-dependent fireball quantities for high-altitude bursts
FBMLI	Determines time-independent fireball quantities for low-altitude bursts

Table 1 (Continued)

Name of Routine	Description
FBMLT	Determines time-dependent fireball quantities for low-altitutde bursts
FBTINT	Determines fireball thermal emission in a given direction
FNNO	Determines solution of differential equation used in high-altitude chemistry model
FOOTPC	Driver routine for fireball footprint plots
FPCIR	Determines circuit performance for single link circuit used for footprint plots
FPINT	Determines parametric values of footprint plot quantities as a function of ground terminal location
FPLNK	Determines link propagation quantities for footprint plots
FPPLOT	Prepares footprint printer page plots
FQAMB	Determines ion-pair production rate below 100 km from electron density and atmospheric parameters
FSKWB	Computer probability of bit error for M-ary wideband FSK system in a noise environment (no fading)
FSKWBQ	Computes the complement of the normal probability distribution
FSKWBY	Computes a summation used in routine FSKWB
FZET	Solves heavy particle range-energy equation
GAIN	Calculates antenna gain
GEOCOR	Computes latitude and longitude of position vector
GNNO	Determines solution to set of equations describing species concentrations for high-altitude chemistry model
GOX	Computes the O_2 incremental absorption
GWAT	Computes the incremental absorption from water vapor

Name of Routine	Description
GWPLME	Determines high-altitude fireball motion caused by gravity and atmospheric winds
HDINT	Computes intergral used in diffusion ionization model
HEAVE	Computes the vertical velocity and time history of the altitude, expansion ratio, and density scale height of a point in a vertically heaving atmosphere
HELP	Prints an error message and can continue or terminate the problem
HERCAN	Computes coefficients used by routine SANCAN
HPCHEM	Partitions energy lost by heavy particles and determines change in neutral and ion species
HTOS	Calculates slant ranges along vector to points that are at specified altitude
IDEFLT	Prepares input default data
INITAL	Determines D-region neutral species concentrations at end of Phase 2 following a burst
INPUT	Reads and checks input data
INPUTP	Performs preliminary processing of input data and prepares summary output
IONLEK	Determines energy in ion leak particles and spatial distribution paramenter
IONOSI	Initializes ionospheric properties for routine IONOSU
IONOSU	Determines properties of the undisturbed ionosphere
JAMND	Determines jammer noise density at specified receiver for a specified jammer location
JULIAN	Computes Gregorian calendar date to a Julian day number
LAGRAN	Computes the initial location and final properties of a Lagrangian cell
LEKSPC	Determines energy histogram for ion leak particles

Table 1 (Continued)

Name of Routine	Description
LINKER	Used on the Honeywell machine for linking (overlay)
LOCATE	Determines array indices and weighting functions for use in link performance models
LOCLAX	Calculates vector transformation matrix
LOSCON	Determines energy in loss cone particles and spatial distribution parameter
MAGDIS	Determines altitude and length along geomagnetic field line of a point on the field line
MAGFIT	Fits a dipole magnetic field to the local magnetic field at specified point
MAGFLD	Determines location of the point on a magnetic field line that is at a specified altitude
MANPTS	Determines mandatory integration points related to beta tubes, low-altitude ionization sources, and heavy particle ionization sources
MATMUL	Performs matrix multiplication between two real matrices
MISCAT	Computes the Mie backscatter and extinction efficiencies given the normalized particle diameter
MODEM1 MODEM2 MODEM3	Determines probability of message error rate for fading environment for three modems
NFSKMF	Computes probability of bit error rate for non-coherent FSK for fading environment
NINT	Determines a normalized integral over the antenna pattern used in computing receiver antenna noise temperature
NORMAL	Calculates the probability that y lies between x and -x for a standard normal distribution
OMEGA	Computes solid angle subtended from any aspect for spheroid, skewed spheroid, torus, cone, and skewed cone

Table 1 (Continued)

Name of Routine	Description
ONEMG5	Calculates magnetic field at specified point
ORBIT	Determines satellite orbit parameters
OZONE	Determines ozone concentrations below 55 km
PCHEM	Determines change in species densities at altitudes above 100 km due to prompt radiation
PCLOUD	Computes the location, shape, and velocity of a dust particle size group
PEDEP	Computes the energy deposited due to prompt radiation
PGROUP	Computes the average backscatter and extinction cross sections for a specified dust particle group
PHEAVE	Determines the heave disturbed atmosphere profile
PHENOM	Driver routine for fireball and debris phenomenology module
PHOTOD	Computes the fraction of O_3 remaining after thermal radiation
PHOTOR	Calculates the negative ion photodetachment and photodissociation rates due to thermal radiation
PIONE	Obtains the initial ion concentrations at a point above 100 km
PLINTP	Obtains the power law interpolation, $y = ax^b$
PLYVAL	Evaluates a polynomial function given the coefficients and argument
PMASS	Computes the mass penetrated between two points assuming that the air density varies exponentially with altitude
PROPEN	Driver routine for calculating propagation effects along a given path

Table 1 (Continued)

Name of Routine	Description
PSDM	Driver routine for post-stabilization debris module for specified debris region
PTHINT	Computes the integral of the electron density, absorption, refraction, scintillation effects, and Faraday rotation along a propagation path
QCOSM	Computes cosmic ion-pair production rate
QFNTN	Computes Marcum's Q function
RADOUT	Computes the radiated power for a burst of a given yield at a specified altitude
RATE	Calculates the reaction rate coefficient for a specified reaction
RICATT	Computes the transient electron density based on an approximate solution to the Ricatti equation
RINTER	Computes intersections between ray path and right circular and skewed spheroids, cones, magnetically defined tubes, and torus
RRMSTP	Calculates ratio of rms to peak frequency deviation of an FM system
SANCAN	Computes two integrals used in analytic signal processing models
SATC	Driver routine for satellite communication calculations
SATCIR	Determines performance quantities for satellite communication circuit
SATLNK	Determines link propagation quantities
SEPA	Calculates the angle between two vectors
SLINK	Determines whether propagation or noise calculations have been made for specified link
SLOBE	Determines maximum side lobe gain
SOIL	Provides the mass density and dielectric constant for a given soil

Table 1 (Continued)

Name of Routine	Description
SOLCYC	Computes the 10.7-cm solar flux
SOLORB	Computes the latitude and longitude of the subsolar point
SOLZEN	Calculates the cosine of the solar zenith angle
SORBIT	Determines satellite location and velocity at specified time
SPCTRM	Defines device data
SPECDP	Computes the neutral species concentrations at the end of Phase 3
SPECDQ	Computes the modification of the neutral species due to delayed radiation
START	Computes a list of mandatory integration points ranked in increasing distance from the transmitter
STRII	Determines scintillation quantities for specified path through fireball
STRIP	Defines fireball striation parameters
SUBVEC	Calculates the difference between two vectors
TATSRT	Computes true anomaly of satellite orbit
TEMPZH	Determines atmospheric temperature below 120 km
TEST	Test input quantities to see if they are within given bounds
TEXK	Computes the excitation temperature for a given energy density equilibrated between the $N_2(VIB)$, $O(^1D)$, the electron kinetic energy and $N(^2D)$
TFUNC	Computes fireball temperature function for high-altitude bursts
TLTFLD	Determines location of the point on a tilted axis that is at a specified altitude

Table 1 (Continued)

Name of Routine	Description
TORBIT	Determines ground terminal location and velocity at specified time
TOROID	Computes the intersection points of a ray path with a toroidal region
TUBE	Computes the intersection point of a ray path with a magnetically contained region
UNITV	Computes a unit vector from a given input vector
USERMD	User routine to compute circuit performance
UVWAV	Determines average wind velocity over a vertical mixing length
UVWD	Determines horizontal wind field above 100 km altitude
VECLIN	Computes the linear combination of two vectors each multiplied by an arbitrary constant
VECM	Computes the product of a vector with a scalar
VOLUME	Computes the volume of a given geometrical region
WATER	Determines water vapor concentration below 45 km altitude
WOBD	Computes the beta energy deposition coefficient, particle release rate, and average energy
WOGD	Computes the delayed gamma-ray energy deposition parameters
WOGP	Provides prompt gamma energy deposition parameters
WOGI	Initializes the gamma-ray energy deposition parameters
WOND	Provides the time-dependent neutron energy deposition parameters

Table 1 (Continued)

Name of Routine	Description
WONP	Provides prompt neutron energy deposition parameters
WON1	Initializes the neutron energy deposition parameters
WOXC	Computes the X-ray energy containment
WOXP	Computes the prompt X-ray energy deposition integral
WOX1	Initializes the neutron energy deposition parameters
XMAG	Computes the absolute magnitude (length) of a vector
ZTTOUT	Converts a local time and Gregorian calendar date to the local time and Gregorian calendar date at Greenwich

SECTION 2
ROUTINE INTERCONNECTIONS AND COMMON BLOCKS

Table 2 lists WESCOM routines and library routines called directly and the common blocks used by each routine. Table 3 lists routines calling a specific routine and Table 4 lists routines using a specific common block.

Table 2. WESCOM routines, library routines, and common blocks used.

ROUTINES	WESCOM ROUTINES CALLED DIRECTLY	LIBRARY ROUTINES CALLED DIRECTLY	COMMON BLOCK USED
CONWES	ATMOSI DATE FOOTPC INPUT IONOSI MAGFIT PHENOM SATC SORBIT ZTTOUT		ALTODN ATMOSN ATMOUP BREG BURST CHEMR CINPUT CIRDES CONST DBREG DCREG DEPDAT DEVICE FBREG HEACOM HEAVET JAMMER MAGLNK MODULT OPTION ORGIN PATH PHEN PROP REGINT SPECW SSYS TIME TSYS WEDEPO WOG WON WOX
ACCUM		ALOG	
AMBABS	ATMOSU GOX GWAT HTOS UNITV VECLIN VECM XMAG	ALOG	ATMOSN CONST
ANLYT2		EXP SQRT	
ANTND	ATMOSU AZELR BETAS FBTINT GEOCOR LOCLAX	ALOG COS SIN SQRT	ANTMP BETAB BREG CINPUT CLINK CONST

Table 2 (Continued)

ROUTINE	WESCOM ROUTINES CALLED DIRECTLY	LIBRARY ROUTINES CALLED DIRECTLY	COMMON BLOCKS USED
ANTND (Continued)	MAGFLD MATMUL NINT PROPEN SUBVEC UNITV VECLIN VECM XMAG		FBREG MAGLNK OPTION PROP SSYS TSYS
ARRLIM	COORDV VOLUME	ALOG COS EXP	CINPUT CONST DBREG RAY
ATMOSF	ATMOSU HEA HELP LAGRAN PEDEP SUBVEC UNITV VECM XMAG	COS EXP SIN SQRT	BREG CONST HEACOM HEAVE1 FBREG
ATMOSI	BKRIAD EXPINT JULIAN OZONE SOLCYC SOLORB SOLZEN TEMPZH WATER	ALOG COS EXP SIN SQRT	ALTODN ATMOUP CONST TIME ZHTEMP
ATMOSU	BKRIAD EXPINT	EXP	ALTODN ATMOSN ATMOUP CONST TIME ZHTEMP
AZELR	LOCLAX MATMUL SEPA SUBVEC XMAG	ATAN2	CONST
BALFIT	MAGDIS	SQRT	CONST LENGTH
BB		ALOG10	
BDPSK	NORMAL	EXP SQRT	CONST DIGMOD

Table 2 (Continued)

ROUTINE	WESCOM ROUTINES CALLED DIRECTLY	LIBRARY ROUTINES CALLED DIRECTLY	COMMON BLOCKS USED
BETAS	CHEMDQ WOBD	ALOG EXP	ANTMP BETAB BREG BURST CINPUT CONST DBREG DEVICE FBREG
BFIELD		ASIN COS SIN SQRT	CONST MAGLNK
BFZ		ALOG EXP	
BKRIAD	BFZ	ALOG EXP	
BLKDTA			ALTODN CHEMR CONST DEPDAT OPTION WEDEPO
BTRACE	BALFIT MAGDIS	SQRT	CONST LENGTH TRACE
CARDIN			OPTION
CHEMD	ATMOSU CMDEDT DEDEP DRATE DTNEP DTNEQ EN2VIB INITAL IONOSU PHOTOR SPECDP SPECDQ VECM	ALOG EXP SQRT	ATMOSN ATMOST BEDIT BREG CHMOVL CINPUT FDSRAT OPTION OUT
CHEMDQ	ATMOSU DRATE DTNEQ IONOSU SPECDQ	ALOG EXP SQRT	ATMOSN ATMOST CINPUT FDSRAT
CHEMEF	CHMION GNNO	ALOG EXP	CHEMAN SPECEF

ROUTINE	WESCOM ROUTINES CALLED DIRECTLY	LIBRARY ROUTINES CALLED DIRECTLY	COMMON BLOCKS USED
CHEMEF (Continued)	RATE TEXK	SQRT	
CHEMHR	ATMOSU EQLAIR EQLMTL PHOTOR RATE	ALOG EXP SQRT	ATMOSN CHEMB FDSRAT OPTION SPEC
CHEMQ	RATE	SQRT	SPECQ
CHMION	ANALYT2 RICATT	EXP SQRT	CHEMAN SPECEF
CHXSPC		ALOG EXP	WEDEPO
CLOSE	DOT VECLIN		
CMDEDT	PEDEP PHOTOD	EXP SQRT	ATMOST BEDIT BREG OPTION OUT WRATE
CMFEDT	ATMOSF PIONF		BREG EDTOVL OPTION SOURCE SPECEF
COMB		ALOG EXP SQRT	CONST
CONSPC		SQRT	WEDEPO
COORDV		COS SIN	CONST
COORDX		ASIN COS SIN SQRT	CONST
CORDTF	AZELR COORDV COORDX GEOCOR LOCLAX MATMUL VECLIN XMAG		CONST
CPSK	ERFC	SQRT	DIGMOD
CROSS			

Table 2 (Continued)

ROUTINE	WESCOM ROUTINES CALLED DIRECTLY	LIBRARY ROUTINES CALLED DIRECTLY	COMMON BLOCKS USED
DATE			ORIGIN
DBMHT	ATMOSU HELP MAGDIS MAGFLD VECM	EXP SQRT	BREG BURST CONST DBREG DEVICE FBREG LENGTH OPTION PHEN
DBMLT	ATMOSU HELP UNITV VECM VOLUME WOBD	EXP SQRT	BURST CONST DEVICE DBREG FBREG PHEN
DBSTAM	DATE GEOCOR MAGFLD PSDM VECM XMAG ZTTOUT		BREG CINPUT CONST DBREG OPTION ORIGIN PHEN TIME
DEBRIS	AZELR CHXSPC CONSPC FZET GEOCOR LEKSPC MAGFLD SEPA VECM	ALOG COS SIN SQRT	BREG CONST DTUBE MAGLNK OPTION WEDEPO
DECODE			
DEDEP	EDEPB EDEPG EDEPND GEOCOR VECM XMAG	COS SIN	BREG BTUBE CINPUT DBREG FBREG MAGLNK OPTION
DELPSK	ERFC	ATAN SQRT	CONST DIGMOD
DIFINT		ALOG EXP	
DISTF		EXP	
DOT			

Table 2 (Continued)

ROUTINE	WESCOM ROUTINES CALLED DIRECTLY	LIBRARY ROUTINES CALLED DIRECTLY	COMMON BLOCKS USED
DPSK	ERFC	EXP SQRT	CONST DIGMOD
DQPSK	ERFC QFNTN	SQRT	DIGMOD
DRATE	RATE	EXP SQRT	WRATE WRATEH
DSTINT	PCLOUD PGROUP RINTER UNITV VECM		CINPUT CONST DCREG FBREG OPTION PROP
DTNEP		ALOG EXP SQRT	ATMOST FDSRAT WRATE
DTNEQ	HELP	ALOG SQRT	ATMOST FDSRAT OUT WRATE
DUSTMI	HELP SOIL	ALOG	BREG BURST DCREG PHEN
EANOM		DCOS DMOD DSIN	
EDEPB	ATMOSU AZELR BFIELD COORDX CROSS EIF E2 GEOCOR LOCLAX MAGFLD MATMUL PMASS RINTER SUBVEC UNITV VECLIN VECM VOLUME WOBD XMAG	ALOG COS EXP SIN SQRT	BREG BURST CONST DBREG FBREG MAGLNK

ROUTINE	WESCOM ROUTINES CALLED DIRECTLY	LIBRARY ROUTINES CALLED DIRECTLY	COMMON BLOCKS USED
EDEPG	ATMOSU AZELR COORDX DISTF HELP MAGFLD PMASS RINTER SUBVEC UNITV WOGD XMAG	ACOS ALOG ASIN COS EXP SIN SQRT	BURST CONST DBREG FBREG
EDEPND	PMASS SUBVEC WOND XMAG	EXP SQRT	BREG BURST DEVICE
EIF		ALOG EXP	
ELDEN	VECM CHEMD ENEF		BREG BURST CINPUT CHMOVL DEVICE OPTION SOURCE
ENEF	ATMOSF ATMOSU CHEMEF CHEMQ DEPEP IONOSU PIONF TEXK UNITV VECM	ALOG EXP SQRT	ATMOSN BREG CHMOVL CINPUT CONST HEACOM OPTION SOURCE SPECEF SPECQ
EN2VIB		EXP	ATMOST
EQCROS	HELP	SQRT	CONST LENGTH
EQLAIR		SQRT	SPEC
EQLMTL		SQRT	SPEC
ERF	ERFC	SQRT	CONST
ERFC	ERF	EXP SQRT	CONST
EUXFIT	WOXC	ALOG	BREG BURST
EXINTP			

Table 2 (Continued)

ROUTINE	WESCOM ROUTINES CALLED DIRECTLY	LIBRARY ROUTINES CALLED DIRECTLY	COMMON BLOCKS USED
EXPINT		ALOG EXP	
E2	EIF	EXP SQRT	
FAC		ALOG EXP SQRT	CONST
FBEN	ATMOSF ATMOSU BFIELD CHEMDQ CHEMHR DEDEP DIFINT GEOCOR HDINT LOCLAX MAGDIS MAGFLD MATMUL RATE SEPA SUBVEC TFUNC UNITV VECLIN VECM XMAG	ALOG COS EXP SIN SQRT	BREG CHEMB CHEMFB CINPUT CONST FBREG LENGTH MAGLNK OPTION
FBINT	ACCUM BFIELD DOT FBEN GEOCOR LOCLAX MAGFLD MATMUL RINTER SEPA STRII SUBVEC UNITV VECLIN VECM XMAG	ALOG COS SIN SQRT	BREG BTUBE BURST CHEMB CHEMFB CINPUT CONST DBREG DEVICE FBREG MAGLNK OPTION PROP REGINT STRIIN
FBITMD		EXP SIN	BREG
FBMHI	ATMOSF ATMOSU ERF	ALOG COS EXP	BREG BURST CONST

Table 2 (Continued)

ROUTINE	WESCOM ROUTINES CALLED DIRECTLY	LIBRARY ROUTINES CALLED DIRECTLY	COMMON BLOCKS USED
FBMHI (Continued)	EUXFIT FBITMD FBMHT IONLEK LAGRAN LOSCON MAGFLD WOXC	SIN SQRT	PHEN
FBMHT	BTRACE COORDX EQCROS FBITMD LOCLAX MAGDIS MATMUL SEPA STRIP VECLIN VECM XMAG	ACOS ALOG COS EXP SIN SQRT	BREG CONST FBREG LENGTH PHEN TRACE
FBMLI	ATMOSF ATMOSU WOXC	ALOG EXP SQRT	BREG BURST CONST PHEN
FBMLT	ATMOSU COORDX LOCLAX MATMUL VECLIN XMAG	EXP SQRT	BREG CONST FBREG PHEN
FBTINT	ACCUM DOT FBEN GEOCOR MAGFLD SUBVEC UNITV VECLIN VECM XMAG	ALOG COS SIN SQRT	ANTMP BREG BURST BTUBE CHEMB DEVICE FBREG MAGLNK OPTION
FNNO		EXP	
FOOTPC	CROSS FBEN FBINT FPINT FPLNK FPPLOT GEOCOR HTOS	ALOG COS SIN	BREG CHEMB CHEMFB CINPUT CONST FBREG FPINTC LENGTH

Table 2 (Continued)

ROUTINE	WESCOM ROUTINES CALLED DIRECTLY	LIBRARY ROUTINES CALLED DIRECTLY	COMMON BLOCKS USED
FOOTPC (Continued)	LOCLAX MAGDIS MAGFLD RINTER SEPA SUBVEC TLTFLD UNITV VECLIN VECM XMAG		MAGLNK OPTION PATH PROP REGINT SSYS TSYS
FPCIR	BDPSK CPSK DELPSK DPSK DQPSK FSKWB MODEM1 MODEM2 MODEM3 NFSKMF USERMD	ALOG10 ATAN2 SIN SQRT	CONST DIGMOD FPCIRC MODULT
FPINT	GEOCOR HELP HTOS SUBVEC UNITV VECLIN	ALOG ALOG10	CONST FPINTC OPTION
FPLNK	AZELR FBTINT FPCIR GAIN LOCLAX MAGFLD MATMUL NINT SLOBE SUBVEC UNITV VECLIN VECM XMAG	ALOG ALOG10 SIN SQRT	ANTMP BREG CINPUT CLINK CONST FBREG FPCIRC MAGLNK OPTION PROP SSYS TSYS
FPPLOT		COS	CONST FPINIC OPTION
FQAMB	ATMOSU DRATE DTNEQ	SQRT	ATMOSN ATMOST FDSRAT OUT

Table 2 (Continued)

ROUTINE	WESCOM ROUTINES CALLED DIRECTLY	LIBRARY ROUTINES CALLED DIRECTLY	COMMON BLOCKS USED
FSKWB	FSKWBY	SQRT	CONST DIGMOD
FSKWBQ		EXP	
FSKWBY	COMB FSKWBQ	ALOG EXP SQRT	DIGMOD
FZET		ALOG SQRT	
GAIN	DOT SEPA	SIN SQRT	
GEOCOR	SEPA	ATAN2	CONST
GNNO	FNNO	ALOG EXP	
GOX		EXP	
GWAT			
GWPLME	BFIELD COORDV DATE GEOCOR MAGFLD SEPA SUBVEC UVWD VECM XMAG ZTTOUT	ACOS ASIN COS SIN SQRT	BREG CONST FBREG ORIGIN PHEN RAY TIME WSTOR
HDINT	MAGDIS	ALOG EXP SQRT	CONST LENGTH
HEAVE	ATMOSU LAGRAN PHEAVE	EXP SQRT	HEAVE1
HELP		EXIT	
HERCAN		EXP	
HPCHEM			SPECEF TSTEF
HTOS	SEPA XMAG	COS SQRT	CONST
IDEFLT	COORDV		BURST CINPUT CIRDES CONST JAMMER MODULT

ROUTINE	WESCOM ROUTINES CALLED DIRECTLY	LIBRARY ROUTINES CALLED DIRECTLY	COMMON BLOCKS USED
IDEFLT (Continued)			OPTION ORIGIN PATH SSYS TSYS
INITAL	DRATE EIF	EXP	ATMOST WRATE
INPUT	BLKDTA CARDIN DECODE IDEFLT INPUTP ORBIT SPCTRM TEST WOG1 WON1 WOX1	ALOG10 EXIT	BURST CINPUT CIRDES CONST DEVICE INPTCM JAMMER MODULT OPTION ORIGIN PATH SPECW SSYS TSYS
INPUTP	BB COORDV CORDIF GEOCOR RRMSTP XMAG		BURST CINPUT CIRDES CONST DEVICE INPTCM JAMMER MODULT OPTION ORIGIN PATH SSYS TSYS
IONLEK			
IONOSI	COORDV FQAMB JULIAN QCOSM SEPA SOLCYC SOLORB ZTTOUT	ALOG COS EXP SQRT	CONST IONOUP MAGLNK TIME
IONOSU	BFZ COORDV FQAMB QCOSM	EXP SQRT	CONST IONOUP MAGLNK TIME

Table 2 (Continued)

ROUTINE	WESCOM ROUTINES CALLED DIRECTLY	LIBRARY ROUTINES CALLED DIRECTLY	COMMON BLOCKS USED
IONOSU (Continued)	RATE SEPA		
JAMND	AZELR GAIN PROPEN SLOBE SUBVEC UNITV VECM XMAG	SQRT	CLINK CONST JAMMER OPTION PROP SSYS TSYS
JULIAN			TIME
LAGRAN		ALOG EXP SQRT	HEAVE1
LEKSPC		SQRT	WEDEPO
LOCATE			
LOCLAX	CROSS UNITV VECM		
LOSCON		ALOG SQRT	
MAGDIS		ALOG EXP SQRT	CONST LENGTH
MAGFIT	COORDV ONEMG5 UNITV VECM	ASIN ATAN COS SIN SQRT	CONST MAGLNK
MAGFLD	DOT UNITV VECLIN XMAG	SQRT	MAGLNK
MANPTS	ATMOSU DOT GEOCOR LOCLAX MAGFLD MATMUL RINTER SUBVEC UNITV VECLIN VECM XMAG	SIN SQRT	BREG BTUBE BURST CINPUT CONST DBREG DEVICE DTUBE MAGLNK OPTION PROP REGINT
MATMUL			

Table 2 (Continued)

ROUTINE	WESCOM ROUTINES CALLED DIRECTLY	LIBRARY ROUTINES CALLED DIRECTLY	COMMON BLOCKS USED
MISCAT		CABS CCOS COS CSIN SIN	
MODEM1	LOCATE	ALOG EXP	
MODEM2	LOCATE	ALOG EXP	
MODEM3	LOCATE	ALOG EXP	
NFSKMF	COMB SANCAN	EXP	CONST DIGMOD
NINT	AZELR DOT GAIN LOCLAX MATMUL OMEGA RINTER SEPA SUBVEC UNITV VECLIN VECM VOLUME XMAG	ACOS ASIN ATAN2 COS SIN	ANTMP CONST FBREG OPTION
NORMAL		EXP	
OMEGA	DOT HELP LOCLAX MATMUL SUBVEC XMAG	COS SIN SQRT	CONST MAGLNK
ONEMG5		SQRT	
ORBIT	EANOM TATSRT	ACOS ASIN ATAN COS SIN SQRT TAN	CONST ORIGIN PATH
OZONE		EXP SIN	CONST TIME
PCHEM	TEXK	EXP SQRT	DEPDAT OPTION

Table 2 (Continued)

ROUTINE	WESCOM ROUTINES CALLED DIRECTLY	LIBRARY ROUTINES CALLED DIRECTLY	COMMON BLOCKS USED
PCHEM (Continued)			SPECEF TSTEF
PCLOUD	LOCLAX MATMUL		BREG CONST DCREG FBREG
PEDEP	DEBRIS PMASS SUBVEC WOGP WONP WOXP XMAG	EXP SQRT	BREG BURST CONST DEVICE DTUBE
PGROUP	MISCAT	ALOG EXP	CONST DCREG
PHEAVE		EXP SQRT	HEAVE1
PHENOM	ATMOSF ATMOSI AZELR BFIELD COORDX DATE DBMHT DBMLT DBSTAM DUSTMI FBMHI FBMHT FBMLI FBMLT GEOCOR GWPLME HELP MAGDIS MAGFLD MAGFIT RADOUT XMAG VECM ZTTOUT	COS SIN	BREG BURST CINPUT CONST DBREG DCREG DEVICE FBREG LENGTH MAGLNK OPTION ORIGIN PHEN TIME
PHOTOD	AZELR	ALOG EXP SIN SQRT	BREG
PHOTOR	SUBVEC XMAG		BREG FBREG FDSRAT

Table 2 (Continued)

ROUTINE	WESCOM ROUTINES CALLED DIRECTLY	LIBRARY ROUTINES CALLED DIRECTLY	COMMON BLOCKS USED
PIONF	ATMOSF ATMOSU AZELR DEBRIS EUXFIT HPCHEM PCHEM PMASS SUBVEC VECLIN VECM WOXP XMAG	ALOG EXP SIN SQRT	BREG BURST CONST DEPDAT DEVICE OPTION SPECEF TSTEF
PLINTP		ALOG	
PLYVAL			
PMASS	ATMOSU	EXP SQRT	CONST
PROPEN	AMBABS AZELR CMFEDT DSTINT FBINT HTOS MANPTS PTHINT START SUBVEC UNITV VECLIN VECM XMAG	COS SIN SQRT	CINPUT CONST EDTOVL MAGLNK OPTION PROP REGINT
PSDM	ARRLIM UVWAV UVWD	COS	CONST SPEEDS RAY WSTOR
PTHINT	ACCUM BFIELD DOT ELDEN GEOCOR MAGFLD SUBVEC UNITV VECLIN XMAG	ALOG SQRT	CINPUT CONST MAGLNK OPTION PROP REGINT
QCOSM		COS EXP SIN	CONST

Table 2 (Continued)

ROUTINE	WESCOM ROUTINES CALLED DIRECTLY	LIBRARY ROUTINES CALLED DIRECTLY	COMMON BLOCKS USED
QFNTN		ALOG10 EXP	
RADOUT	HELP	ALOG EXP	BREG FBREG PHEN
RATE		EXP	CHEMR
RICATT	EIF	ALOG EXP	
RINTER	BFIELD CLOSE DOT GEOCOR LOCLAX MAGFLD MATMUL SUBVEC TOROID TUBE UNITV VECLIN VECM XMAG	COS SIN SQRT	CONST MAGLNK RGEOM
RRMSTP	PLYVAL	ALOG10	
SANCAN	ERF FAC HERCAN	EXP SQRT	CONST
SATC	ANTND ATMOSI DECODE GEOCOR HTOS IONOSI JAMND MAGFIT PROPEN SATCIR SATLNK SLINK SUBVEC TORBIT UNITV VECLIN VECM XMAG		CHEMB CIRDES CLINK JAMMER OPTION PATH PROP SSYS TIME STSYS
SATCIR	BDPSK CPSK DELPSK DPSK	ALOG10 ATAN2 SIN SQRT	CINPUT CONST DIGMOD MODULT

Table 2 (Continued)

ROUTINE	WESCOM ROUTINES CALLED DIRECTLY	LIBRARY ROUTINES CALLED DIRECTLY	COMMON BLOCKS USED
SATCIR (Continued)	DQPSK FSKWB MODEM1 MODEM2 MODEM3 NFSKMF USERMD		OPTION SIGCOM
SATLNK	AZELR GAIN GEOCOR SLOBE SUBVEC UNITV VECM XMAG	ALOG10 SQRT	CINPUT CLINK CONST OPTION PROP SIGCOM SSYS TSYS
SEPA	DOT XMAG	ACOS ASIN	CONST
SLINK	DECODE		CIRDES CLINK SSYS TSYS
SLOBE		SIN	CONST
SOIL	HELP		DCREG
SOLCYC		COS	ORIGIN TIME CONST
SOLORB		COS SIN	CONST TIME
SOLZEN		ACOS COS SIN SQRT	CONST TIME
SORBIT	COORDV EANOM TATSRT	ASIN ATAN2 COS EXIT SIN SQRT	CONST OPTION PATH
SPCTRM			SPECW
SPECDP		ALOG EXP SQRT	ATMOSN ATMOST WRATE WRATEH
SPECDQ		EXP	ATMOST WRATE

Table 2 (Continued)

ROUTINE	WESCOM ROUTINES CALLED DIRECTLY	LIBRARY ROUTINES CALLED DIRECTLY	COMMON BLOCKS USED
START			FBREG PROP REGINT
STRII	ACCUM CROSS DOT HELP SUBVEC UNITV VECLIN	ALOG SQRT	CONST PROP STRIIN
STRIP		SQRT	BREG FBREG
SUBVEC			
TATSRT		ATAN SQRT TAN	CONST
TEMPZH			ALTODN CONST TIME ZHTEMP
TEST			
TEXK		ALOG EXP SQRT	
TFUNC			
TLTFLD	MATMUL VECLIN XMAG		CONST
TORBIT	COORDX LOCLAX MATMUL VECLIN VECM XMAG		CINPUT CONST PATH
TOROID	DOT LOCLAX MATMUL VECLIN VECM	SQRT	RGEOM
TUBE	DOT MAGFLD SUBVEC		RGEOM

Table 2 (Continued)

ROUTINE	WESCOM ROUTINES CALLED DIRECTLY	LIBRARY ROUTINES CALLED DIRECTLY	COMMON BLOCKS USED
TUBE (Continued)	UNITV VECLIN		
UNITV		SQRT	
USERMD			DIGMOD
UVWAV	RAY SPEEDS		
UVWD		COS EXP	CONST RAY WSTOR
VECLIN			
VECM			
VOLUME	HELP	COS SIN SQRT	CONST
WATER		ALOG EXP SIN	CONST TIME
WOBD			DEVICE
WOGD	EXINTP		DEVICE WOG
WOGP	EXINTP		WOG
WOG1			DEVICE SPECW WOG
WOND	EXINTP PLINTP		WON
WONP	EXINTP PLINTP		WON
WON1		ALOG EXP SQRT	DEVICE SPECW WON
WOXC	EXINTP	ALOG EXP	WOX
WOXP	EXINTP		WOX
WOX1		ALOG EXP	DEVICE SPECW WOX
XMAG		SQRT	
ZTTOUT		EXIT	CONST TIME

Table 3. WESCOM routine called by a specific routine.

SUBROUTINE	CALLED BY	SUBROUTINE	CALLED BY	SUBROUTINE	CALLED BY
AMBABS	PROPEN	AZELR	ANTND CORDTF DEBRIS EDEPB EDEPG FPLNF JAMND NINT PHENOM PHOTOD PIONF PROPEN SATLNK	CARDIN	INPUT
ANLYT2	CHMION			CHEMD	ELDEN
ANTND	SATC			CHEMDQ	BETAS FBEN
ARRLIM	PSDM			CHEMEF	ENEF
ATMOSF	CMFEDT ENEF FBEN FBMHI FBMLI PHENOM PIONF	BALFIT	BTRACE	CHEMHR	FBEN
				CHEMQ	ENEF
				CHMION	CHEMEF
		BB	INPUTP	CHXSPC	DEBRIS
ATMOSI	CONWES PHENOM SATC	BDPSK	EPCIR SATCIR	CLOSE	RINTER
ATMOSU	AMBABS ANTND ATMOSF CHEMD CHEMDQ CHEMHR DBMHT DBMLT EDEPB EDEPG ENEF FBEN FBMHI FBMLI FBMLT FQAMB HEAVE MANPTS PIONF PMASS	BETAS	ANTND	CMDEDT	CHEMD
		BFIELD	EDEPB FBEN FBINT GWPLME PHENOM PTHINT RINTER	CMFEDT	PROPEN
				COMB	FSKWBY NFSKMF
				CONSPC	DEBRIS
		BFZ	BKRIAD IONOSU	COORDV	ARRLIM CORDTF GWPLME IDEFLT INPUTP IONOSI IONOSU MAGFIT SOPPIT
		BKRIAD	ATMOSI ATMOSU		
		BLKDTA	INPUT		
		BTRACE	FBMHT		

Table 3 Continued)

SUBROUTINE	CALLED BY	SUBROUTINE	CALLED BY	SUBROUTINE	CALLED BY
COORDX	CORDTF EDEPB EDEPG FBMHT FBMLT PHENOM TOPBIT	DOT	CLOSE FBINT FBTINT GAIN MAGFLD MANPTS NINT OMEGA PTHINT RINTER SEPA STRII TOPOID TUBE	EIF	EDEPB E2 INITAL RICATT
CORDTF	INPUTP			ELDEN	PTHINT
CPSK	FPCIR SATCIR			ENEF	EDEPB
CROSS	EDEPB FOOTPC LOCLAX STRII	DPSK	FPCIR SATCIR	EN2VIB	CHEMD
DATE	CONWES DBSTAM GWPLME PHENOM	DQPSK	FPCIR SATCIR	EQCROS	FBMHT
DBMHT	PHENOM	DRATE	CHEMD CHEMDQ FOAMB INITAL	EQLAIR	CHEMHR
DBMLT	PHENOM	DSTINT	PROPEN	EQLMTL	CHEMHR
DBSTAM	PHENOM	DTNEP	CHEMD	ERF	ERFC FBMHI SANCAN
DEBRIS	PEDEP PIONF	DTNEQ	CHEMD CHEMDQ FOAMB	ERFC	CPSK DELPSK DPSK DQPSK ERF
DECODE	INPUT SATC SLINK	DUSTMI	PHENOM	EUXFIT	FBMHI PIONF
DEDEP	CHEMD FNEF FBEN	EANOM	ORBIT SORBIT	EXINTP	WOGD WOGP WOND WONP WOXC WOXP
DELPSK	FPCIR SATCIR	EDEPB	DEDEP	EXPINT	ATMOSI ATMOSU
DIFINT	FBEN	EDEPG	DEDEP	E2	EDEPB
DISTF	EDEPG	EDEPND	DEDEP	FAC	SANCAN
				FBEN	FBINT FBTINT FOOTPC

Table 3 (continued)

SUBROUTINE	CALLED BY	SUBROUTINE	CALLED BY	SUBROUTINE	CALLED BY
FBINT	FOOTPC PROPEN	GAIN	FPLNK JAMND NINT SATLNK	HERCAN	SANCAN
FBITMD	FBMHI FBMHT	GEOCOR	ANTND CORDTF DBSTAM DEBRIS DEDEP EDEPB FBEN FBINT FBTINT FOOTPC FPINT GWPLME INPUTP MAPPTS PHENOM PTHINT RINTER SATC SATLNK	HPCHEM	PIONF
FBMHI	PHENOM			HTOS	AMBABS FOOTPC FPINT PROPEN SATC
FBMHT	FBMHI PHENOM			IDEFLT	INPUT
FBMLI	PHENOM			INITAL	CHEMD
FBMLT	PHENOM			INPUT	CONVES
FBTINT	ANTND FPLNK			INPUTP	INPUT
FNNO	GNNO			IONLEK	FBMHI
FOOTPC	CONWES			IONOSI	CONWES SATC
FPCIR	FPLNK	GNNO	CHEMEF	IONOSU	CHEMD CHEMDQ ENEF
FPINT	FOOTPC	GOX	AMBABS		
FPLNK	FOOTPC	GWAT	AMBABS	JAMND	SATC
FPPLOT	FOOTPC	GWPLME	PHENOM	JULIAN	ATMOSI IONOSI
FQAMB	IONOSI IONOSU	HDINT	FBEN	LAGRAN	ATMOSF FBMHI HEAVE
FSKWB	FPCIR SATCIR	HEAVE	ATMOSF	LEKSPC	DEBRIS
FSKWBQ	FSKWBY	HELP	ATMOSF DBMHT DBMLT DTNEQ DUSTMI FDEPG FQCROS FPINT OMEGA PHENOM RADOUT SOIL STRII VOLUME	LOCATE	MODEM1 MODEM2 MODEM3
FSKWBY	FSKWB				
FZET	DEBRIS				

Table 3 (Continued)

SUBROUTINE	CALLED BY	SUBROUTINE	CALLED BY	SUBROUTINE	CALLED BY
LOCLAX	ANTND AZELR CORDTF EDEPB FBEN FBINT FBMHT FBMLT FOOTPC FPLNK MANPTS NINT OMEGA PCLOUD RINTER TORBIT TOROID	MANPTS	PROPEN	PCLOUD	DSTINT
		MATMUL	ANTND AZELR CORDTF EDEPB FBEN FBINT FBMHT FBMLT FPLNK MANPTS NINT OMEGA PCLOUD RINTER TLTFLD TORBIT TOROID	PEDEP	ATMOSF CMDEDT
				PGROUP	DSTINT
				PHEAVE	HEAVE
				PHENOM	CONWES
				PHOTOD	CMDEDT
				PHOTOR	CHEMD CHEMHR
LOSCON	FBMHI			PIONF	CMFEDT ENEF
		MISCAT	PGROUP		
MAGDIS	BALFIT BTRACE DBMHT FBEN FBMHT FOOTPC HDINT PHENOM	MODEM1	FPCIR SATCIR	PLINTP	WOND WONP
		MODEM2	FPCIR SATCIR	PLYVAL	RRMSTP
		MODEM3	FPCIP SATCIR	PMASS	EDEPB EDEPG EDFPND PEDEP PIONF
MAGFIT	CONWES PHENOM SATC	NFSKMF	FPCIR SATCIR		
MAGFLD	ANTND DBMHT DBSTAM DEBRIS EDEPB EDEPG FBEN FBINT FBMHI FBTINT FOOTPC FPLNK GWPLME MANPTS PHENOM PTHINT RINTER TURE	NINT	ANTND FPLNK	PROPEN	ANTND JAMND SATC
		NORMAL	BDPSK	PSDM	DBSTAM
		OMEGA	NINT	PTHINT	PROPEN
		ONEMGS	MAGFIT	QCOSM	IONOSI IONOSU
		ORBIT	INPUT	QFNTN	DQPSK
		OZONE	ATMOSI	RADOUT	PHENOM
		PCHEM	PIONF		

Table 3 (Continued)

SUBROUTINE	CALLED BY
RATE	CHEMEF CHEMHR CHEMO DRATE FBEN IONOSU
RICATT	CHMION
RINTER	DSTINT EDEPB EDEPG FBINT FOOTPC MANPTS NINT
RRMSTP	INPUTP
SANCAN	NFSKMF
SATC	CONWES
SATCIR	SATC
SATLNK	SATC
SEPA	AZELR DEBRIS FBEN FBINT FBMHT FOOTPC GAIN GEOCOR GWPLME HTOS IONOSI IONOSU NINT
SLINK	SATC
SLOPE	FPLNK JAMND SATLNK
SOIL	DUSTMI
SOLCYC	ATMOSI IONOSI
SOLORB	ATMOSI IONOSI
SOLZEN	ATMOSI
SORBIT	CONWES
SPCTRM	INPUT
SPECDP	CHEMD
SPECDQ	CHEMD CHEMDQ
START	PROPEN
STRII	FBINT
STRIP	FBMHT
SUBVEC	ANTND ATMOSF AZELR EDEPB EDEPG EDEPND FBEN FBINT FBTINT FOOTPC FPINT FPLNK GWPLME JAMND MANPTS NINT OMEGA PEDEP PHOTOR PIONF PROPEN PTHINT RINTER SATC SATLNK STRII TUBE
TATSRT	ORBIT SORBIT
TEMPZH	ATMOSI
TEST	INPUT
TEXK	CHEMEF ENEF PCHEM
TFUNC	FBEN
TLTFLD	FOOTPC
TORBIT	SATC
TOROID	RINTER
TUBE	RINTER
UNITV	AMBABS ANTND ATMOSF DBMLT DSTINT EDEPB EDEPG ENEF FBEN FBINT FBTINT FOOTPC FPINT FPLNK JAMND LOCLAX MAGFIT MAGFLD MANPTS NINT PROPEN PTHINT RINTER SATC SATLNK STRII TUBE

Table 3 (Continued)

SUBROUTINE	CALLED BY	SUBROUTINE	CALLED BY	SUBROUTINE	CALLED BY
USERMD	FPCIR		FPLNK	XMAG	AMBABS
	SATCIR		GWPLME		ANTND
			JAMND		ATMOSF
UVWAV	PSEM		LOCLAX		AZELR
			MAGFIT		CORDTF
UVWD	GWPLME		MANPTS		DBSTAM
	PSDM		NINT		DEDEP
			PHENOM		EDEPB
VECLIN	AMBABS		PIONF		EDEPG
	ANTND		PROPEN		EDEPND
	CLOSF		RINTER		FBEN
	CORDTF		SATC		FBINT
	EDEPB		SATLNK		FBMHT
	FBEN		TORBIT		FBMLT
	FBINT		TOROID		FBTINT
	FBMHT				FOOTPC
	FBMLT	VOLUME	ARRLIM		FPLNK
	FBTINT		DBMLT		GWPLME
	FOOTPC		EDEPB		HTOS
	FPINT		NINT		INPUTP
	FPLNK				JAMND
	MAGFLD	WATER	ATMOSI		MAGFLD
	MANPTS				MANPTS
	NINT				NINT
	PIONF	WOBD	BETAS		OMEGA
	PROPEN		DBMLT		PEDEP
	PTHINT		EDEPB		PHENOM
	RINTER				PHOTOR
	SATC	WOGD	EDEPG		PIONF
	STRII				PROPEN
	TLTFLD				PTHINT
	TORBIT	WOGP	PEDEP		RINTER
	TOROID				SATC
		WOG1	INPUT		SATLNK
VECM	AMBABS				SEPA
	ANTND	WOND	EDEPND		TLTFLD
	ATMOSF				TORBIT
	CHEMD	WONP	PEDEP		
	DBMHT			ZTTOUT	CONWES
	DBMLT	WON1	INPUT		DBSTAM
	DBSTAM				GWPLME
	DEBPIS				IONOSI
	DEDEP	WOXC	EUXFIT		PHENOM
	DSTINT		FBMHI		
	EDEPB		FBMLI		
	ELDEN	WOXP	PEDEP		
	ENEF		PIONF		
	FBEN				
	FBINT				
	FBMHT	WOX1	INPUT		
	FBTINT				
	FOOTPC				

Table 4. Routines using a specific common block.

COMMON BLOCK	USED IN	COMMON BLOCK	USED IN	COMMON BLOCK	USED IN
ALTODN	CONWFS	BETAR	ANTND	BTUBE	DEDEP
	ATMOSI		BETAS		FBINT
	ATMOSU				FBTINT
	BLKDTA	BREG	CONWFS		MANPTS
	TEMPZH		ANTND		
			ATMOSF	BURST	CONWFS
ANTMP	ANTND		BETAS		BETAS
	BETAS		CHEMD		DAMHT
	FBTINT		CMDEDT		DBMLT
	FPLNK		CMFEDT		DUSTMT
	NINT		DAMHT		EDEPB
			DBSTAM		EDEPG
ATMOSN	CONWFS		DEPRIS		EDEPND
	AMBARS		DEDEP		ELDEN
	ATMOSU		DUSTMT		EUXFIT
	CHEMD		EDEPB		FBINT
	CHEMDQ		EDEPND		FBMHI
	CHEMHR		ELDEN		FBMLI
	ENEF		ENEF		FBTINT
	FOAMB		EUXFIT		IDEFLT
	SPECDP		FBEN		INPUT
			FBINT		INPUTP
			FBITMD		MANPTS
ATMOST	CHEMD		FBMHI		PEDEP
	CHEMDQ		FBMHT		PHENOM
	CMDEDT		FBMLI		PTONF
	DTNEP		FBMLT		
	DTNEQ		FBTINT		
	EN2VIB		FOOTPC	CHEMAN	CHEMEF
	FOAMB		FPLNK		CHMION
	INITAL		GWPLME		
	SPECDP		MANPTS		
	SPECDQ		PCLOUD	CHEMB	CHEMHR
			PEDEP		FBEN
ATMOUP	CONWFS		PHENOM		FBINT
	ATMOSI		PHOTOD		FBTINT
	ATMOSU		PHOTOR		FOOTPC
			PTONF		SATC
			RADOUT		
BEDIT	CHEMD		STRIP		
	CMDEDT			CHEMFB	FBEN
					FBINT
					FOOTPC

Table 4 (Continued)

COMMON BLOCK	USED IN
CHEMH	CONWES
	BLKDTA
	RATE
CHMOVL	CHEMD
	ELDEN
	ENEF
CINPUT	CONWES
	ANTND
	ARRLIM
	BETAS
	CHEMD
	CHEMDQ
	DBSTAM
	DEDEP
	DSTINT
	ELDEN
	ENEF
	FREN
	FRINT
	FOOTPC
	FPLNK
	IDEFLT
	INPUT
	INPUTP
	MANPTS
	PHENOM
	PROPEN
	PTHINT
	SATCIR
	SATLNK
	TORBIT
CIRDES	CONWES
	IDEFLT
	INPUT
	INPUTP
	SATC
	SLINK
CLINK	ANTND
	FPLNK
	JAMND
	SATC
	SATLNK
	SLINK

COMMON BLOCK	USED IN
CONST	CONWES
	AMBABS
	ANTND
	ARRLIM
	ATMOSF
	ATMOST
	ATMOSU
	AZELR
	BALFIT
	BDPSK
	BETAS
	BFIELD
	BLKDTA
	BTRACE
	COMB
	COORDV
	COORDX
	CORDTF
	DRMHT
	DRMLT
	DBSTAM
	DEBRIS
	DELPSK
	DPSK
	DSTINT
	EDEPB
	EDEPG
	ENEF
	EQCROS
	ERF
	FREC
	FAC
	FBEN
	FBINT
	FBMHI
	FBMHT
	FBMLI
	FBMLT
	FOOTPC
	FPCIR
	FPINT
	FPLNK
	FPPLOT
	FSKWB
	GEOCOR
	GWPLME
	HDINT
	HTOS
	IDEFLT
	INPUT
	INPUTP
	IONOSI

COMMON BLOCK	USED IN
	IONOSU
	JAMND
	MAGDIS
	MAGFIT
	MANPTS
	NFSKMF
	NINT
	OMEGA
	ORBIT
	OZONE
	PCLOUD
	PEDEP
	PGROUP
	PHENOM
	PIONF
	PMASS
	PROPEN
	PSDM
	PTHINT
	QCOSM
	RINTER
	SANCAN
	SATCIR
	SATLNK
	SEPA
	SLOBF
	SOLCYC
	SOLORB
	SOLZEN
	SORBIT
	STRTI
	TEMPZH
	TLTFLD
	TORBIT
	UVWD
	VOLUMF
	WATER
	ZTTOUT
DRREG	CONWES
	ARRLIM
	BETAS
	DRMHT
	DRMLT
	DBSTAM
	DEDEP
	EDEPB
	EDEPG
	FRINT
	MANPTS
	PHENOM

Table 4 (Continued)

COMMON BLOCK	USED IN
DCREG	CONWES
	DSTINT
	DUSTMI
	PCLOUD
	PGROUP
	PHENOM
	SOIL
DEPDAT	CONWES
	BLKDTA
	PCHEM
	PIONF
DEVICE	CONWES
	BETAS
	DBMHT
	DBMLT
	EDEPND
	ELDEN
	FBINT
	FBTINT
	INPUT
	INPUTP
	MANPTS
	PEDEP
	PHENOM
	PIONF
	WOBD
	WOGD
	WOG1
	WON1
	WOX1
DIGMOD	BDPSK
	CPSK
	DELPSK
	DPSK
	DQPSK
	FPCIR
	FSKWB
	FSKWBY
	NFSKMF
	SATCIR
	USERMD
DTURB	DEBRIS
	MANPTS
	PEDEP
EDTOVL	CMFEDT
	PROPEN
FREG	CONWES
	ANTND
	ATMOSF
	BETAS
	DBMHT
	DBMLT
	DEDEP
	DSTINT
	EDEPB
	EDEPG
	FREN
	FRINT
	FBMHT
	FBMLT
	FBTINT
	FOOTPC
	FPLNK
	GWPLME
	NINT
	PCLOUD
	PHENOM
	PHOTOR
	RADOUT
	START
	STRIP
FDSRAT	CHEMD
	CHEMDQ
	CHEMHR
	DTNEP
	DTNEQ
	FQAMB
	PHOTOR
FPCIRC	FPCIR
	FPLNK
FPINTC	FOOTPC
	FPINT
	FPPLOT
HEACOM	CONWES
	ATMOSF
	ENEF
HEAVF1	CONWES
	ATMOSF
	HEAVE
	LAGRAN
	PHEAVE
INPTCM	INPUT
	INPUTP
IONOUP	IONOST
	IONOSU
JAMMER	CONWES
	IDEFLT
	INPUT
	INPUTP
	JAMND
	SATC
LENGTH	BALFIT
	BTRACE
	DBMHT
	EQCROS
	FBEN
	FBMHT
	FOOTPC
	HDINT
	MAGDIS
	PHENOM
MAGLNK	CONWES
	ANTND
	BFIELD
	DEBRIS
	DEDEP
	EDEPB
	FBEN
	FBINT
	FBTINT
	FOOTPC
	FPLNK
	IONOSI
	IONOSU
	MAGFIT
	MAGFLD
	MANPTS
	OMEGA
	PHENOM
	PROPEN
	PTHINT
	RINTER

Table 4 (Continued)

COMMON BLOCK	USED IN	COMMON BLOCK	USED IN	COMMON BLOCK	USED IN
MODULT	CONWES	URIGIN	CONWES	RAY	ARRLIM
	FPCIR		DATE		GWPLME
	IDEFLT		DBSTAM		PSDM
	INPUT		GWPLME		UVWAV
	INPUTP		IDEFLT		UVWD
	SATCIR		INPUT		
			INPUTP	REGINT	CONWES
OPTION	CONWES		ORBIT		FBINT
	ANTND		PHENOM		MANPTS
	BLKDTA		SOLCYC		PROPEN
	CARDIN				PTHINT
	CHEMD	OUT	CHEMD		START
	CHEMHR		CMDEDT		
	CMDEDT		DTNEQ	RGEOM	RINTER
	CMFEDT		FQAMB		TORDID
	DBMHT				TUBE
	DBSTAM				
	DEBRIS	PATH	CONWES	SIGCOM	SATCIR
	DEDEP		IDEFLT		SATLNK
	DSTINT		INPUT		
	ELDEN		INPUTP		
	ENEF		ORBIT	SOURCE	CMFEDT
	FBEN		SATC		ELDEN
	FBINT		SORBIT		ENEF
	FBTINT		TORBIT		
	FOOTPC			SPEC	CHEMHR
	FPINT	PHEN	CONWES		EQLAIR
	FPLNK		DBMHT		EQLMTL
	FPPLOT		DBMLT		
	IDEFLT		DBSTAM	SPECEF	CHEMEF
	INPUT		DUSTMI		CHMION
	INPUTP		FBMHI		CMFEDT
	JAMND		FBMHT		ENEF
	MANPTS		FBMLI		HPCHEM
	NINT		FBMLT		PCHEM
	PCHEM		GWPLME		PIONF
	PHENOM		PHENOM		
	PIONF		RADOUT	SPECQ	CHEMQ
	PROPEN				ENEF
	PTHINT	PROP	CONWES		
	SATC		ANTND	SPECW	CONWES
	SATCIR		DSTINT		INPUT
	SATLNK		FBINT		SPCTRM
	SORBIT		FPLNK		WOG1
			JAMND		WON1
			MANPTS		WOX1
			PROPEN		
			PTHINT	SPEEDS	PSDM
			SATC		UVWAV
			SATLNK		
			START		
			STRII		

Table 4 (Continued)

COMMON BLOCK	USED IN	COMMON BLOCK	USED IN
SSYS	CONWES	WEDEPO	CONWES
	ANTND		BLKDTA
	FPLNK		CHXSPC
	IDEFLT		CONSPC
	INPUT		DEBRIS
	INPUTP		LEKSPC
	JAMND		
	SATC	WOG	CONWES
	SATLNK		WOGD
	SLINK		WOGP
			WOG1
STRIIN	FRINT		
	STRII		
		WON	CONWES
			WOND
TIME	CONWES		WONP
	ATMOSI		WON1
	ATMOSU		
	DRSTAM		
	IONOSI	WOX	CONWES
	IONOSU		WOXC
	JULIAN		WOXP
	OZONE		WOX1
	PHENOM		
	SATC	WRATE	CMDEDT
	SOLCYC		DRATE
	SOLORB		DTNEP
	SOLZEN		DTNEQ
	TEMPZH		INITAL
	WATER		SPECDP
	ZTTOUT		SPECDQ
TRACE	BTRACE	WRATEH	DRATE
	FBMHT		SPECDP
TSTEF	HPCHEM	WSTOR	GWPLME
	PCHEM		PSOM
	PIUNF		UVWD
TSYS	CONWES	ZHTEMP	ATMOSI
	ANTND		ATMOSU
	FPLNK		TEMPZH
	IDEFLT		
	INPUT		
	INPUTP		
	JAMND		
	SATC		
	SATLNK		
	SLINK		

SECTION 3
ROUTINE DESCRIPTIONS

A description of inputs and outputs transferred through the call statement and a list of inputs and outputs transferred through labeled common blocks are given in comment statements at the beginning of each routine. A description of quantities in labeled common blocks is given in Table 5.

Most of the routines used in the WESCOM code are modified versions of routines developed for the WEPH code. However, as indicated in the following descriptions routines developed for the SATL, ROSCOE, and WOE codes have also been modified for use in the WESCOM code.

Table 5. Quantities stored in labeled common blocks.

COMMON BLOCK	QUANTITY	DESCRIPTION
ALTODN (Atmosphere Common)	ALTKM	Altitudes used for atmospheric calculations in routine ATMOSF
	ZHT	Altitudes used for temperature and ozone calculations in routine ATMOSI
ANTMP (Noise Common)	BEAM	Antenna beam efficiency
	DEPTH	Effective distance into the fireball producing thermal radiation (km)
	FREQN	Frequency (MHz)
	KEYN	Code describing location of fireball in antenna beam
	KPLME	Code describing fireball z-axis curvature
	N	Fireball index
	NCFB	Index of fireball closest to receiver in beam center
	RBO	Antenna beam width (radians)
	RC	Side lobe gain relative to RGO
	RGO	Main beam gain
	RXKO	Side lobe specification
	SRFBE SRFBX	Slant ranges to entrance and exit intersections with fireball
	TANT	Normalized antenna temperature
	TASUM	Antenna temperature summation for fireball loop (K)
	TIME	Calculation time (s)
	UV	Transformation matrix from tangent plane to earth centered coordinates
	VBEAM	Antenna pointing direction vector (km)
	VR	Receiver location vector (km)
	VSPA	Sight path vector to fireball (km)
	VZZ	Fireball reference vector (km)
ATMOSN (Atmosphere Common)	ACO2 . . . AO3	Concentration of CO_2, H, ... O_3 (cm^{-3})

Table 5 (Continued)

COMMON BLOCK	QUANTITY	DESCRIPTION
ATMOST (Atmosphere Common)	CCO2 CH . . . CO_3	Concentration of CO_2, H, ... O_3 (cm^{-3})
	HRHO	Density scale height (km)
	P	Pressure (dynes cm^{-2})
	RHO	Density (gm cm^{-3})
	TEM	Temperature (K)
ATMOUP (Atmosphere Common)	ACO2T AHO2T . . . AO3T	Concentration of CO_2, HO_2, ... O_3 (cm^{-3})
	FDAY	Day profile of mean molecular weight
	FHR120	Density scale height term
	GAMT	Coefficient of M_i in equation for Y_i
	HRHO	Density scale height
	HRO110	Density scale height at 110 km
	PP	Pressure (dynes cm^{-2})
	RHO	Density (gm cm^{-3})
	SA	(TIF-TZ)/TIF
	SB	Approximate derivative of density scale height at 110 km
	SNIZ	Species densities at 120 km (cm^{-3})
	TAU	Temperature gradient at 120 km
	TIF	Exospheric temperature (K)
	TT	Temperature (K)
	TZ	Temperature at 120 km (K)
BEDIT (D-region Edit Common)	EDP	Energy deposited by prompt radiation (ergs gm^{-1})
	EXPD	Fraction of O_3 remaining after thermal radiation
	INDEX	Indices of bursts affecting D-region neutral species
	NPBC	Index of last burst in INDEX

COMMON BLOCK	QUANTITY	DESCRIPTION
BETAB (Beta Sheath Common)	DBBETA	Absorption through beta sheath (dB)
	ETAS	Beta sheath reflection coefficient
	FSCA	Scaled frequency used for reflection coefficient calculation
	HPBETA	Altitude of field point (km)
	MBETA	0 Beta sheath absorption 1 Absorption and reflection coefficient
	NBETA	Fireball index
	RHOBET	Fireball air density (gm cm^{-3})
BREG (Burst Common)	AENE	Apogee N_e (cm^{-3})
	AHF	Apogee reference altitude (km)
	AHMAXF	Apogee maximum altitude (km)
	AHMINF	Apogee minimum altitude (km)
	AHSNE	Apogee N_e scale height along longitudinal axis (cm^{-3} km-1)
	AHSNF	Apogee density scale height along longitudinal axis (km)
	AHTF	Apogee temperature scale height along longitudinal axis (km)
	ALPHUV	UV parameter
	ARHOF	Apogee mass density at fireball bottom (gm cm^{-3})
	ARLF	Apogee longitudinal dimension (km)
	ARTF	Apogee transverse dimension (km)
	ATF	Apogee temperature (K)
	ATILTF	Apogee tilt angle (radians)
	AVFBO	Apogee earth centered vector location (km)
	AXL	Apogee longitudinal positions (km)
	DBV3	Debris volume when fireball is 3000 K (km^3)
	DECANB	Magnetic declination angle at burst point (radians)
	DIPANB	Magnetic dip angle at burst point (radians)
	ENERGY	Number of photons in 4.135 to 7.255 eV band (1.E-18 photons)
	EQRHOF	Mass density at bottom of fireball at t_{eq} (gm cm^{-3})
	FNEUT	Burst point density scaling parameter
	FUVT	Fraction of hydroenergy converted to UV
	HB	Burst altitude (km)

Table 5 (Continued)

COMMON BLOCK	QUANTITY	DESCRIPTION
BREG (Continued)	HBOT2	Altitude of fireball bottom when fireball temperature is 2000 K (km)
	HSB	Density scale height at burst point (km)
	HSNFAO	Average scale height between bottom and center of initial fireball (km)
	HSTOP	Stopping altitude for ballistic fall of ionization (km)
	HS2000	Density scale height at bottom of fireball when fireball temperature is 2000 K (km)
	IBURST	Burst index
	IDAYB	Time of day at burst time (day or night)
	IFBRM	Fireball merge flag
	KFB	0 if fireball bottom goes above HSTOP, 1 if below
	KINDFA	Apogee fireball shape
	LHVB	1 if burst causes heave
	LMCF	1 if low altitude burst, 0 if high altitude burst
	MRGID	Merge index
	PB	Pressure at burst point (dynes cm^{-2})
	RCHEX	Charge exchange characteristic radius (km)
	RDUV	Downward UV radius (km)
	RDZERO	Initial downward radius (km)
	REFT	Initial vortex surface temperture (K)
	RHOB	Burst point mass density (gm cm^{-3})
	RHOFO	Initial bottom mass density (gm cm^{-3})
	RHUV	Horizontal UV radius (km)
	RHZERO	Initial horizontal radius (km)
	RH2000	Fireball density when fireball temperature is 2000 K (gm cm^{-3})
	RH3000	Fireball density when fireball temperature is 3000 K (gm cm^{-3})
	RIONL	Ion leak characteristic radius (km)
	RLOSC	Loss cone characteristic radius (km)
	RM	Magnetic containment radius (km)
	RUZERO	Initial upward radius (km)
	TAPOGE	Apogee time (s)
	TB	Burst time (s)

Table 5 (Continued)

COMMON BLOCK	QUANTITY	DESCRIPTION
BREG (Continued)	TEMB	Temperature at burst point (K)
	TEQ	Magnetic containment time (s)
	TFO	Initial fireball temperature (K)
	TFZ	Magnetic freezing time (s)
	TMAX	Time for all parcels to fall (s)
	TMRG	Merge time (s)
	TTC	Time of completion of torus formation (s)
	T1	Time of end of first expansion phase (s)
	T2	Time at end of second expansion phase (s)
	T3000	Time when fireball temperature is 3000 K (s)
	VBO	Earth centered vector to burst location (km)
	VMAXD	Heavy particle velocity (km s^{-1})
	VMFBO	Earth centered vector location of dipole for burst (km)
	VKO	Earth centered vector location of heavy particle reference location
	VMIND	Heavy particle velocity (km s^{-1})
	W	Burst yield (MT)
	WCHEX	Charge exchange yield (MT)
	WILD	Ion leak yield (MT)
	WLCD	Loss cone downward yield (MT)
	WUV	UV yield (MT)
	XEMAX	Position of parcel in apogee fireball that stops at equator (km)
	XEST	Position of parcel in apogee fireball that goes above HSTOP (km)
	XMFB	Wake parameter
	XMSD	Wake parameter
BTUBE (Beta Tube Common)	HBETA1	Altitude of lower beta tube intersection (km)
	HBETA2	Altitude of upper beta tube intersection (km)
	KBS	Beta sheath flag
BURST (Burst Input Common)	ICONJ	Burst location flag
	ID	Device index
	IS	Surface index
	NB	Number of bursts
	TBI	Burst time (s)

Table 5 (Continued)

COMMON BLOCK	QUANTITY	DESCRIPTION
BURST (Continued)	VBIO	Earth centered vector to burst location (km)
CHEMAN (F-region Chemistry Common)	ALPHA1	Atomic ion recombination rate (cm^3/s)
	ALPHA2	Molecular ion recombination rate (cm^3/s)
	AMOLP	Molecular ion concentration (cm^{-3})
	BETA1	Effective loss rate due to volume expansion (s^{-1})
	DELEV	Energy returned from chemistry (eV/cm^3)
	DELT	Time interval (s)
	EXPAND	Time average volume expansion ratio
	Q	Total ion pair production rate ($cm^{-3}\ s^{-1}$)
	RHO21	Ratio of density at time t_2 to density at time t_1
	XK(I)M	Mean rate coefficient for reaction I
CHEMB (Fireball Chemistry Common)	FE	Entrainment fraction
	FEQN	Entrainment fraction at 2000 K
	FUVTC	Fraction of hydroenergy converted to UV
	LFPCJ	Conjugate region flag
	LFPCS	Footprint calculation flag
	Q	Ion pair production rate ($cm^{-3}\ s^{-1}$)
	RAL	Aluminium density ($gm\ cm^{-3}$)
	RHO	Air density ($gm\ cm^{-3}$)
	RHOALQ	Aluminium density at time TEQM ($gm\ cm^{-3}$)
	RHOEQ	Air density at TEQ ($gm\ cm^{-3}$)
	RHOEQM	Air density at TEQM ($gm\ cm^{-3}$)
	RHOEQN	Air density at TEQN ($gm\ cm^{-3}$)
	RHOHB	Burst point air density ($gm\ cm^{-3}$)
	RHOI	Initial air density ($gm\ cm^{-3}$)
	RHOUQ	Uranium density at time TEQM ($gm\ cm^{-3}$)
	RU	Uranium density
	TEQC	Magnetic equilibrium time (s)
	TEQM	Time after burst when temperature is TFEM (s)
	TFB	Fireball temperature (K)
	TFEM	Non-equilibrium metal ion temperature (K)
	TFEN	Non-equilibrium neutral air species temperature (K)
	TFI	Initial temperature (K)

Table 5 (Continued)

COMMON BLOCK	QUANTITY	DESCRIPTION
CHEMB (Continued)	TOB	Burst time (s)
	XT	Scaled distance from fireball bottom
CHEMFB (Fireball Chemistry Common)	ENEFP	Electron density (cm^{-3})
	FPXL	Distance from earth's surface measured along geomagnetic field line (km)
	HSNEFP	Electron density scale height (km)
	HSTFFP	Temperature scale height (km)
	JNFBFP	Fireball index
	TFBFP	Temperature (K)
CHEMR	AR, BR, CR	Reaction rate coefficient parameters
CHMOVL (F-region Chemistry Common)	ENEC	Electron density (cm^{-3})
	ENPC	Positive ion density (cm^{-3})
	HPC	Altitude (km)
	IALT	Altitude index
	IONC	Ionization flag
	NPBX	Number of prior bursts
	VEIC	electron-ion collision frequency (s^{-1})
	VEMC	Electron-neutral collision frequency (s^{-1})
	VHEAVE	Heave velocity (km/s)
	VIMC	Ion-neutral collision frequency (s^{-1})
	VPOC	Earth centered vector to field point (km)
CINPUT (Input Common)	IDAY	Time of day (day or night)
	JNDB	Debris region index
	JNDC	Dust cloud index
	JNFB	Fireball index
	JTIME	Calculation time index
	LNCNT	Output line count
	NPROB	Problem number
	NT	Number of calculation times
	PROB	Problem heading
	T	Calculation times (s)
	TESTIP	Input test flag

Table 5 (Continued)

COMMON BLOCK	QUANTITY	DESCRIPTION
CIRDES (Circuit Common)	IDL	System indexes for downlink
	ISSL	System indexes for satellite-to-satellite link
	ITI1	Ground terminal index
	ITI2	Satellite terminal index
	ITI3	Satellite terminal index
	ITI4	Ground terminal index
	IUL	System indexes for uplink
	NC	Number of circuits
CLINK (Link Common)	INDEX	Circuit index
	JLINK	Link index
	K1, K2, K4, K4	System indexes for specified link
	LFLAG	Propagation calculation flag
	LINK	Circuit index
	L1, L2, L3, L4	Terminal indexes
	NFLAG	Noise calculation flag
CONST (Constant Common)	G	Acceleration of gravity (km s^{-2})
	PI	π
	RADIAN	$\pi/180$
	RE	Earth's radius
	RHOG	Air density at earth's surface (gm cm^{-3})
	XNHAT	Earth centered unit vector to geographic pole (km)
DBREG (Debris Region Common)	DB	Beta sheath thickness (cm)
	DISTD	Debris distribution parameter
	FEI	Fraction of beta energy that escapes debris region
	FEO	Fraction of escaping energy deposited in beta sheath
	HBETA	Beta source altitude (km)
	HD	Debris altitude (km)
	HMAXD	Maximum debris truncation altitude (km)
	HMIND	Minimum debris truncation altitude (km)
	HSND	Debris scale height (km)
	IXDBB(L)	Burst index associated with L*th* dust cloud

Table 5 (Continued)

COMMON BLOCK	QUANTITY	DESCRIPTION
DBREG (Continued)	IXDBFB	Fireball index associated with L*th* debris region
	KBET	Beta sheath flag
	KINDD	Debris region geometry flag
	NDB	Number of debris regions
	RLBETA	North-south radius of beta source plane (km)
	RLD	Longitudinal debris radius (km)
	RTBETA	East-west radius of beta source plane (km)
	RTD	Transverse debris radius (km)
	TILTD	Debris tilt angle (radians)
	VDBO	Earth centered vector to debris reference point (km)
	VOLD	Debris volume (km^3)
	WBD	Beta source fission yield (MT)
	WFD	Gamma source fission yield (MT)
	XLO	Larmor radius outside debris region (cm)
DCREG (Dust Cloud Common)	ABAR	Particle size group boundary values (cm)
	DIECR	Real part of index of refraction
	DIECI	Imaginary part of index of refraction
	FNP	Fraction of particles in each group
	IMAXP	Index of maximum particle group lofted
	IXDCFB(L)	Fireball index associated with L*th* dust cloud
	JGROUP	Group index
	NDC	Number of dust clouds
	NPG	Number of particle groups
	RHODP	Particle mass density (gm cm^{-3})
	SIGB	Average backscatter cross section for each group (m^2)
	SIGE	Average extinction cross section for each group (m^2)
	TNP	Total number of particles in all groups
	XMLOD	Dust loading factor (MT/MT)
DEPDAT (Prompt Energy Common)	ERGU(L)	Photon energy for UV group L (erg)
	PREFF(L,I)	Pressure efficiency for energy group L and species I
	SIGU(L,I)	UV absorption cross section for energy group L and species I (cm^2)

Table 5 (Continued)

COMMON BLOCK	QUANTITY	DESCRIPTION
DEPDAT (Continued)	THRESH(I)	Effective threshold for absorption of UV photons by species I (erg)
DEVICE (Device Common)	FEDG	Fraction of weapon energy radiated as prompt gammas
	FEDH	Fraction of weapon energy in hydro
	FEDN	Fraction of weapon energy in neutrons
	FEDX	Fraction of weapon energy radiated as X-rays
	FF	Fission fraction
	FMAL	Fraction of weapon mass that is aluminum
	FMUR	Fraction of weapon mass that is uranium
	FTHERM	Fraction of fissionable material that is fissionable by thermal neutrons
	WI	Weapon yield (MT)
	WMASS	Weapon mass (g)
DIGMOD (Signal Processing Common)	A	Ratio of bit period to decorrelation time
	BETA	Scintillation index function
	DGLRAT	1 - 1/MARY
	DISPAR	Dispersion parameter
	EBNO	Bit energy-to-noise ratio
	ENNOR	Chip energy-to-noise ratio
	GAMMA	Normalized energy-to-noise ratio
	GPR	Function of number of modulation states
	MARY	Number of modulation states
	NINFOB	ℓn_2(MARY)
	S4	Scintillation index
	TAU	Decorrelation time (s)
	WT	Product of chip period and frequency separation
DTUBE (Debris Kinetic Energy Common)	LDKE	Radiation source flag
EDTOVL (F-region Burst Edit Common)	HFTEST	Test altitude (km)
	JNFEDT	Last burst index
	JPBEDT	Index of last burst producing F-region ionization
	VPO	Earth centered vector to test location (km)

Table 5 (Continued)

COMMON BLOCK	QUANTITY	DESCRIPTION
FBREG	AFB, AFC, BFB, BFC	Coefficients for parcel location
	BVAL	Oval of Cassini parameter
	CFB, CFC	Coefficients for parcel location
	ENE1DF	Diffusion ionization parameter (cm^{-3})
	HF	Fireball reference altitude (km)
	HLDF	Hydrostatic scale length (km)
	HMAXF	Maximum altitude (km)
	HMINF	Minimum altitude in burst region
	HMINFC	Minimum altitude in conjugate region (km)
	HSNF	Density scale height along longitudinal axis (km)
	KINDF	Shape indicator
	KPB	Burst region parcel indicator (0 = none)
	KPC	Conjugate region parcel indicator
	NFB	Number of fireballs
	POWER	Thermal power radiated in specified bands (10^{-18} photons s^{-1})
	RDOT	Radial expansion velocity (km s^{-1})
	RHOF	Bottom density (gm cm^{3})
	RLF	Longitudinal radius (km)
	RTF	Transverse radius (km)
	RLFC	Conjugate longitudinal radius (km)
	RGEOM	Radial geometry factor used in FBEN
	RMAXDF	Radius from earth center to maximum altitude on field line (km)
	RMAXF	Distance from earth center to field line at equator (km)
	RPDF	Radius from earth's center to diffusion ionization peak (km)
	RTREF	Radius of reference Oval of Cassini (km)
	RVL	LAFBP - vortex longitudinal radius (km)
	RVT	LAFBP - vortex transverse radius (km)
	SPLEX	Power law exponent
	SSCAI	Inner scale length (km)
	SSCAO	Outer scale length (km)
	TDEB	Debris temperature (K)
	TF	Temperature (K)

Table 5 (Continued)

COMMON BLOCK	QUANTITY	DESCRIPTION
FBREG (Continued)	TILTF	Tilt angle (radians)
	TVORT	Vortex surface temperature (K)
	VARNEN	Electron density variance (cm^{-6})
	VFBO	Earth centered vector defining central field line
	VFBVEL	Earth centered vector defining velocity of fireball ($km\ s^{-1}$)
	VOV	Vortex volume (km^3)
	XLLDF	Hydrostatic scale length along field line in diffusion fireball (km)
	XLMDF	Netural density vertical scale height in diffusion fireball (km)
	XLPDF	Distance from earth's surface to peak of diffusion ionization (km)
FDSRAT (Fireball Photodissociation Common)	FDIS3 . . . FDIS9	Photodissociation rate (s)
	FDT1 . . . FDT8	Photodetachment rate (s)
FPCIRC (Footprint Circuit Common)	BWL	Noise bandwidth (MHz)
	DNOSA	Ambient noise density ($W\ Hz^{-1}$)
	DNOSD	Disturbed noise density ($W\ Hz^{-1}$)
	ENTOT	Electron density integral (cm^{-2})
	FREQGH	Frequency (GHz)
	FZEROL	Frequency selective bandwidth (Hz)
	IMOD	Modulation index
	KALSN	Signal-to-noise option
	KFMFP	FM modulation flag
	PERFP	Probability of bit or message error (s^{-1})
	SIGFS	Ambient signal strength (W)
	SIGND	Disturbed signal strength (W)
	SPHIL	rms phase fluctuation (radians)
	SPSIL	rms angle of arrival fluctuation (radians)
	S4L	Scintillation strength index

Table 5 (Continued)

COMMON BLOCK	QUANTITY	DESCRIPTION
FPCIRC (Continued)	TAUZL	Decorrelation time (s)
FPINTC (Footprint Interpolation Common)	HR	Receiver altitude (km)
	KFMFP	FM modulation flag
	NI1	Scan number ending first set of contours
	NI2	Scan number starting second set of contours
	NN	Total number of scans
	NPK	Number of paths for specified scan
	NPKM	Index of path with maximum propagation effects
	QT	Propagation quantities
	QTI	Interpolated propagation quantities
	SKD	Distance from origin to paths
	TLAMAX, TLAMIN	Minimum and maximum latitudes for scan (deg)
	TLATFL	Latitude of central field line (deg)
	TLATRD	Latitude of calculation paths for scan (deg)
	TLATRI	Latitude of paths for interpolated propagation quantities (deg)
	TLOMAX, TLOMIN	Minimum and maximum longitudes for scan (deg)
	TLONFL	Longitude of central field line (deg)
	TLONRD	Longitude of calculation paths for scan (deg)
	TLONRI	Longitude of paths for interpolated propagation quantities (deg)
	VPO	Earth centered vector to field point (km)
	VR	Earth centered vector to receiver terminal (km)
	VXP	Earth centered path direction vector (km)
HEACOM (Heave Interpolation Common)	HPINT	Altitude (km)
	NINT	Number of interpolated points
	RHOINT	Density (gm cm^{-3})
	TINT	Time after burst (s)
HEAVE1 (Heave Common)	A . . . ZRSS	Calculation quantities used in heave model

Table 5 (Continued)

COMMON BLOCK	QUANTITY	DESCRIPTION
INPTCM (Input Common)	BCORD1 . . . VROO	Transfer of internal input quantities between routines INPUT and INPUTP
IONOUP (Ionosphere Common)	BA BB	Booker interpolation parameters
IONOUP (Continued)	BNER	Electron density at reference point (cm^{-3})
	BZ	Transition altitudes (km)
	BZR	Reference altitude (km)
	H1	Upper altitude of production rate fits (km)
	XION	Ionosphere fit quantities
JAMMER (Jammer Common)	DJAM	Jammer noise density (W Hz^{-1})
	IJS	Index of satellite terminal
	IJT	Index of ground terminal
	NJ	Number of jammers
	VJO	Earth centered vector to jammer (km)
LENGTH (Field Line Geometry Common)	COSLO	Colatitude of earth intercept (cosine)
	RMAX	Radius from earth center to maximum altitude (km)
	XLMAX	Length along field line from earth's surface to maximum altitude (km)
MAGLNK (Magnetic Dipole Common)	COSLTO	Colatitude of south pole (cosine)
	PHIO	Latitude of south pole (radians)
	SINLTO	Colatitude of south pole (sine)
	VMFO	Earth centered vector to north pole
	XMVO	Magnetic moment (gauss km^3)
MODULT (Modulation Common)	AMDAT	Modulation parameters
	LPMIDX	Modulation index
	LPMAOD	Modulation type
	NM	Number of modems
OPTION (Option Common)	IBI, ICXI, IGI, IGDI, IILI, ILCI, INDI, IUVI, IXI	Radiation options

Table 5 (Continued)

COMMON BLOCK	QUANTITY	DESCRIPTION
OPTION (Continued)	ID1, ID2, KALCD1, KALCD2, MD1, MD2	Dummy variables
	IFPE IFPLOT IFPP IFPS	Footprint output options
	IOUT IOUTE IOUTP	Output options
	KALCFP	Footprint calculation option
	KALCS	Satellite circuit calculation option
	LFDO LFIDO LFIN LFINT LFNO LFPLOT	File numbers
	MAMB MFREGI MNATN MWIND	Model options
ORIGIN (Origin Common)	IDAYSO	Day of the month
	IMONSO	Number of the month
	IYRSO	Number of the year in the 1900s (1974 is 74)
	PLATO	North latitude (radians)
	PLONO	East longitude (radians)
	SBARO	Sunspot number
	ZTO	Local zone time (decimal hours)
OUT (Output Common)	A	Attachment rate (s)
	ALPHAD	Electron-ion recombination coefficient ($cm^3\ s^{-1}$)
	ALPHAI	Ion-ion recombination coefficient ($cm^3\ s^{-1}$)
	D	Detachment rate (s)
PATH (Propagation Path Common)	LPSGOM	Satellite geometry option
	LPTGOM	Ground terminal geometry option
	NGT	Number of ground terminals
	NST	Number of satellites
	SORBP	Satellite orbit parameters

Table 5 (Continued)

COMMON BLOCK	QUANTITY	DESCRIPTION
PATH (Continued)	TORBP	Ground terminal motion parameters
	VSO	Earth centered vector to satellite (km)
	VSOV	Earth centered satellite velocity vector (km s^{-1})
	VTIO	Earth centered vector to ground terminal (km)
	VTO	Earth centered vector to ground terminal (km)
	VTOV	Earth centered ground terminal velocity vector (km s^{-1})
PHEN (Phenomenology Common)	PH1 . . . PH6	Temporary storage of quantities used in phenomenology models
PROP (Propagation Common)	DBSTOP	Maximum circuit signal loss (dB)
	DBSUM	Absorption due to ionization (dB)
	DBWVAO	Absorption due to water vapor and molecular oxygen (dB)
	DJAMS	Jammer noise density (W Hz^{-1})
	DNOISA	Ambient noise density (W Hz^{-1})
	DNOISE	Disturbed noise density (W Hz^{-1})
	DREGDB	D-region absorption (dB)
	ENFAR	Faraday rotation (radians)
	ENSUM	Electron density integral (cm^{-2})
	FREQ	Frequency (MHz)
	FZERO	Frequency selective bandwidth (Hz)
	FZEROR	Frequency selective bandwidth for reverse propagation direction (Hz)
	IXFBNM	Fireball index
	KDIR	Propagation direction flag
	KODE	Propagation effects code
	LJLINK	Link index
	LL	Circuit index
	LLINK	Propagation index
	LNINK	Noise index

Table 5 (Continued)

COMMON BLOCK	QUANTITY	DESCRIPTION
PROP (Continued)	MODE	Calculation option
	SMAX	Slant range between terminals (km)
	SPHI	rms phase fluctuation (radians)
	SPSI	rms angle of arrival fluctuations (radians)
	SPSIR	rms angle of arrival fluctuation for reverse propagation direction (radians)
	S4S	Scintillation strength index
	TAUZ	Decorrelation time (s)
	TAUZR	Decorrelation time for reverse propagation direction (s)
	VRO	Earth centered vector to receiver terminal (km)
	VROV	Earth centered receiver terminal velocity vector (km/s)
	VSP	Earth centered propagation direction vector (km)
	VXO	Earth centered vector to transmitter terminal (km)
	VXOV	Earth centered transmitter terminal velocity vector (km s^{-1})
	XVBAR	Relative velocity between striations and propagation path (km s^{-1})
RAY (Atmospheric Wind Common)	ARRAY	Air parcel location
REGINT (Region Propagation Common)	DBCODE	Absorption maximum
	DBDC	Dust cloud attenuation (dB)
	DLO	Minimum integration step size (km)
	DL2	Maximum integration step size (km)
	DSNOM	Nominal integration step size (km)
	ENCODE	Ionization maximum
	INDMP	Mandatory points flag
	KODEA	geometrical region code
	KODEG	Incremental absorption code
	KODEP	Ionization code
	NGAMMA	Number of low-altitude ionization sources
	NHOUT	Output flag
	NMP	Number of mandatory points
	NPBFRG	Number of F-region ionization bursts

Table 5 (Continued)

COMMON BLOCK	QUANTITY	DESCRIPTION
REGINT (Continued)	SGAMMA	Slant range from transmitter to point of maximum ionization due to low-altitude ionization source (km)
	SMP	Slant range from transmitter to mandatory points (km)
	SMPMAX	Maximum slant range to mandatory point (km)
	SMPMIN	Minimum slant range to mandatory point (km)
	SRBT	Slant range from transmitter to beta tube intersections (km)
	SRFB	Slant range from transmitter to fireball intersections (km)
RGEOM (Geometry Common)	RDVEC	Position vector (km)
	SPHAT	Path direction vector (km)
	XMHAT	Magnetic pole direction vector (km)
SIGCOM (Circuit Common)	BWL	Noise bandwidth (MHz)
	DJAMSL	Jammer noise density (W Hz^{-1})
	DNOSA	Ambient noise density (W Hz^{-1})
	DNOSD	Disturbed noise density (W Hz^{-1})
	ENTOT	Electron density integral (cm^{-2})
	FREQGH	Frequency (GHz)
	FZEROL	Frequency selective bandwidth (Hz)
	IMOD	Modulation index
	ISIGPR	Signal processing flag
	KALSN	Signal-to-noise ratio flag
	NCIR	Circuit index
	SIGFS	Ambient signal strength (W)
	SIGND	Disturbed signal strength (W)
	SPHIL	rms phase fluctuations (radians)
	SPSIL	rms angle of arrival fluctuation (radians)
	S4L	Scintillation strength index
	TAUZL	Decorrelation time (s)
SOURCE (Heavy Particle Ionization Command)	LPRT	Ionization flag
SPEC (Fireball Ionization Common)	BAL	Number of aluminum atoms
	BN	Number of nitrogen atoms
	BO	Number of oxygen atoms

Table 5 (Continued)

COMMON BLOCK	QUANTITY	DESCRIPTION
SPEC (Continued)	BU	Number of uranium atoms
	CALO . . . CUP	Species concentration (cm^{-3})
	EC1 . . . EC23	Equilibrium constants
	SAL . . . SU	Normalized values for BAL to BU
SPECEF (F-region Ionization Common)	CO2 . . . O2	Species concentrations (cm^{-3})
	PRES	Pressure (dynes cm^{-2})
	QAMB	Ion-pair production rate (cm^{-3} s^{-1})
	RHO	Air density (gm cm^{-3})
	TEL	Electron temperature (K)
	TVIBN2	Molecular nitrogen vibrational temperature (K)
	T1F, T2F	Time at beginning and end of deionization time step (s)
SPECQ (F-region Ionization Common)	AO2 . . . COP	Species concentrations (cm^{-3})
	TE	Electron temperature (K)
	TG	Gas temperature (K)
	TV	Molecular nitrogen vibrational temperature (K)
SPECW (Device Spectrum Common)	FEDGD	Prompt gamma yield fraction
	FEDHD	Hydro yield fraction
	FEDND	Neutron yield fraction
	FEDXD	X-ray yield fraction

Table 5 (Continued)

COMMON BLOCK	QUANTITY	DESCRIPTION
SPECW (Continued)	FFD	Fission fraction
	FMALD	Fraction of weapon mass in aluminum
	FMURD	Fraction of weapon mass to uranium
	SPECGD	Gamma ray spectrum specification
	SPECND	Neutron spectrum specification
	SPECXD	X-ray spectrum specification
	WMASSD	Weapon mass (gm)
SPEEDS (Atmospheric Wind Common)	UVW	Air velocity ($m\ s^{-1}$)
SSYS (Satellite Systems Common)	ISAD	Antenna direction option
	ISASL	Side lobe option
	ISATYP	Antenna specification option
	ISMOD	Not used
	ISRN	Input noise specification option
	ISTMOD	Modulation index
	NSANT	Number of antennas
	NSRCV	Number of receivers
	NSXMT	Number of transmitters
	SADAT	Antenna quantities
	SASLG	Side lobe gain relation to main beam (dB)
	SRBW	Receiver noise bandwidth (MHz)
	SRNTEM	Noise temperature (K)
	STFREQ	Transmitter frequency (MHz)
	STPWR	Transmitter power (W)
	VSAD	Earth centered antenna direction vector (km)
STRIIN (Scintillation Common)	CTHETZ	Colatitude of point (cos)
	DNESB	Electron density variance (cm^{-6})
	DSMX	Maximum slant range of ionization from transmitter (km)
	EN	Power law exponent
	FREQH	Frequency (Hz)
	ISTOP	Striation velocity flag
	LINK	Propagation path index
	RP	Radius from earth center to field point (km)
	RTH	Equivalent radius (km)

Table 5 (Continued)

COMMON BLOCK	QUANTITY	DESCRIPTION
STRIIN (Continued)	ST	Slant range between transmitter and receiver (km)
	SX	Slant range from transmitter to field point (km)
	VBHAT	Unit vector (earth centered) normal to magnetic field (km)
	VSPHAT	Earth centered propagation direction vector (km)
	VV1	Earth centered velocity vector for transmitter (km s^{-1})
	VV2	Earth centered velocity vector for fireball (km s^{-1})
	VV3	Earth Centered velocity vector for receiver (km s^{-1})
	XLI	Inner scale length (km)
	XLO	Outer scale length (km)
TIME (Origin Common)	CHI	Zenith angle of the sun (radians)
	FST	Fractional summer - one on 1 July and zero on 1 January in northern hemisphere and reversed in southern hemisphere
	FYR	Fractional season year - zero on 1 January in northern hemisphere and zero on 1 July in southern hemisphere
	GAT	Greenwich apparent time (decimal hours)
	HL	Local apparent time (decimal hours)
	IDAYS	Day of the month in Greenwich time zone
	IDORN	Time of day (+ 1 day, - 1 night)
	IMONS	Number of the month in the Greenwich time zone
	IYRS	Number of the year in the 1900s (1974 is 74)
	PLAT	North latitude of origin (radians)
	PLON	East longitude of origin (radians)
	SBAR	Average 10.7 - cm solar flux (1.0×10^{-22} W/m^2 Hz))
	UT	Universal time corresponding to the zone time ZT (decimal hours)
	ZT	Zone time for the 15-degree longitude interval containing PLON (decimal hours)
TRACE (Geometry Common)	AHMIN	Altitude of lowest air parcel in apogee fireball (km)

Table 5 (Continued)

COMMON BLOCK	QUANTITY	DESCRIPTION
TRACE (Continued)	ALT	Altitude of air parcel in apogee fireball (km)
	CONJ	Conjugate flag
	DELH	Altitude separation between air parcels in apogee fireball (km)
	DELV	Velocity change between air parcels in apogee fireball (km s^{-1})
	HALT	Altitude of air parcel at time T
	RAPOG	Radius from earth's center to air parcel apogee altitude (km)
	T	Calculation time (s)
	TAC	Fireball apogee time (s)
	TPAP	Time when air parcel reaches apogee (s)
	TPHS	Time when air parcel reaches stopping altitude (s)
	VHBOT	Velocity of lowest air parcel in apogee fireball at apogee (km s^{-1})
	XJP	Air parcel index
	XLT	Distance from earth's surface to air parcel at time T measured along magnetic field line (km)
TSTEF (Heavy Particle Ionization Common)	BUF2(1)	Change in electron concentration (cm^{-3})
	BUF2(2)	Change in $N(^4S)$ concentration (cm^{-3})
	BUF2(3)	Change in $N(^2D)$ concentration (cm^{-3})
	BUF2(4)	Change in O concentration (cm^{-3})
	BUF2(5)	Change in N_2 concentration (cm^{-3})
	BUF2(6)	Change in O_2 concentration (cm^{-3})
	BUF2(7)	Change in N^+ concentration (cm^{-3})
	BUF2(8)	Change in O^+ concentration (cm^{-3})
	BUF2(9)	Change in O excitation energy and electron thermal energy per electron (eV/electron)
	BUF2(11)	Change in N_2^+ concentration (cm^{-3})
	BUF2(12)	Change in O_2^+ concentration (cm^{-3})
	DAIXX	X-ray energy deposited (erg gm^{-1})
	FLUX	Fluence of the L*th* UV group (erg gm^{-1})
TSYS (Ground Terminal Systems Common)	FREQ02	Frequency (MHz)
	I02MOD	Modulation index
	ITASL	Side lobe option
	ITATYP	Antenna specification flux

Table 5 (Continued)

COMMON BLOCK	QUANTITY	DESCRIPTION
TSYS (Continued)	ITRN	Input noise specification option
	ITTMOD	Modulation index
	KALCSN	Signal-to-noise calculation option
	NTANT	Number of antennas
	NTRCV	Number of receivers
	NTXMT	Number of transmitters
	STNO2	Signal to noise ratio (dB)
	TADAT	Antenna quantities
	TASLG	Side lobe gain relative to main beam (dB)
	TRBW	Receiver noise bandwidth (MHz)
	TRNTEM	Noise temperature (K)
	TTFREQ	Transmitter frequency (MHz)
	TTPWR	Transmitter power (W)
WEDEPO (Heavy Particle Ionization Common)	ALPHA1	Elastic portion of the heavy-particle stopping cross section for O on N (eV cm^2 $atom^{-1}$)
	ALPHA2	Elastic portion of the heavy-particle stopping cross section for Al on N (eV cm^2 $atom^{-1}$)
	AM	Mass of mass-15 particle
	BETA1	Coefficient of the square root of the energy in the inelastic portion of the heavy-particle stopping cross-section for O on N ($\sqrt{eV}$ cm^2 $atom^{-1}$)
	BETA2	Coefficient of the square root of the energy in the inelastic portion of the heavy-particle stopping cross-section for Al on N ($\sqrt{eV}$ cm^2 $atom^{-1}$)
	CMTKM	cm to km (km cm^{-1})
	EMTERG	MT to ergs (ergs MT^{-1})
	EMTTEV	MT to eV (eV MT^{-1})
	EPSLN	eV to ergs (ergs eV^{-1})
	IWK	Number of energy groups used in approximating the heavy particle energy deposition
	SM	Mass of mass-15 particle
WOG (Gamma Deposition Common)	PMG	Penetrated air mass array for which energy deposition parameters precomputed (gm cm^{-2})
	UBARGP	Prompt gamma ray energy deposition coefficient (cm^2 gm^{-1})
	UBARGD	Delayed gamma ray energy deposition coefficient (cm^2 gm^{-1})

Table 5 (Continued)

COMMON BLOCK	QUANTITY	DESCRIPTION
WON (Neutron Deposition Common)	CHB	Burst point nonuniform air correction factor
	CHD	Deposition point nonuniform air correction factor
	ENL	Mean free path array
	EXPQNE	Neutron elastic scatter energy deposition coefficient (cm^2 gm^{-1})
	PMN	Penetrated air mass array for which energy deposition parameters precomputed (gm cm^{-2})
	SIGMAN	Mean total cross section (cm^2 gm^{-1})
	UBARNC	Neutron capture energy deposition coefficient (cm^2 gm^{-1})
	UBARNP	Prompt neutron energy deposition coefficient (cm^2 gm^{-1})
WOX (X-ray Deposition Common)	FCONTX	X-ray energy containment within mass depth PMXBAR
	PMXBAR	Normalizing air mass penetrated (gm cm^{-2})
	PMXR	Normalized penetrated air mass array for which energy deposition parameters precomputed (gm cm^{-2})
	UBARX	X-ray energy deposition coefficient (cm^2 gm^{-1})
WRATE (D-region Chemistry Common)	XK1 . . . XK243	Reaction rate coefficients
	A1 . . . A8	Initial ionization and dissociation parameters
WRATEH (D-region Chemistry Common)	XK27 . . . XK50	Reaction rate coefficients
WSTOR (Atmospheric Wind Common)	IDAY	Day of month
	IMON	Number of month
	IYR	Number of the year in the 1900s (1974 is 74)
	JALT	Altitude index
	TIML	Local time (decimal hours)

Table 5 (Continued)

COMMON BLOCK	QUANTITY	DESCRIPTION
WTOR (Continued)	U	East-west wind velocity (ms^{-1})
	V	North-south wind velocity (ms^{-1})
	WW	Vertical wind velocity (ms^{-1})
ZHTEMP (Atmospheric Common)	TZH	Temperature array (K)

CONTROL ROUTINE

This routine is the main control routine for the WESCOM code. A simplified flow chart for the routine is shown in Figure 1.

The problem loop refers to a given input specification and the problem number is changed each time control is transferred to the input module and new input data obtained.

After input data are obtained, routines ATMOSI, MAGFIT, and IONOSI are called to initialize the ambient atmosphere and magnetic field models. Next, a loop over calculation times is started and routine PHENOM is called to obtain the fireball and debris region geometry and intrinsic properties. The location of the satellites(s) at the calculation time is found by calling routine SORBIT.

Next, a test is made to see if circuit or footprint calculations have been requested and either routine SATC or FOOTPC is called. When the calculation time loop is completed control is returned to routine INPUT to obtain the next problem case.

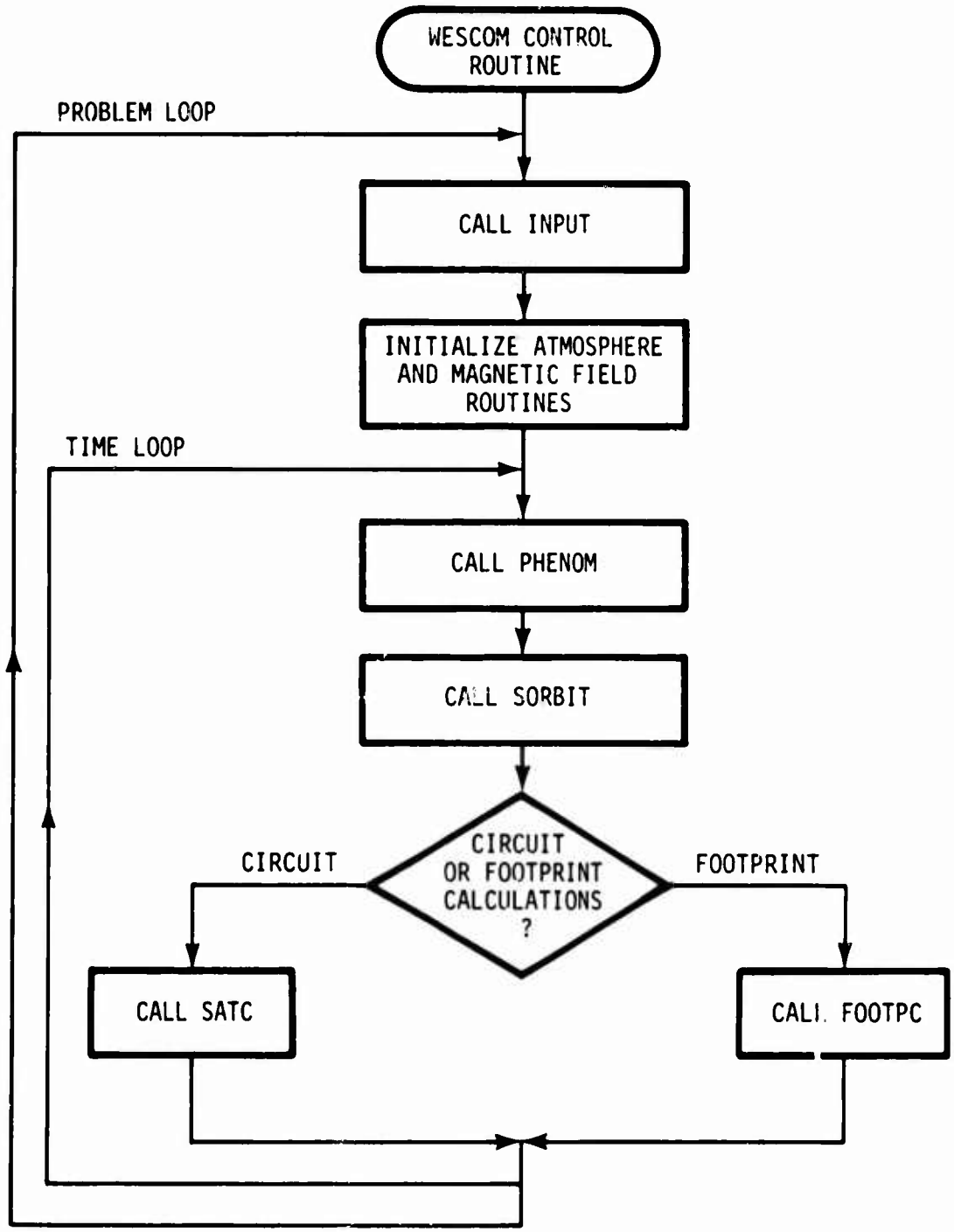

Figure 1. Flowchart for WESCOM control routine.

SUBROUTINE AMBABS

This routine determines resonance absorption due to molecular oxygen and water vapor along a specified propagation path for a specified frequency.

The absorption is determined by integrating the incremental absorption computed at points along the path. The integration is started at the lowest point on the path and integration step sizes in path length corresponding to 3-km altitude steps are used (but not larger than 20-km path length step). If the lowest point on the path is between the transmitter and receiver terminals, the integration between the lowest point and receiver is computed first and then the integration between the lowest point and the transmitter determined. The integration in a given direction is stopped when either the incremental absorption goes to zero or the product of the incremental absorption and the remaining path length becomes less than 0.1 dB.

Routine GWAT is called to obtain the incremental absorption due to water vapor and routine GOX is called to obtain the incremental absorption due to molecular oxygen. Inputs to these routines include the atmospheric pressure, temperature, and water vapor concentration. These quantities are obtained at each calculation point from routine ATMOSU.

SUBROUTINE ANTND

This routine is the driver for the antenna noise temperature module. Given a receiver location, it obtains the ambient noise density (W Hz^{-1}) and the noise density due to thermal radiation from each fireball visble to the receiver. A simplified flowchart for the routine is shown in Figure 2.

After determining geometry quantities associated with the receiver location, the antenna and receiver characteristics are determined. Then the ambient noise density is determined if the receiver noise characteristics are given as input. If the system noise characteristics are given, the ambient noise is assumed to be included in the input specification.

Next, a fireball loop is started and a normalized integral over the antenna pattern is determined by calling routine NINT. Then, an index is set up which ranks the fireballs according to the normalized integral, in descending order. This index is used in the next fireball loop to minimize the number of thermal emission calculations.

A new fireball loop is begun to sum the contributions from each fireball to the total antenna noise temperature, TASUM. Each fireball is checked to see if the unattenuated contribution assuming a maximum fireball temperature is at least five percent of the current value of the antenna noise temperature. If not, it is skipped. If it is, the actual thermal emission from the fireball is determined by calling routine FBTINT. After calling routine FBTINT the fireball contribution is checked again and further calculations skipped if its contribution is less than five percent. If the fireball thermal radiation is still significant the beta sheath absorption is determined for low-altitude fireballs by calling routine BETAS and the path absorption for both low- and high-altitude fireballs estimated from the D-region absorption determined for the path between the transmitter and receiver. This absorption is generally a reasonable estimate of the absorption outside the fireball since only fireballs in the main beam will produce significant thermal noise. However, this approximation can be tested by exercising the noise test option as part of the input specification. When this is done the absorption between the fireball edge and the receiver antenna is found by calling routine PROPEN.

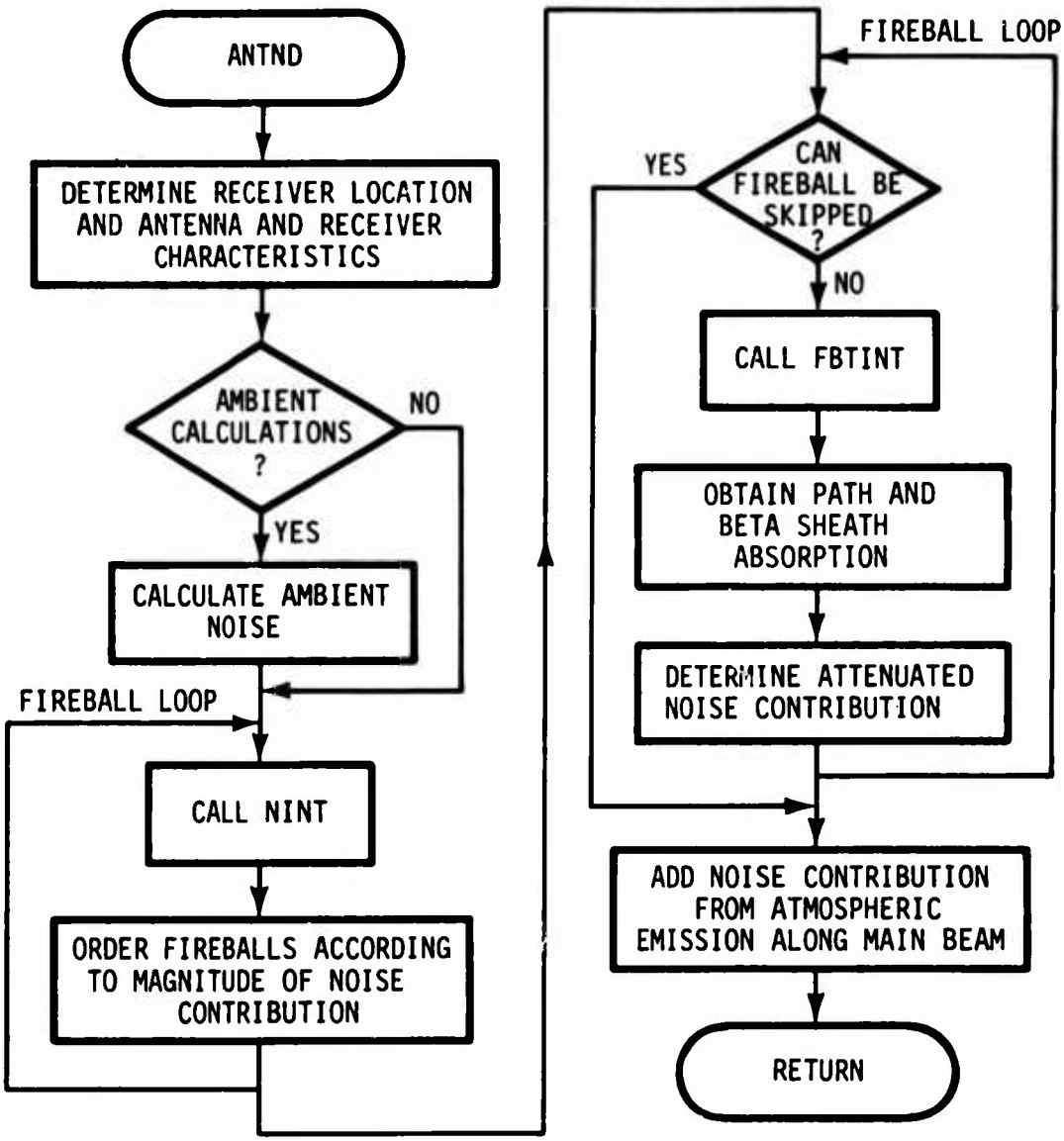

Figure 2. Flowchart for subroutine ANTND.

The final calculation in routine ANTND is the noise contribution produced by emissions along the main path. This is computed from the absorption along the path between transmitter and receiver.

SUBROUTINE ARRLIM

This routine determines the debris region location and size from debris marker particles that have been displaced from the debris stabilization location by atmospheric winds.

The location of the debris center is found by averaging the locations of the marker particles. The minimum and maximum latitude and east-longitude positions are saved for use in determining the debris radius.

The debris radius is determined as the average of the north-south and east-west dimensions plus the radius at debris stabilization time. The debris characteristic radius and distribution parameter are found for use in beta particle ionization calculations.

SUBROUTINE ATMOSF

This routine computes properties of the natural or heaved atmosphere at points above 100 km. The routine is a modified version of routine ATMOSF developed for the WOE code. A simplified flow chart for the routine is shown in Figure 3.

If there are no bursts prior to the calculation time, the properties of the air at the specified altitude are the same as in the natural atmosphere and are obtained from routine ATMOSU.

If one or more bursts prior to the calculation time can cause heave (bursts above 120 km) and if the operational mode discussed below is equal to 1, wake heave parameters are determined for each fireball. The wake heave causes the air motion below the fireball to be consistent with the air motion in the fireball. A loop over bursts is made and the energy deposited at 110 km beneath the specified point is calculated for each burst.

If any of the bursts produce heave the Lagrangian coordinates of the bottom and top of each fireball producing wake heave are found and then routine HEAVE is called. Routine HEAVE determines the location of the air that is at the specified altitude at the calculation time and at the time of each prior burst (whether it is a heave burst or not). The heaved air is assumed to move along a vertical path. The HEAVE routine also provides the ratio of the density at each altitude to the density at the initial altitude (altitude at time of first burst) and the vertical mass scale height. Routine ATMOSU is then called to determine the density, pressure, temperature, neutral particle concentrations, and mean molecular weight at the initial altitude.

There are four operational modes for routine ATMOSF determined by the input parameter MODE. For MODE = 1, an output array is prepared giving the altitude, density or density ratio, and density scale height at the time of each burst and at the calculation time. The mass density (gm/cm^3) is stored in the array for the initial altitude and the density ratio returned by the HEAVE routine is stored for other altitudes. When the time interval between bursts or between the last burst and the calculation time is large, the altitude and density ratio at intermediate times are found for use in interpolation calculations.

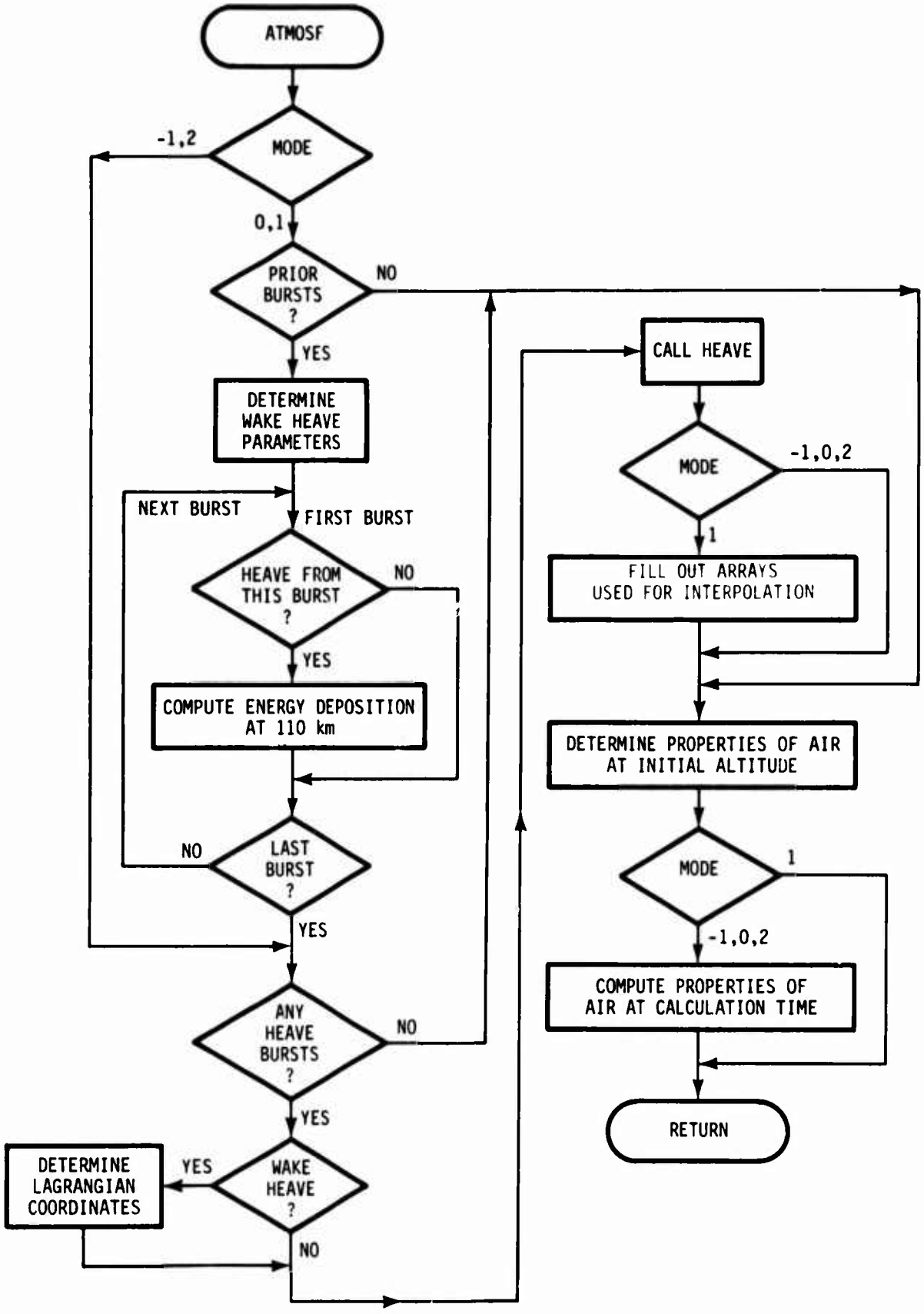

Figure 3. Flowchart for subroutine ATMOSF.

For MODE = 0 output quantities are given for the final altitude only. The gas temperature and pressure are computed from

$$T(h_f) = T(h_i) \left(\frac{\rho(h_f)}{\rho(h_i)} \right)^{\gamma-1}$$

and

$$P = P(h_i) \left(\frac{\rho(h_f)}{\rho(h_i)} \right)^{\gamma}$$

where the subscripts i and f refer to the initial and final altitude respectively and γ is the gas constant. The third operational mode (MODE = -1) is used when calls to ATMOSF are made for the same vertical column of air and the same calculation time as a previous call, but at a different final altitude. For MODE = -1, the energy deposition matrix needed as input to the HEAVE routine is not recalculated. The output for MODE = -1 is the same as for MODE = 0.

The final operational mode (MODE = 2) is used when calls to ATMOSF are made for the same air parcel as a previous call but at an earlier time. The output is the same as for MODE = 0 and also includes the altitude of the air parcel.

SUBROUTINE ATMOSI

This routine determines properties of the atmosphere as a function of altitude at a specified location and time for use by routine ATMOSU. The routine is a modified version of routines ATMOSU and SPECMIN developed for ROSCOE. The major modifications include combining the initialization computations into a single separate routine and the use of an expontential formulation described by Booker* for fitting atmospheric properties as a function of altitude. The formulation provides continuous derivatives and replaces the high order polynomials used in the models developed for ROSCOE.

The first step in the atmosphere initialization process is the determination of solar quantities needed to evaluate the solar-flux dependent Fourier coefficients used in computing the temperature gradient at the lower boundary (120 km) of the high-altitude model and the exospheric temperature. The required solar quantities are obtained by calls to routine JULIAN, SOLCYC, SOLORB, and SOLZEN (a call to routine ZTTOUT used in the ROSCOE model to determine the date and time at Greenwich is made prior to calling routine ATMOSI).

Next, routine TEMPZH is called to obtain the atmospheric temperature profile at the location and season specified as input. This temperature profile is used to determine the molecular scale temperature used in evaluating atmospheric intrinsic properties. Atmospheric properties at the boundary of the low- and high-altitude models are determined and the solar quantities are used to evaluate the high-altitude temperature model.

The remaining computations in routine ATMOSI are calculations of minor neutral species concentrations at the altitude matrix given by ALTKM in the labeled common block ALTODN. This altitude matrix is different than the one (AHT) used to evaluate the temperature and water vapor profiles. The calculations are similar to those given in routine SPECMIN developed for ROSCOE except that the

---

*Booker, H.G., "Fitting of Multi-Region Ionospheric Profiles of Electron Density by a Single Analytic Function of Height," *J. Atmos. Phys.*, vol 39, pp 619-123, 1977.

exponential formulation is used to obtain integrals and derivatives and interpolation of altitude dependent quantities and the species concentrations at the matrix altitude values are the output that will be used by routine ATMOSU.

SUBROUTINE ATMOSU

This routine determines properties of the atmosphere at a specified time and point in space. The routine is a modified version of routine ATMOSU developed for ROSCOE.

The routine uses data prepared by routine ATMOSI (during an initialization call) to determine atmospheric quantities at a specified altitude. For altitudes below 120 km a low-altitude model is used to determine the intrinsic properties and major species concentrations. The basic parameter in the mode is g/T_M, the ratio of the acceleration of gravity to the molecular scale temperature determined in routine ATMOSI.

For altitudes above 120 km a high-altitude model is used that determines species concentrations and intrinsic properties in terms of the temperature gradient at 120 km (TAU), the exospheric temperature (TIF) and the species concentrations at the lower boundary determined in routine ATMOSI.

After the intrinsic properties and major species concentrations are determined, the minor species concentrations are evaluated if the calculation flag JJ is greater than 2. The minor species concentrations are found by calling routine BKRIAD to interpolate the values determined in routine ATMOSI.

SUBROUTINE BALFIT

This routine fits a fourth order curve to the ballistic equation solution for use in determining the position of an ionized air parcel on a geomagnetic field line.

The fit is used for locations between two points on the field line (ℓ_o and ℓ_1) given as input. First, the velocity and acceleration of the air parcel at ℓ_1 and the time for the parcel to reach ℓ_1 are determined. Then coefficients C and D are found for use in the following equation for parcel position versus time between ℓ_o and ℓ_1.

$$\ell = \ell_o + v_o(t-t_o) + \frac{\dot{v}_o}{2}(t-t_o)^2$$

$$+ C(t-t_o)^3 + D(t-t_o)^4$$

where ℓ is the distance along the geomagnetic field line from the earth's surface to the air parcel and the time t must be between t_o and t_1 (time for the parcel to reach ℓ_1).

SUBROUTINE BETAS

This routine computes the one-way path absorption and the back-scatter coefficient for normal incidence on the beta sheath ionization region. The routine is a modified version of routine BETAS developed for the WEPH code.

The calculations are for a sharply bounded fireball/debris geometry where it is assumed that the debris is within the fireball and that the air temperature and density outside the fireball have ambient values. Only the path absorption calculation is used in the WESCOM code.

Beta sheath ionization relations are used to compute the ion-pair production rate, q, at two points within the beta sheath: a point at the fireball surface and a point outside the surface where the ion-pair production rate is reduced by about a factor of e^{-2}. For each of these points (assumed to be at the same altitude) routine CHEMDQ is called to obtain the electron density and electron-neutral collision frequency. Then the electron density within the sheath is approximated with an exponential function,

$$N_e = N_{ei}\, e^{-\frac{X}{H}}$$

where

N_{ei} = electron density at fireball surface

X = distance from fireball surface

H = ionization scale height determined from electron density calculations at two points.

The one-way path absorption is found from

$$A_{BS} = \int_0^{\infty} \frac{4.6 \times 10^4\, N_e \nu}{\omega^2 + \nu^2}\, dX \quad .$$

Substituting for N_e

$$A_{BS} = \frac{4.6 \times 10^4 \, N_{ei} H\nu}{\omega^2 + \nu^2} \text{ dB}$$

where

ω = wave frequency (radians s^{-1})

ν = collision frequency (s^{-1})

H = scale height (km).

SUBROUTINE BTRACE

This routine determines the motion of an ionized air parcel along a geomagnetic field line given the location and velocity of the air parcel at an initial time.

The procedure used is to divide the field line into segments and to calculate the time when the parcel reaches the end of each segment and the parcel velocity and acceleration at these times. The parcel motion is determined by calling routine BALFIT which uses the parcel properties at one point to determine the parcel location and properties at the end of a time step.

After the parcel properties are found at equal intervals along the field line (including the portion between the starting point and the earth) a 4th order interpolation procedure is used to determine the location of the parcel at a specified input time. If the parcel crosses the equator a flag (CONJ) is set and the time for the parcel to reach the equator is given as output in addition to the time for the parcel to reach the earth's surface.

SUBROUTINE CHEMD

This routine is the driver routine for the D-region chemistry module. Th routine is a modified version of routine CHEMD developed for ROSCOE. Figure 4 shows a simplified flow diagram for the routine.

Inputs to the routine are the location of the D-region point at which ionization is to be calculated and the calculation time. Outputs from the routine are electron density, total positive ion density, and collision frequencies.

Subroutines ATMOSU and IONOSU are called to find the ambient air properties at h_c. Subroutine DRATE is called to determine the values of the reaction rate coefficients. The initial values of the neutral species are set equal to the ambient values at h_c.

Next, routine DEDEP is called to determine the energy deposited per gram at h_c and t_c by delayed radiation and the ion-pair production rate is computed by multiplying by 1.79×10^{10} times the density and adding the ambient ion-pair production rate. Routine CMDEDT is called to determine which of the previous bursts must be considered as prompt energy sources. For each burst to be considered the prompt energy deposited per gram and the photodissociation rate for ozone are stored.

Next, a time loop over each burst that must be considered plus the calculation time is established and calculations are started for the first time interval. The time interval is between t_1 and t_2 where t_1 is the time of the first burst that must be considered and t_2 is either the time of the next burst that must be considered or the calculation time (t_c). Routine INITAL determines the change in neutral species caused by the burst at the end of Phase 2. Routine PHOTOR determines the photodissociation and photodetachment rates caused by thermal radiation from previous bursts at the end of the time interval (t_2). Routine SPECDP determines the neutral species concentrations at t_2 and Routine DTNEP determines the electron and total positive ion densities at t_2.

After the last time interval ($t_2 = t_c$) routines SPECDQ and DTNEQ are called to determine the effect of delayed radiation on the neutral and ion species concentrations. The electron and positive ion densities returned by CHEMD are the larger of those due to prompt and delayed radiation.

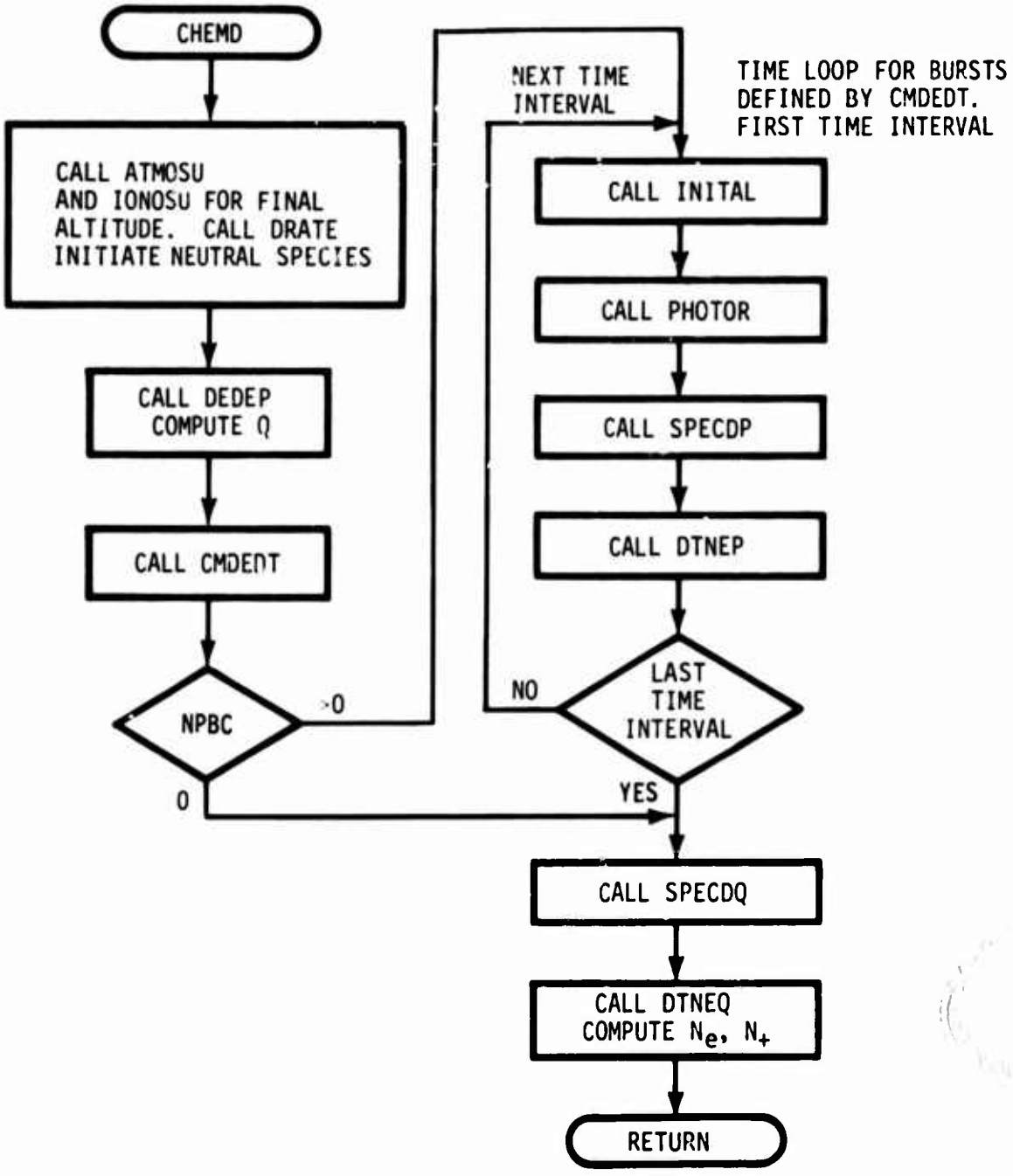

Figure 4. Flowchart for subroutine CHEMD.

ROUTINE CHEMDQ

This routine is a driver routine to determine ionization at a specified D-region altitude. The ionization determined is the same as would be obtained with routine CHEMD for a steady-state ionization source if the effect of prompt energy deposition on the neutral species is neglected. If the ionization source is not specified, an ambient value is determined and used to calculate the ionization.

First, routine ATMOSU is called to obtain the ambient neutral species at the altitude of interest and routine DRATE is called to determine the values of the reaction rate coefficients. Then, if the input value of the ion-pair production rate (Q) is zero, routine IONOSU is called to obtain the ambient ion-pair production rate.

Next, routine SPECDQ is called to determine the change in neutral species and routine DTNEQ is called to determine the electron and ion densities due to the ion-pair production rate. The final calculations are for the electron and ion collision frequencies.

SUBROUTINE CHEMEF

This routine computes E- and F-region chemistry for times after the prompt energy deposition phase has been completed. The routine is a modified version of routine CHEMEF developed for ROSCOE.

Input and output is provided through the labeled common block SPECEF. Common block SPECEF contains the initial and final times, t_1 and t_2, for the specified time interval, and a subscripted variable (dimension 2) for each chemical parameter. The first array location for each variable contains the value at time t_1, and the second location will contain the updated value at time t_2.

The operations performed by CHEMEF are sequential, with very little branching and no looping or iteration. The operations are as follows:

1. Compute the heavy-particle temperature at times t_1 and t_2.
2. If the electron temperature TEL(1) differs from the excitation temperature TV1BN2(1), compute the total excitation energy density and equilibrate it to define a new effective excitation energy. Routine TEXK computes the new temperature.
3. Compute the average volume expansion parameter and mean reaction rate coefficients. The rate coefficients at each temperature are obtained from routine RATE.
4. Call routine CHMION to compute the change in species due to the ion reactions.
5. Compute the mean value of each species due to the ion chemistry.
6. Compute change in species due neutral reactions. Routine GNNO is used to determine changes due to reactions of atomic nitrogen.
7. Compute the change in pressure and heavy particle temperature due to the chemical energy release.
8. Compute the change in excitation energy density and the new equilibration temperature. Routine TEXK computes the new temperature. Set the electron temperature equal to the excitation temperature.

ROUTINE CHEMHR

This subroutine computes the electron and total positive ion densities at a specified point within a heated region overlay for a specified evaluation time. This routine is a modified version of routine CHEMHR developed for ROSCOE. Figure 5 shows a simplified flow diagram for the routine.

First, the fraction of the ions that remain atomic (f_A), the molecular ion production rate (q_M), and the atomic ion production rate (q_A) are computed. If $f_A > 0.99$ and the point of interest is within the fireball the ionization sources considered are nonequilibrium air ionization and the atomic ion production rate. If $f_A > 0.99$ and the point of interest is outside the fireball, only the ionization due to the molecular ion production rate is considered and a simple recombination loss equation is used to determine the electron and positive ion density.

If $f_A \leq 0.99$ the thermal equilibrium properties of air and metal species are determined by calling routine EQLAIR and EQLMTL (see Figure 6). An iteration loop is used to insure species conservation. After each call to routine EQLAIR the O_2 density is modified to account for reactions with nitrogen.

Next, effective reaction rate coefficients are computed (see Figure 7). In computing the reaction rate coefficients, the equilibrium values of the species are used if the temperature is greater than T_{EN} (approximately 2000 K). If the temperature is less than T_{EN}, and $T_{FI} > T_{EN}$, nonequilibrium values for NO, NO_2, O, and O_3 are determined. If $T_{FI} \leq T_{EN}$, ambient values for NO and NO_2 are used and the O and O_3 are assumed to be equal to the thermal equilibrium values. A partial correction to the neutral species is made to account for effects of delayed radiation. For points outside the fireball the effect of photodetachment due to fireball thermal radiation is determined by calling routine PHOTOR.

After the effective reaction rate coefficients are determined the nonequilibrium metal ionization and the equilibrium ionization due to the molecular ion-pair production rate are evaluated. Then the nonequilibrium air

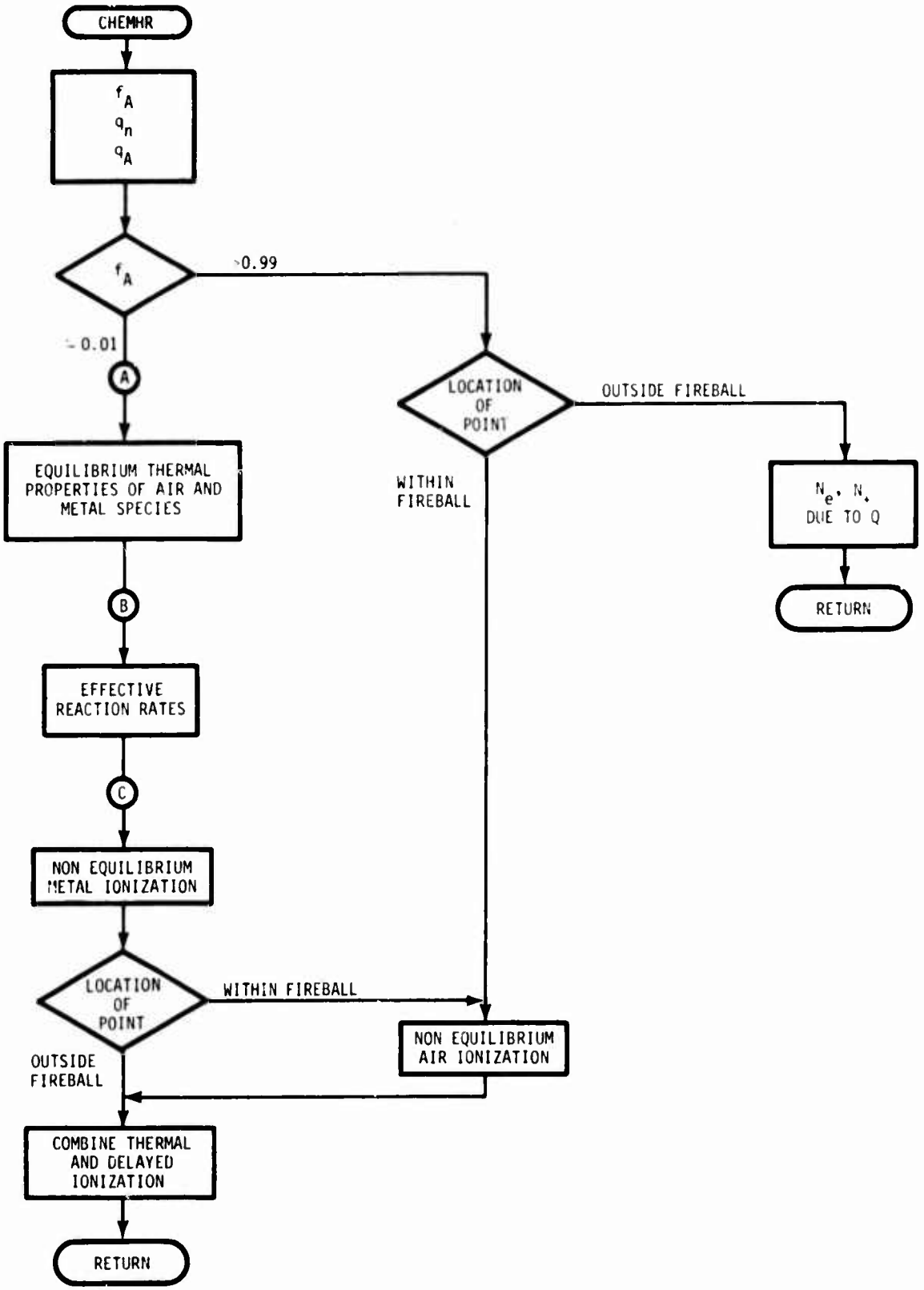

Figure 5. Flowchart for subroutine CHEMHR.

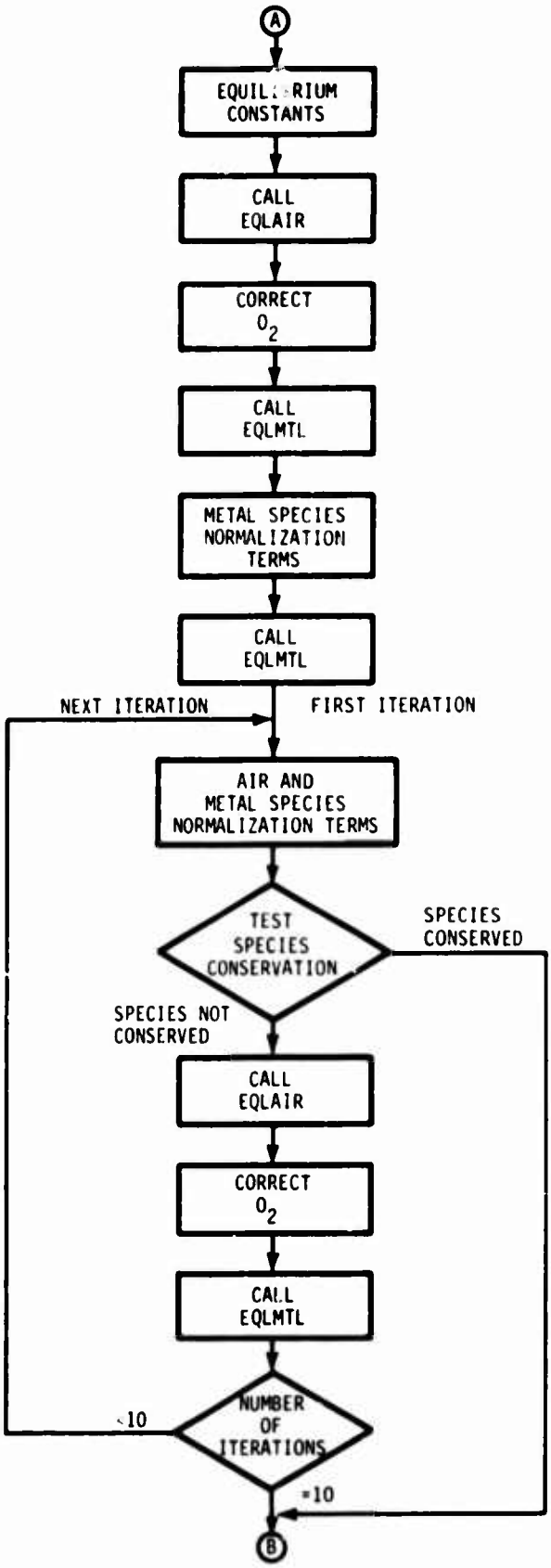

Figure 6. Detail for equilibrium thermal properties of air and metal species block in Figure 5.

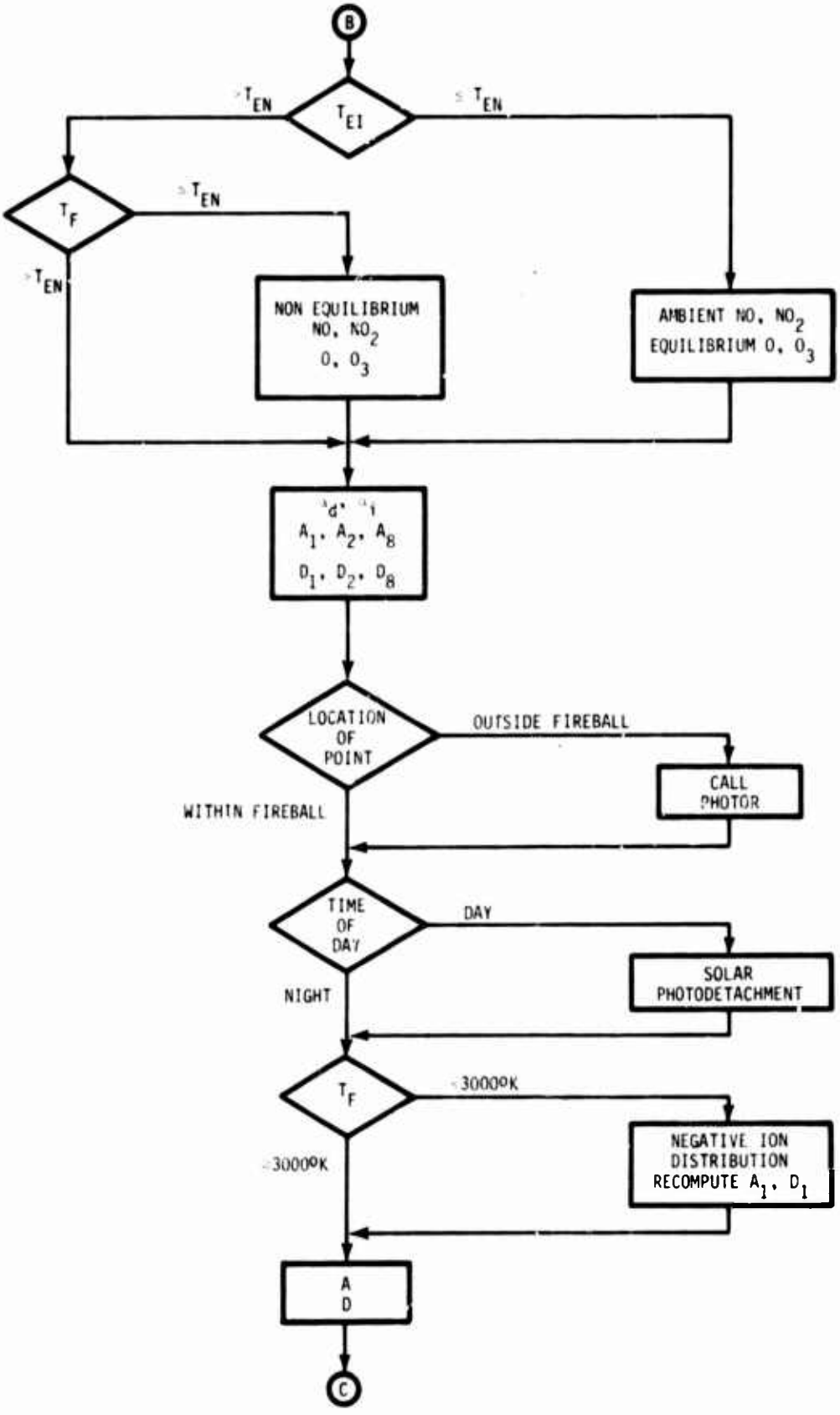

Figure 7. Detail for effective reaction rate block in Figure 5.

ionization and the ionization due to the atomic ion production rate are determined.

The electron density returned by routine CHEMHR is the sum of that due to thermal ionization and that due to delayed radiation.

SUBROUTINE CHMION

This routine computes the change in species concentrations due to E- and F-region ion chemistry. The routine is essentially the same as routine CHMION developed for ROSCOE.

Initial values for the species concentrations are obtained from labeled common block SPECEF and mean reaction rate coefficients and the ion production rate are obtained from labeled common block CHEMAN. The new species concentrations at the time t_2 will be returned through SPECEF common (under variable subscript 2). The energy released, DELEV, is returned to CHEMEF through CHEMAN common.

Mean ion loss rates due to each reaction are computed accounting only for volume expansion. A check is made to determine if the N_2 or O_2 could be significantly depleted during the time interval. If so, improved mean values for N_2 and O_2 are determined. Next, if the loss rate due to reaction with NO is within 10 percent of the total N^+ loss rate, an improved mean value of NO is computed.

In final preparation for the ion solutions the total ion production rate is proportioned into N^+, O^+, and M^+ production rates. The N^+ and O^+ solutions are computed by routine ANLYT2. The transient solution for M^+ is computed by routine RICATT. This is then combined with the equilibrium solution for M^+. Finally, the change in neutral species concentrations is computed and the energy release determined.

SUBROUTINE CMDEDT

This routine edits the bursts to form a list for use in D-region chemistry calculations. The routine is essentially the same as routine CMDEDT developed for ROSCOE. The bursts chosen are those which affect neutral species or ionization due to prompt energy deposition or photodissociation of O_3. For each burst the prompt energy deposited and the photodissociation rate for O_3 are computed and stored. A flow diagram for routine CMDEDT is shown in Figure 8.

A burst is included in the burst list if the prompt energy deposition or photodissociation of O_3 changes the neutral species sufficiently to affect the reaction rate coefficients used for equilibrium ionization calculations. The equilibrium electron density can be approximated by

$$N_e = \sqrt{\frac{q}{\alpha}} \frac{D + \sqrt{q\alpha}}{A + D + \sqrt{q\alpha}}$$

where D, A, and α are effective reaction rates. Tests are made to see if the production of O, N, and $O_2(^1\Delta)$ results in a detachment rate larger than

$$0.1(D + \sqrt{q\alpha})$$

and whether the production of O_3 and O result in an attachment rate larger than D. In performing the tests ambient values of the neutral species are used to compute A and D. Since the detachment rate, D, depends on the composition of negative ions, a fit to the ratio of O_2^- to total negative ion density is used and only detachment from O_2^- considered. Changes in the neutral species can also affect the effective recombination coefficient but by using an effective value which is small bursts affecting α will be included in the bursts affecting the detachment rate.

Routines EDEPD and PHOTOD are called to determine the prompt energy deposition and the photodissociation rate for O_3 due to thermal radiation. Approximate relations are used to estimate the amount of O, $O_2(^1\Delta)$, and N produced by the burst and the decay of these species between the burst and

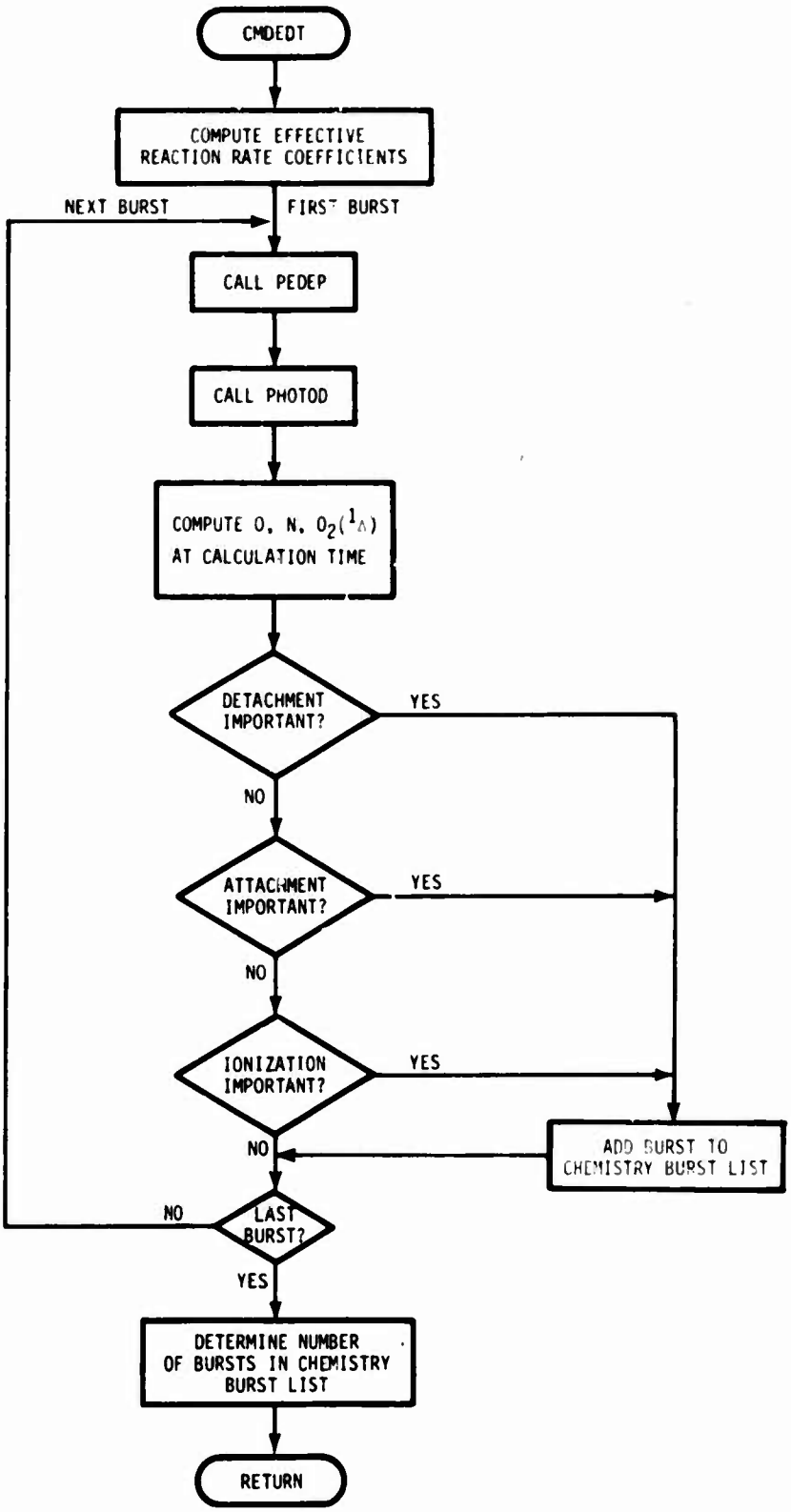

Figure 8. Flowchart for subroutine CMDEDT.

calculation time.

If the burst does not affect the neutral species sufficiently to be included in the burst list, a test on the prompt ionization remaining at the calculation time is made to see if it is significant in comparison to that product by delayed radiation. First a test is made to see if a saturation impulse is important by comparing the positive ion density due to an ionization impulse with the positive ion density due to the ion-pair production rate. The ionization due to prompt energy deposition is not important if

$$\frac{1}{\alpha t} \leq 0.1 \sqrt{\frac{q}{\alpha}}$$

or rearranged

$$\sqrt{q\alpha}\, t > 10 \ .$$

If the burst could be important a further test is made with the actual ionization produced by the burst. For this test the electron density at the calculation time due to the impulse is estimated from

$$N_e(\text{impulse}) \approx \frac{N_e}{1 + N_e \alpha t} \frac{D + A\, e^{-(A+D)t}}{D + A}$$

and compared with the electron density due to delayed radiation.

The detachment rate used in computing the electron density due to prompt radiation is computed using the neutral species concentrations at the time of burst. This maximizes the electron density due to prompt radiation.

SUBROUTINE CMFEDT

This routine edits the burst to form a test for use in E- and F-region chemistry calculations. The bursts chosen are those that produce a specified level of initial ionization (set at 3×10^7 cm^{-3} for the WESCOM code) at a specified altitude (currently chosen as 200 km unless the lowest altitude on the path is above 200 km).

The air properties and neutral species densities at the test point are found for each burst from routine ATMOSF. Then routine PIONF is called to determine the initial ionization caused by the burst and the result compared to the minimum values used to select bursts and E- and F-region ionization sources. In computing prompt ionization in routine PIONF air motion due to heave is neglected. While this can result in overestimating the initial ionization, it reduces the calculation time in routine PIONF.

SUBROUTINE DBMHT

This routine determines time-dependent quantities for debris regions produced by high-altitude bursts.

For high-altitude bursts, geometrical debris regions are only used for gamma radiation effects. For beta radiation the altitude and dimensions of an ellipse in the horizontal plane are defined.

Up to four debris regions can be defined to model the location of the fission debris for a given burst. One debris region is used to model the ionized debris distributed within the fireball. Two debris regions are used to model debris settling down the geomagnetic field lines in the burst and opposite hemispheres. For bursts detonated below 120 km a debris region is used to model neutral debris falling back over the burst point.

First the ambient atmospheric scale heights at the bottom of the fireball and at the debris settling altitude (taken to be 150 km) are found by calling routine ATMOSU. Then parameters related to the fireball are defined and for times greater than the fireball apogee times the amount of debris that is in the fireball (FDI), and the amount of debris that has reached the settling altitude in each region (FDNB and FDNC) are calculated. These values are estimated from the air parcel data calculated for the fireball region assuming that the debris density distribution is similar to the fireball ionized air mass distribution. For bursts below about 120 km (FNEUT > 0.1) and times after the magnetic equilibrium time (TEQ), the fraction of debris that will fall back over the burst point is accounted for.

If the ionized debris fraction is greater than five percent, an ionized debris region is defined. A skewed spheroid debris geometry is used and the current fireball scale height is used for the debris distribution. A beta source plane is defined at the altitude HBETA determined in routine FBMHT that includes effects of magnetic freezing of the beta tube.

After the ionized debris region is defined, tests are made to see if more than five percent of the debris has fallen down the field lines to 150-km altitude. If the amount is more than five percent, a debris region is defined. A spheroid geometry is used, but by the use of truncation altitudes a pancake-

like region is defined. Beta source planes at 150 km are defined for use in determining beta ray ionization. If the wind option (given as input) is exercised, separate beta source planes are defined for each hemisphere. Otherwise, a single beta source plane in the burst hemisphere is defined.

For bursts below 120 km and times after TEQ a debris region that falls back over the burst point until reaching 150 km is modeled.

SUBROUTINE DBMLT

This routine determines time-dependent quantities for debris regions produced by low-altitude bursts.

For low-altitude bursts, a geometrical debris region is defined for use in computing effects of delayed beta and gamma radiation. The right circular spheroid (untilted) and toroid geometries used for the fireball (KINDF = 1 and KINDF = 3) are also used for the debris region. For times before toroid formation the debris region dimensions are found from

$$RTD = RTBF$$

$$RLD = \frac{RLF}{RTF} RTBF$$

where RTD and RLD are the debris axis dimensions perpendicular and parallel to the vertical direction respectively and RLF and RTF are similar dimensions for the fireball. The quantity RTBF is the horizontal debris radius defined by routine FBMLT. The debris region is truncated with minimum and maximum altitude slices if the fireball region is truncated.

The vector location of the debris origin is determined and routine VOLUME is used to obtain the debris volume. The debris stabilization time and debris geometry at stabilization time are stored for use in modeling wind effects. If the debris stabilizes above 200 km, the vertical radius is limited to 50 km and if the debris stabilizes below 200 km the debris vertical radius at stabilization time is not allowed to be less than 4 km.

Several additional quantities are calculated for use in beta ionization calculations. First, the dimensions of a horizontal ellipse that can be used to determine the maximum extent of the beta tube are calculated from the quantities RLBF and RTBF defined in routine FBMLT. Then, quantities required in beta sheath calculations are determined.

SUBROUTINE DBSTAM

This routine is a driver routine for determining post-stabilization debris geometry due to atmospheric winds.

The atmospheric wind model is used to determine debris geometry for debris regions above 100-km altitude and for times after the debris stabilization times. For earlier times or for debris altitudes below 100 km the debris geometry determined by the fireball/debris models (routines DBMLT and DBMHT) are used. These models include a nominal debris expansion due to winds, but do not include debris lateral motion (debris offset) due to atmospheric winds.

For debris regions above 100 km and times after the debris stabilization time the geographic location of the debris center and the local time at the debris stabilization time (start time for wind effects model) are computed. The debris parameters at stabilization time are written out on the detailed output file (file LFDO) if detailed phenomenology data has been requested (input option). Then routine PSDM is called with the debris data at stabilization time to determine the debris geometry at the current calculation time due to atmospheric winds.

SUBROUTINE DEBRIS

This routine is a driver routine to determine the energy deposition at a specified point due to charge exchange, loss cone, and ion leak particles. Figure 9 shows a simplified flowchart for the routine.

First, a check is made to see if the deposition point is in the magnetic conjugate region of the burst. If it is, energy deposition due to debris kinetic energy sources is neglected.

If the deposition point is in the burst region, the reduced range for loss cone and charge exchange particles is computed and the particle energy lost in transversing the mass penetrated from the burst to the deposition points is found by calling routine FZET. Then, tests are made to see if the energy due to loss cone particles is to be computed. These tests include an input option, a test on the amount of debris kinetic energy in loss cone particles, and a test on the upper intersection altitude for loss cone particles. Only the upper intersection altitude is tested (rather than testing to see if the field point is between the lower and upper intersection altitudes as is done for beta particles) because vertical air motion (heave) can move the air in which the particles initially deposit their energy.

If the loss cone particle energy deposition is to be computed, routine CONSPC is called to obtain the energy spectrum and the energy deposited neglecting the spatial distribution is computed. Next, the effect of the spatial distribution is found by computing the location of the 100-km point on the geomagnetic field line passing through the deposition point of interest. The distance of this point from where the field line passing through the burst point reaches 100 km is used to compute the distribution function.

Following calculations for the loss cone particles, the energy deposition neglecting the spatial distribution for ion leak and charge exchange particles is computed. To account for the spatial distribution for charge exchange and ion leak particles a plane normal to the geomagnetic field lines at the burst point is used as the distribution plane. The position of the magnetic field line that passes through the field point in the distribution plane is determined for use in the distribution function.

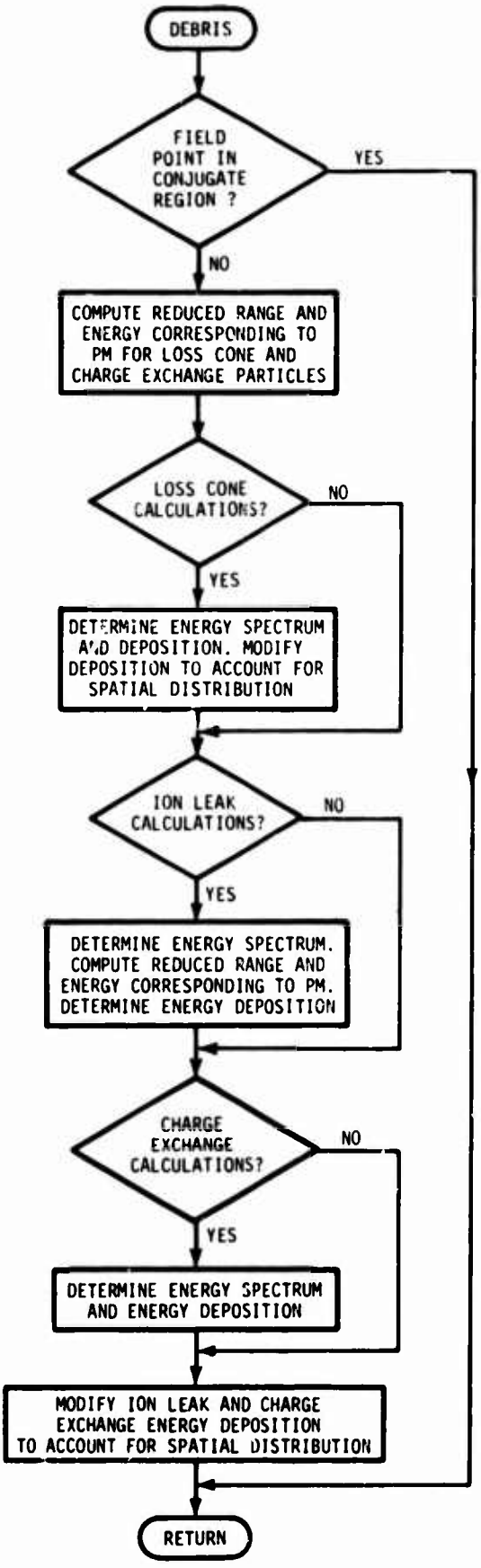

Figure 9. Flowchart for subroutine DEBRIS.

SUBROUTINE DEDEP

This routine determines the delayed energy deposition rate (ergs gm^{-1} s^{-1}) due to weapon radiation.

A loop over debris regions is initiated and routines EDEPG and EDEPB are called to obtain the energy deposited per gram by gamma rays and beta particles, respectively. The call to routine EDEPG is skipped if the air density at the field point is less than 10^{-11} gm cm^{-3} (about 125 km) and the call to routine EDEPB is skipped if the field point is outside the beta tube.

Delayed energy deposition due to neutrons is computed by setting up a burst loop and calling routine EDEPND. Routine EDEPND determines the neutron energy deposition due to capture reactions and elastic scattering reactions occurring after the time used for prompt energy deposition.

SUBROUTINE DSTINT

This routine determines the attenuation due to progagation through dust clouds.

A loop over dust clouds defined by phenonemonology module is started and for each dust cloud routine PCLOUD is called to determine the geometry for each dust cloud particle group. Then routine RINTER is called to see if the ray path intersects the region. If it does, routine PGROUP is called to determine the extinction coefficient and the attenuation is calculated. If detailed output has been requested the dust cloud intersections and attenuations are written out on file LFDO.

SUBROUTINE DTNEP

This routine determines the electron and total positive ion densities at a specified time after burst due to prompt radiation. The routine is similar to routine DTNEP developed for ROSCOE.

First α_i and A and initial values of α_d and D are determined. These values are used to compute initial values for N_e and N_+ .

The initial value of N_e is tested against the electron density that would be produced by delayed radiation for the same reaction rate coefficients. If the electron density due to prompt radiation is less than 1/10 the value due to delayed radiation or if the electron density due to prompt radiation is less than 10^3 electrons cm^{-3}, the electron and positive ion densities due to prompt radiation are set to zero and no further calculations are made.

If after the above tests prompt ionization can still be important, the positive and negative ion compositions and new effective values for α_d and D are computed. These revised values are then used to recompute the electron and total positive ion densities.

SUBROUTINE DTNEQ

This routine determines the steady-state reaction rate coefficients and the corresponding electron and total positive ion densities due to delayed radiation. The routine is essentially the same as routine DTNEQ developed for ROSCOE.

The ion-pair production rates producing O_2^+ and NO^+ are determined from the total ion-pair production rate. Next attachment and detachment rates are computed. The detachment rate includes the effects of photodetachment from thermal radiation from each burst occuring prior to the calculation time. Then positive and negative ion transfer rates are determined including effects of photodissociation from thermal radiation.

Initial values for the ratios R_{p1} through R_{p10} (positive ion ratios) and R_{n1} through R_{n9} (negative ion ratios) are chosen and used to compute effective reaction rate coefficients and equilibrium electron and ion densities. The electron and ion densities are then used to recompute the ratios R_{p1} through R_{p10} and R_{n1} through R_{n9}. The above procedure is repeated until the effective recombination coefficient and effective detachment rate change by less than 1 percent.

SUBROUTINE DUSTMI

This routine computes time-independent quantities used in dust region calculations.

First, the scaled burst height (ratio of burst height to the pressure equilibrium radius computed in routine FBMLI) is tested to see if the burst will cause a dust cloud. If the scaled burst height is less or equal to 3 a dust cloud is defined. For the first cloud defined the particle size group parameters are computed (same for all dust clouds). Eight particle groups are used in the current model (see Table 6), with the boundaries chosen to keep the spatial overlap of adjacent groups relatively uniform. The fraction of the particles in each size group, FNP(I), is computed from the assumed size distribution with 0.001- and 10.0-cm minimum and maximum particle sizes.

For each dust cloud the mass loading factor, XMLOD, is computed and the diameter of the largest particle lofted, ATRY, is computed rounded to the nearest particle group boundary; ie, the nearest value of ABAR. The index of the largest group lofted, IMAXP, is then the group for which the maximum size is the rounded value of ATRY. Finally, the total number of particles included in all the groups, designated TNP, is computed. It should be noted that all these particles are not lofted; only those contained in particle-size groups up through IMAXP are lofted.

Table 6. Time-independent particle group parameters.

Group Index I	Minimum Diameter (cm) ABAR(I)	Maximum Diameter (cm) ABAR(I+1)	Fraction of Particles FNP(I)
1	0.001	0.09	≈1.000
2	0.09	0.4	1.356E-6
3	0.4	1.0	1.463E-8
4	1.0	2.0	8.750E-10
5	2.0	3.25	9.587E-11
6	3.25	5.25	2.222E-11
7	5.25	7.5	4.540E-12
8	7.5	10.0	1.370E-12

FUNCTION EDEPB

This routine computes the energy deposition rate (ergs gm^{-1} s^{-1}) due to beta particles. The model is based on formulations developed for ROSCOE. A simplified flowchart for the routine is shown in Figure 10.

The average beta particle energy, beta particle release rate, and energy deposition coefficient are found from routine WOBD. Then routine ATMOSU is called to determine atmospheric properties at the beta source altitude. If the debris is distributed in a constant altitude plane, a correction term is found for use in computing the debris integral along the geomagnetic field line through the field point. The correction term is a function of the location of the field line at the beta source altitude.

For beta source altitudes above 80 km a debris pancake (elliptical region in a constant altitude plane) is used to model the beta source. For lower beta source altitudes, the actual debris shape (spheroid or toroid) is used. The beta source geometry is used to determine the integral of debris along the geomagnetic field line intersecting the field point, the altitude of the debris center, and the magnetic field strength at the debris center. For field points within the debris region (source altitudes below 80 km) the debris region is divided into two parts; one below and one above the field point.

The integrals are used to compute the energy deposition within the beta tube. For beta source altitudes below 80 km the energy deposited within the beta sheath is computed if requested (input option to routine). The beta sheath energy deposition is computed and added to that calculated for the beta tube.

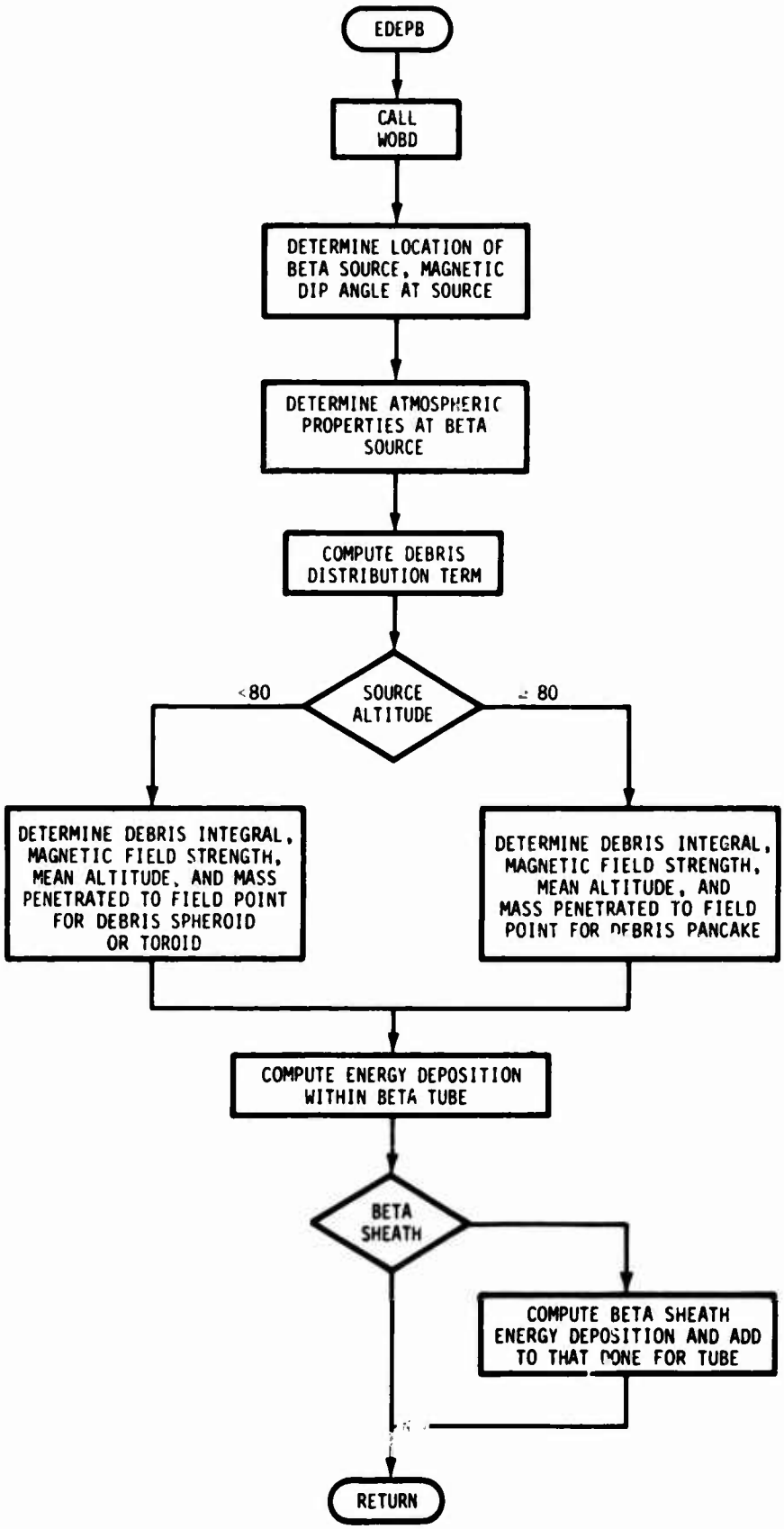

Figure 10. Flowchart for function EDEPB.

FUNCTION EDEPG

This routine computes the energy deposition rate (ergs gm^{-1} s^{-1}) at a given point in space due to gamma radiation from the fission debris. A simplified flowchart for routine EDEPG is presented in Figure 11.

First, the debris truncation altitudes and the vertical dimensions are calculated. Then, the mass penetrated from the field point to the debris center is computed. If a point source calculation has been requested (input option), the mass penetrated and slant range between the field point and debris center are used to compute the gamma ray energy deposition.

If a point source has not been requested, the dimensions and volume of the debris region are found and the mass penetrated is computed to the debris edges. Then, tests are made to see if analytical solutions can be used or whether a numerical solution is required to compute the energy deposition. A numerical solution is used when the debris geometry is a toroid or tilted spheroid or has been truncated so that the top is below the center, when the debris vertical or radial distribution is not uniform, and when the step sizes based on allowable changes in mass penetrated are smaller than the debris size.

The coordinate system used in computing the step sizes is one where the r coordinate is measured along a constant-altitude plane at the altitude of the debris center. The Δr and Δz step sizes for which the change in mass penetrated from the field point is less than ΔM gm cm^{-2} are determined from

$$\Delta r = \frac{(r_2 - r_1)\Delta M}{M_2 - M_1}$$

$$\Delta z = \frac{\Delta M a}{M_c - M_t} \quad ,$$

where ΔM is chosen as 10 gm cm^{-2} and

M_c = mass penetrated from field point to r_o , z_o

M_t = mass penetrated from field point to r_o , z_t

r_o , z_o = coordinate of debris center

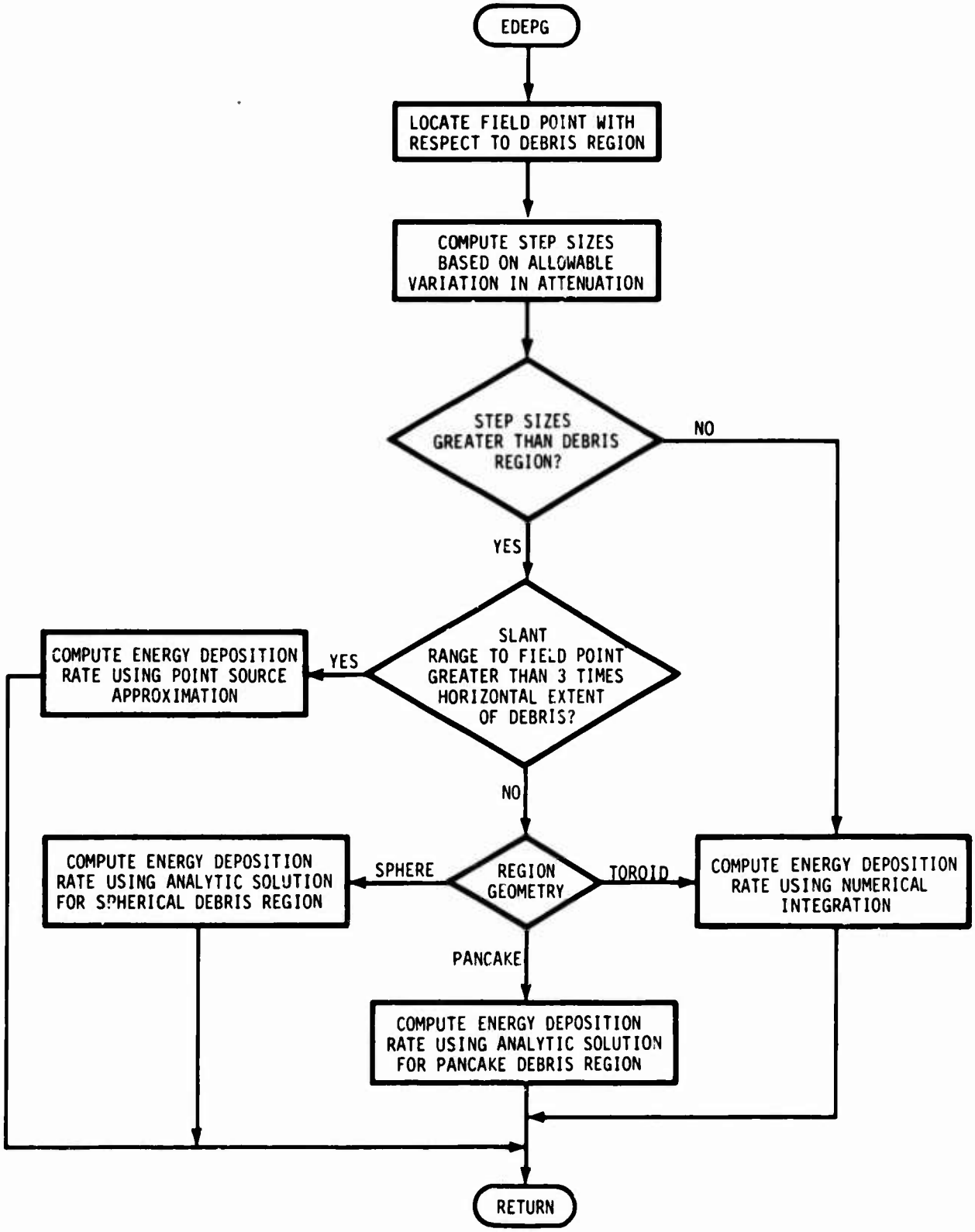

Figure 11. Flowchart for function EDEPG.

z_t = z coordinate of top of debris region

r_1 , r_2 = minimum and maximum horizontal distances from field point to debris plane at $z = z_o$

M_1 , M_2 = mass penetrated from field point to r_1 , z_o and r_2 , z_o

a = radius of sphere, radius of toroid arm, or semithickness of pancake.

If Δr and Δz are greater than the horizontal and vertical dimensions of the debris region, $A_\gamma(M)$ is essentially constant over the debris region. If $A_\gamma(M)$ is constant and the slant range to the debris center is greater than three times the largest horizontal debris radius, a point-source approximation is used to compute the ion-pair production rate. If $A_\gamma(M)$ is constant and the slant range is smaller than above, analytical expressions are used for spherical and pancake debris geometries. For all other conditions, a numerical integration procedure is used.

When the numerical integration procedure is used, a second set of Δr and Δz step sizes is determined to ensure that the numerical integration gives good agreement with the volume of the debris region. These step sizes are found from the following:

	$\Delta' r$	$\Delta' z$
Sphere	$\frac{2a}{7}$	$\frac{2a}{7}$
Toroid	$\frac{2b}{7}$	$\frac{2a}{7}$
Pancake	$\frac{2b}{7}$	$2a$

where b is the largest horizontal radius of the debris region.

The Δz step size is taken as the smaller of that determined on the basis of the variation in $A_\gamma(M)$ and that determined for volume accuracy, with a minimum step size of 1 km.

A minimum Δr step size is then chosen from

$$\Delta r = \text{minimum} \left(\Delta r', \sqrt{\frac{10^{-3}}{\rho_d}} \right) ,$$

where ρ_d equals the mass density at the debris center, to restrict the step size for low debris altitudes where the mass penetrated is a strong function of r. As a further restriction, the minimum Δr step size is not allowed to exceed 500 km for debris altitudes less than 50 km or 1000 km for debris altitudes greater than 50 km.

For each Δz step in the integration procedure, the mass penetrated to two points in the debris region at altitude z is found with routine PMASS. A new Δr step size is computed from

$$\Delta r = \frac{(s_2 - s_1)\Delta M}{M_1 \ell n(M_2/M_1)} ,$$

where s_1 is the slant range to a point in the debris region closest to the field point, and s_2 is the slant range to a point chosen to make $M_2 - M_1$ about 85 gm cm^{-2}. The minimum of the above Δr step size and the one previously determined is used for the integration over r. The mass penetrated to each volume element between r_1 and r_2 is found by interpolating between M_1 and M_2:

$$M = M_1 \left(\frac{M_2}{M_1} \right)^{\frac{s - s_1}{s_2 - s_1}} .$$

if r becomes larger than r_2, the two points r_1 and r_2 are changed so that r_2 becomes r_1, and r_2 is again chosen so that $M_2 - M_1$ is about 85 km. Within each integration region, the Δr step size is uniform except where it is necessary to reduce the step size to match a debris boundary. The Δz step size is always uniform.

To eliminate numerical integration when the ion-pair production rate

q is small, a point-source estimate is made at each step in z with the debris at r_1 , z . If the point-source calculation of q is less than a minimum value (chosen as one-tenth of the natural ion-pair production rate), integration over r is not performed.

The vertical debris distribution is accounted for in computing the debris density at each step in z . For times after debris stabilization the debris may have a radial distribution defined by the debris distribution parameter. This is approximately accounted for in the numerical integration by first increasing the radial dimension of the debris to include debris in the tail of the distribution and by modifying the contribution to the energy deposition integral for each step in r to account for the debris distribution.

The last calculation in the routine is to account for the reduced mass in the fireball if the debris is within a low-altitude fireball. Corrections to the energy deposited at the field point due to the reduced mass in the fireball are made when the fireball associated with the debris region is below 40 km and the fireball temperature is greater than 300 K.

FUNCTION EDEPND

This routine computes the energy depositon rate (ergs gm^{-1} s^{-1}) at a given point in space due to neutron elastic collisions and capture reactions.

Before computing the neutron energy deposition, tests are made to see if the energy deposition would be negligible in comparison to gamma and beta energy deposition rates. Detailed neutron calculations for a particular burst are not made if

$$\frac{10^{24} W f_N}{R^2}\left(\frac{t_c}{t}\right)^2 \leq 0.1\ E_{rf} \qquad t < t_c$$

$$\frac{10^{24} W f_n}{R^2} e^{-\frac{t}{\tau}} \leq 0.1\ E_{rf} \qquad t \geq t_c$$

where

E_{rf} = energy deposition rate due to gammas and betas (ergs gm^{-1} s^{-1})

R = slant range to burst point (cm)

$$t_c = \frac{1.3 \times 10^{-6}}{\rho}$$

$$\tau = \frac{5 \times 10^{-5}}{\rho}$$

and f_n is the fraction of the weapon yield in neutron kinetic and capture energy.

For bursts considered, the mass penetrated from the burst point to the deposition point and the vertical mass above the burst point used are poor for such cases and, in general, other ionization sources will dominate.

Once the shortest distance has been found, the neutron-decay beta flux and the ion-pair production rate are determined.

SUBROUTINE ENEF

This routine computes the electron density (cm^{-3}) and electron collision frequencies (s^{-1}) at a specified location above 100 km. A simplified flowchart for subroutine ENEF is presented in Figure 12.

First, the location and properties of the air that is at the calculation point at the calculation time are found at the time of all bursts prior to the calculation time and at the calculation time by calling routines ATMOSF and IONOSU. Then the ion-pair production rate at the calculation time due to gamma rays and beta particles is found from routine DEDEP.

The first F-region prompt source is found by testing logical parameter LPRT, which was set up in routine CMFIDT. The prompt ionization due to this burst is computed by routine PIONF. Routine PIONF also modifies the neutral particle concentrations according to the number of ions produced and determines a new excitation temperature.

The end of the deionization time interval is taken to be the next prompt source (or the calculation time if there are no more prompt sources), subject to the constraint that the mass density of the air cannot change by more than a factor of two during the interval. If the density ratio during an inter-burst time interval changes by more than a factor of two, an intermediate time is taken such that the density change to this time is exactly a factor of two. An exponential interpolation is used to compute the density at the intermediate time and linear interpolation to compute the altitude of the air parcel. The remaining interval will be further checked on the next iteration and broken up again if necessary. In addition, to prevent large time steps immediately after burst, calculations are made at 1 and 3 seconds after each burst.

To avoid the possibility of overlooking large peaks or nulls in the density time-history during a long inter-burst time interval, an array of intermediate times and the properties of the air at those times has been computed during the call to ATMOSF, above. These times are merged with the burst time array for use in breaking up time-intervals and interpolating to find the properties of the air at intermediate times.

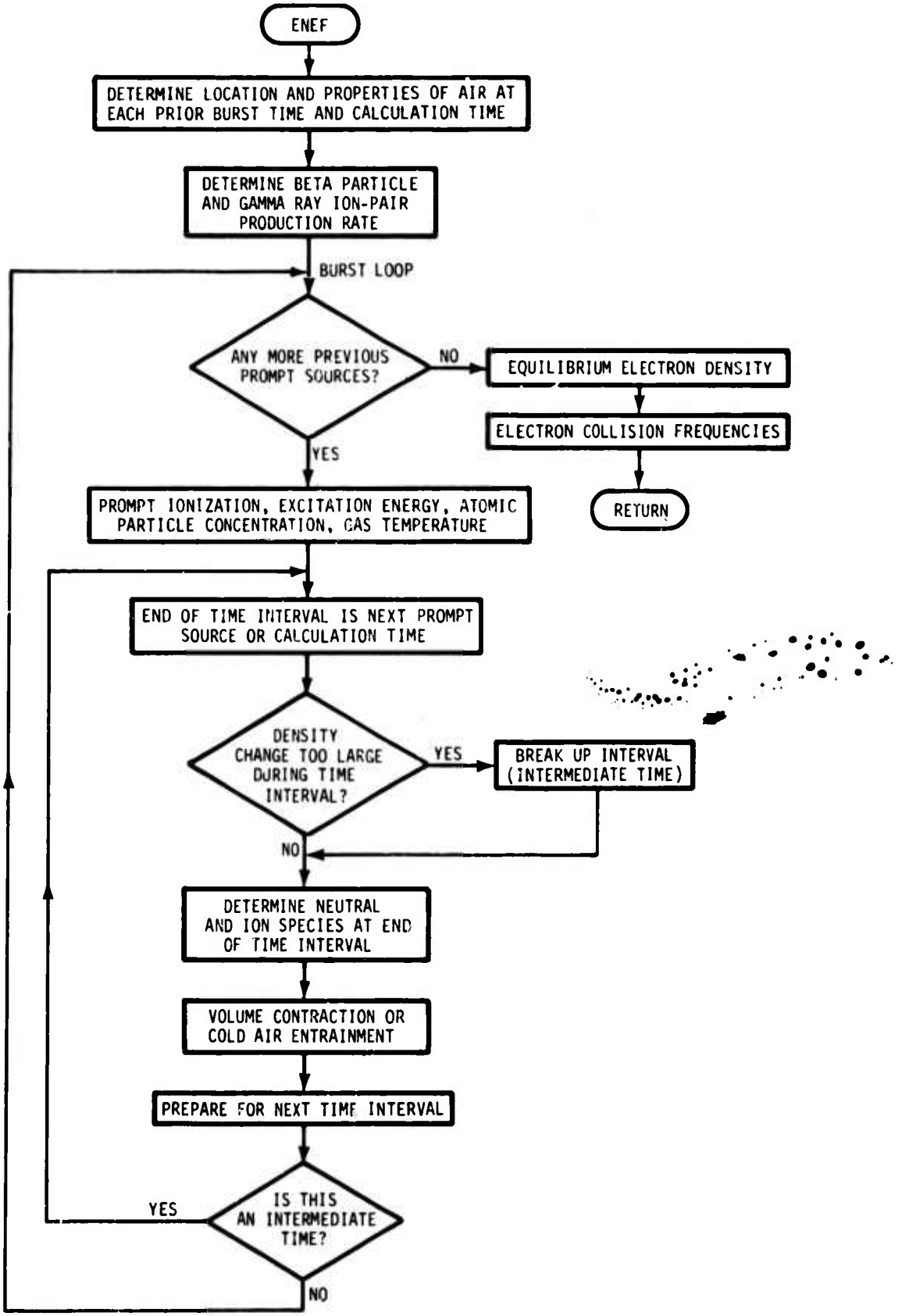

Figure 12. Flowchart for subroutine ENEF.

Once the time-interval for deionization is established, the changes in ion and neutral species densities are found from routine CHEMEF. If the mass density decreases during the time interval, the electron, ion, and neutral particle concentrations are modified due to volume expansion and the gas temperature is decreased due to adiabatic expansion in routine CHEMEF. If the density increases, the particle concentrations and gas temperature are modified due to cold air entrainment and volume contraction. A new excitation temperature is obtained from routine TEXK.

If the end of the time interval just computed is an intermediate time, the next time interval is taken to the time of the next prompt source. Control is returned to the block which determines whether the remaining interval need be subdivided again. If the end of the time interval just completed is not an intermediate time, control is returned to the beginning of the burst loop. If there is another prompt ionization source, the the prompt ionization from that source is computed and all the subsequent calculations repeated.

If there are no more prompt sources, the electron density due to natural and weapon ion-pair production rates is found from routine CHEMQ with neutral and ion species for the most recent time interval. The electron density at the calculation time is then computed as the maximum of that due to prompt radiation and the ion-pair production rates. The logical parameter ION is set to equal to 1, 2, 3, or 7, depending on whether the dominant ionization source is natural, beta particle, gamma ray, or prompt ionization, respectively.

The final step in routine ENEF is the computation of electron-neutral and electron-ion collision frequencies.

ROUTINE FBEN

This routine determines fireball ionization, collision frequencies, and incremental absorption at a specified point within the fireball. A simplified flowchart for the routine is shown in Figure 13.

For fireballs produced by low-altitude bursts and for fireballs produced by high-altitude bursts for times less than the time to reach apogee (t_{ap}) the air at the calculation point is assumed to have come from a position in the initial fireball which was at the same number of scale heights above the bottom as the calculation point is at the calculation time. The initial mass density is taken as the atmospheric density at the initial point at the time of the burst and is calculated by routine ATMOSU or ATMOSF.

The mass density at the calculation time is computed from the initial mass density and the ratio of the initial and current fireball scale heights. For fireballs produced by low-altitude bursts the mass density is taken as the larger of the above and the pressure equilibrium value. If the pressure equilibrium value is larger, the additional mass density is assumed to be due to entrainment.

For fireball reference altitudes below 100 km the ion-pair production rate caused by beta particles and gamma rays is found from routine DEDEP. For toroid geometries it is possible for the calculation point to be within the hole of the toroid. For this case routine CHEMDQ is used to compute the steady-state ionization neglecting effects of prompt ionization and assuming ambient temperature.

For calculation points within the fireball routine CHEMHR is called to obtain the ionization and collision frequencies. If the burst altitude is below about 85 km and the calculation point is within the debris region, the metal species densities are computed prior to calling routine CHEMHR. Also, if the fireball temperature is below 2000 K the air density and entrainment fraction at the time the air was at 2000 K the air are computed.

For fireballs produced by high-altitude bursts and calculation times after the time to reach apogee the fireball ionization is calculated as the sum of ballistic ionization and diffusion ionization. At the first call to routine

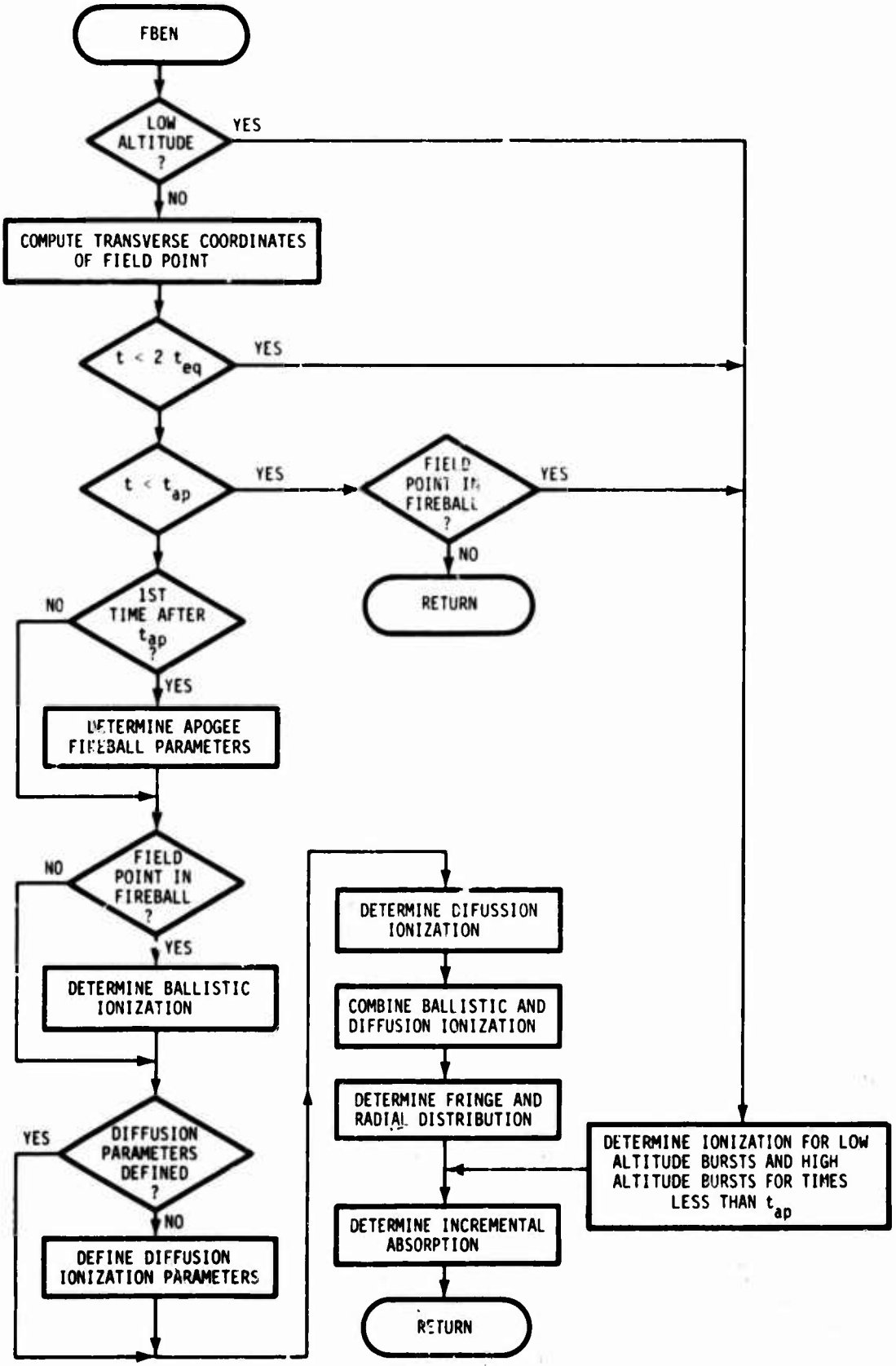

Figure 13. Flowchart for subroutine FBEN.

FBEN after t_{ap} the apogee fireball ionization along the longitudinal axis is fit with two exponential terms. The exponential parameters are determined from the models described above. Then a test is made to see if the field point is within the ballistic ionization region. If it is, the ballistic ionization is computed by finding the location within the apogee fireball where the air at the calculation point came from and computing the ionization at apogee and the change in ionization since apogee.

Diffusion ionization parameters are calculated once for each calculation time. Then, the diffusion ionization is determined and combined with the ballistic ionization. For field points near the top of the fireball, the electron density is reduced empirically to approximate additional volume expansion not modeled. Also, a transverse radial ionization distribution is used to modify the ionization in terms of the transverse location of the field point.

After obtaining the ionization and collision frequencies, the incremental absorption is computed. If the electron density is large enough that the plasma frequency is greater than the wave frequency, the incremental absorption is set equal to 1×10^{10} dB km^{-1}.

When footprint calculations are made the electron density and temperature are computed at several points along the longitudinal axis and stored in common block CHEMFB as part of preliminary calculations. Then, these data are used to fit the electron density and temperature at points within the fireball that are along propagation paths in each scan. The logical flag LFPCS is set to an integer greater than 0 when the interpolation calculations are to be used in routine FBEN.

SUBROUTINE FBINT

Routine FBINT is a driver routine for the module that determines environment and propagation quantities for propagation through fireball regions. A simplified flowchart for the routine is shown in Figure 14.

After integral values are initialized to zero for each fireball a fireball loop is set up and routine RINTER is called to determine whether the propagation path intersects the fireball. If an intersection exists, fireball quantities are stored in labeled common block CHEMB. For low-altitude bursts the metal species densities (aluminum and uranium) are computed by adding the metal densities from each debris region associated with the fireball. Path intersections with debris regions are also found for low-altitude bursts for later use in selecting path integration segments. A beta sheath ionization flag is set for debris regions produced by the same burst that produced the fireball. Beta sheath ionization from other debris regions is ignored.

Next, path integration segments are determined. For fireballs from high-altitude bursts one segment is used for burst region intersections and another for conjugate regions intersections. For fireballs from low-altitude bursts up to eight path segments can be defined to describe different ionization regions within the fireball.

After the integration segments have been defined a numerical integration of propagation quantities is performed for each segment. A running sum over the segments and over fireballs, if the path intersects more than one fireball, is kept and added to the path propagation quantity terms.

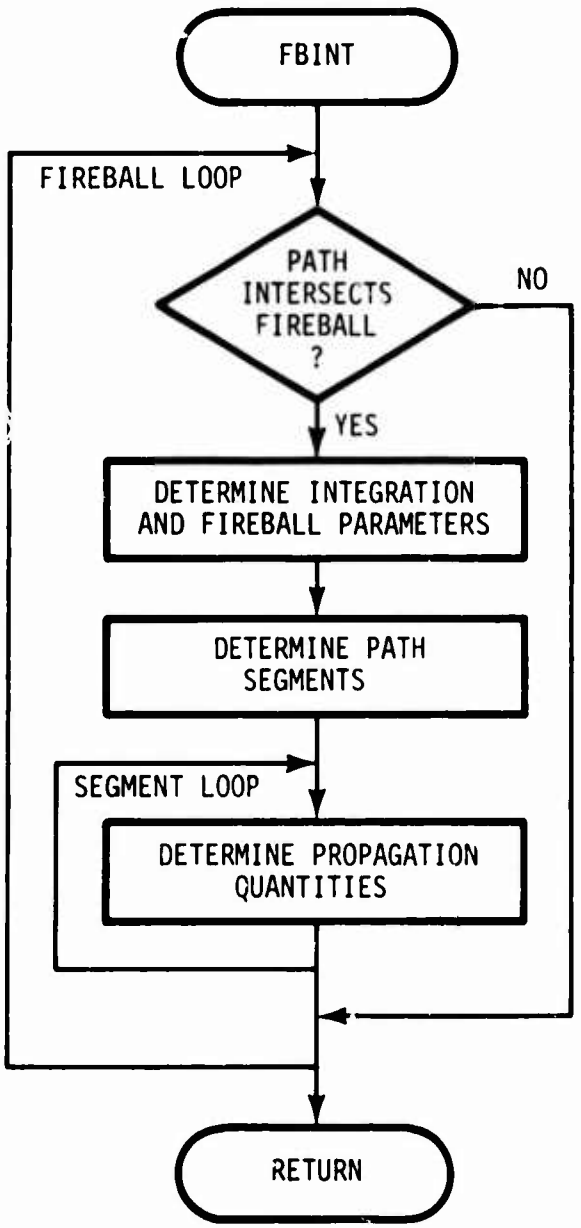

Figure 14. Flowchart for subroutine FBINT.

SUBROUTINE FBMHI

This routine determines time-independent scaling quantities for fireballs from high-altitude bursts.

Routine FBMHI is called for each burst detonated above 75 km. The high-altitude model flag, LMCF, is set to zero indicating a high-altitude burst but may be reset to one (a low-altitude burst) later as indicated below.

First, the debris loss-cone and ion-leak parameters are found by calling routines LOSCON and IONLEK. This includes the amount of debris kinetic energy in loss-cone and ion-leak particles which is not available to produce the fireball. Next, charge exchange and UV fractions are found and the heave flag is set (no heave for bursts detonated below 120 km).

Next, the initial fireball horizontal, downward, and upward dimensions are determined. Iteration procedures are used to determine the amount of X-ray energy contained within the horizontal radius and the effect of non-uniform air and work done against the magnetic field. An iteration procedure is also used to find the downward radius in a non-uniform, possibly heaved atmosphere. After the initial dimensions measured from the burst point are found the location and dimensions of an equivalent spheroid are calculated.

Next, quantities defining the fireball rise and expansion and the initial fireball properties (density, scale height, mass, and volume) are computed. A test is made to see if the maximum fireball altitude neglecting drag forces will be above 250 km. If it is not, the high-altitude model flag is set to one (low-altitude burst) and control is returned to the calling routine.

The location of the loss-cone reference point (used in computing loss-cone ionization) is determined by calling routine MAGFLD to determine the location of the point on the field line through the burst point that is at 100 km altitude. Also, routine EUXFIT is called to determine the fraction of ionizing UV energy. The Lagrangian coordinates of the bottom and top of the initial fireball (used in the fireball wake heave model) are found by calling routine LAGRAN.

The last calculations performed are to determine fireball properties

when the fireball reaches apogee and at the magnetic equilibrium time. The apogee quantities are found by calling routine FBMHT and the equilibrium properties (mass density) by calling routine FBITMD.

SUBROUTINE FBMHT

This routine determines time-dependent quantities for high-altitude bursts.

The routine is divided into two major computational blocks; one for times less than the time for the fireball to reach apogee (determined in routine FBMHI) and one for later times. An input logical flag (MODE) is used to determine apogee fireball quantities (MODE = 0) or fireball quantities at a calculation time (MODE = 1).

For MODE = 0 or for times less than the apogee time for MODE =1, the fireball geometric and intrinsic properties are determined from time-independent quantities calculated in routine FBMHI and scaling relations defined for several time periods after burst. For MODE = 0 the fireball quantities (apogee quantities) are stored in labeled common block BREG.

For MODE = 1 and times after the time to reach apogee the location of ionized air marker parcels are determined for use in defining ballistic and diffusion ionization. Twenty parcels are equally spaced along the longitudinal axis of the apogee fireball. At later times the locations of the highest and lowest parcels in the burst hemisphere and the highest and lowest parcels in the conjugate hemisphere (if any parcels cross the magnetic equator) are found. The parcel locations are used to define coefficients that define the location of a parcel in the apogee fireball in terms of its location at a later time.

As a part of the preliminary calculations the time (TMAX) for all the parcels to fall below a stopping altitude and the location (XEMAX) in the apogee fireball separating parcels that remain in the burst region from those crossing the equator are found. Ionization associated with parcels that are above the stopping altitude is termed ballistic ionization. Ionization associated with parcels that fall below the stopping altitude is called diffusion ionization. If parcels cross the equator, parcel location scaling coefficients and fireball dimensions are separately defined for the conjugate region.

The parcel locations are determined by calling routine BTRACE. Inputs and outputs to routine BTRACE are through labeled common block TRACE. The

quantity TPHS is the time for the parcel to fall below the stopping altitude, the quantity TPAP is the time for the parcel to reach apogee and the quantity CONJ is a flag that is set to a negative number if the parcel crosses the equator.

SUBROUTINE FBTINT

This routine determines the thermal emission of a fireball in a specified direction.

The thermal emission is specified in terms of an effective fireball temperature that accounts for fireball emissivity and temperature along a path through the fireball in the specified direction. For low-altitude bursts the fireball is modeled as an isothermal region and the fireball temperature and emissivity at the fireball edge are used to compute the effective fireball temperature.

For high-altitude bursts both the emissivity and the fireball temperature are functions of position within the fireball. The effective fireball temperature is computed from

$$T_e = \int_0^R \alpha(r)T(r)e^{-\int_0^r \alpha(x)dx}dr$$

where

α = incremental absorption within the fireball (nepers)
T = temperature within the fireball (K)
r = the distance from the edge of the fireball along the specified path
R = distance through the fireball along the specified path .

For emissions from the bottom of the fireball (paths from the antenna that have a positive elevation angle in the fireball), the integration is performed along the path from the receiver according to the above equation. Routine FBEN is called to obtain α and T as a function of position within the fireball.

For emissions from the top of the fireball a direct integration of the above equation could require an excessive number of integration steps since most of the contribution occurs near the bottom of the fireball. In order to limit the number of steps, an integration of fireball absorption in the upward

direction through the fireball is performed first and emissivity quantities at each integration step saved. Then an integral in the reverse direction is performed using the integration steps determined from the absorption integral.

SUBROUTINE FOOTPC

This routine is the driver routine for determining fireball region footprint plots. A simplified flow chart for the routine is shown in Figure 15.

Footprint plots are not prepared for low-altitude bursts. Absorption and the integral of electron density for a path from the satellite through the fireball center are given as output along with the location of the corresponding ground terminal.

For high-altitude bursts the fireball ionization and temperature are fit and the fit parameters stored in labeled common block CHEMFB. Then a scan loop is started where a scan consists of a series of propagation paths from the satellite through the fireball. The scans are defined by points along the longitudinal axis of the fireball, starting at the fireball bottom. The propagation paths in each scan are chosen to be in a plane normal to the fireball longitudinal axis and the local vertical at the point on the axis defining the scan. An attempt is made to define five paths that intersect the fireball (one through the longitudinal axis and two on each side of the axis).

For each path the location of the ground terminal is computed and propagation quantities determined from routine FBINT. Routine FPLNK is called to determine link quantities including the effects of noise. Two additional paths with ambient propagation quantities are defined for each scan to locate the fireball edges. Then routine FPINT is called to obtain parametric values of the quantities to be plotted as a function of ground terminal location. After all the scans have been completed routine FPPLOT is called to prepare printer page plots.

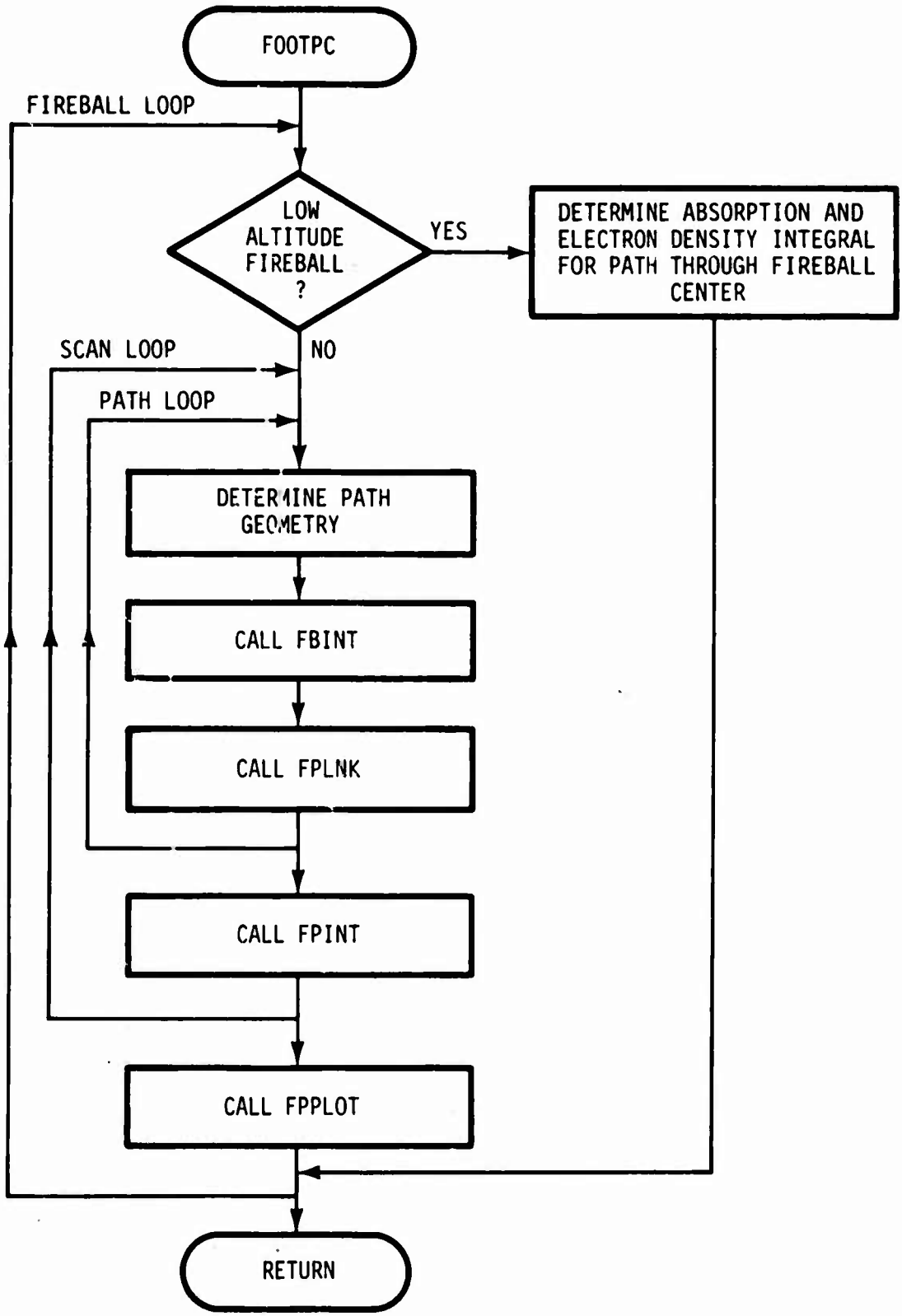

Figure 15. Flowchart for subroutine FOOTPC.

SUBROUTINE FPCIR

This routine determines signal processing quantities for single link circuits used for footprint plots.

For FM systems the signal-to-noise ratio is calculated including the effect of intermodulation noise. For digital systems the bit energy-to-noise ratio is computed and depending on the modulation system either analytic models are used to determine the bit error rate or data base models are used to determine the message error rate.

SUBROUTINE FPINT

This routine determines parametric values of footprint plot quantities as a function of ground terminal location.

Calculations are performed for each plot quantity and stored in file LFIDO. First, the maximum value of the plot quantity is found and then parametric values between the minimum value (stored in a data statement) and the maximum value are determined.

Next, the location, in terms of distance from the longitudinal axis in the scan plane, of paths that will have the parametric values of the plot quantity are determined by interpolation. A linear interpolation is used at the edges and an exponential interpolation elsewhere.

After the location of the paths corresponding to the parametric values have been determined, the ground terminal location for each path is computed and the results stored for use by the plot routine.

SUBROUTINE FPLNK

This routine determines link propagation quantities for footprint plots.

The transmitter and receiver terminal locations are defined from the footprint calculation option (downlink for KALCFP = 1 and uplink for KALCFP = 2) and the terminal systems data defined from the systems data stored for index 1. Routines GAIN and SLOBE are used to determine the antenna main beam and side lobe gains.

If a system's noise temperature was not specified as input, the ambient noise level at the receiver is computed. Then a test is made to see if noise due to fireball thermal emissions should be calculated. The fireball noise is always calculated for paths in the first scan (see description of routine FOOTPC) and the maximum temperature saved. For paths in the second or subsequent scans the fireball noise is only calculated when the maximum temperature for the first scan is greater than 250 degrees Kelvin. If fireball thermal noise is to be calculated, routine NINT is called to determine a normalized integral over the antenna pattern and routine FBTINT is called to calculate the thermal emission from the fireball.

After the noise has been determined the signal power noise density, and scintillation quantities are stored in labeled common block FPCIRC for plotting and for use by routine FPCIR to determine circuit performance. If there are angular fluctuations due to scintillation, a beam spread loss is computed and the signal strength reduced.

SUBROUTINE FPPLOT

This routine prepares footprint printer page plots of environment, propagation, and systems performance quantities.

The data to be plotted are on file LFIDO which is rewound at the start of each plot. A plot grid is determined and grid points located at 10 degree intervals in latitude and longitude for an elliptical projection. Then, for each scan (see description of routire FOOTPC for description of a scan) the latitude-longitude data defining contour points are obtained from file LFIDO and plot locations and plot symbols determined for each contour point. The contour points always start at the minimum value (QTMIN defined in a data statement). If two or more contour points are at the same plot location, the symbol for the largest contour value is used to define the point.

After the plot data have been computed the printer page plot is prepared on the summary output file (file LFNO).

An external plot file can be prepared by setting ID1 (dummy control integer in the OPTION common block) to an integer greater than zero. This can be done in the routine INPUT if it is desired to control preparation of the external file as part of the input specification. Data are written on file LFPLOT which is set to 7 in the control routine. The following describes the data written on the plot file.

For each calculation time and each fireball the ordinate and abscissa scales (applicable for each plot for that calculation time and fireball) and the number of plots are written on the file as follows:

TLAMAX, TLAMIN, TLOMAX, TLOMIN, NPLOT

where

TLAMAX, TLAMIN = maximum and minimum values of ordinate scale (north latitude in degrees)

TLOMAX, TLOMIN = maximum and minimum values of abscissa scale (east longitude in degrees)

NPLOT = number of plots for the calculation time and fireball.

Then for each plot two records are written on the file, the first record describes the plot and the grid as follows:

```
IQT,KFMFP,QTMINX,IXL,KK,((Y1(I),((X1(J=I),
KK,I=1,IXL)
```

where

IQT = plot number
- 1 = absorption (dB)
- 2 = electron density integral (cm^{-2})
- 3 = reciprocal of correlation time (s^{-1})
- 4 = scintillation index
- 5 = phase standard deviation (radians)
- 6 = bit error rate or message error rate if KFMFP=0 (s^{-1})
- = reciprocal of signal-to-noise ratio if KFMFP=1

QTMINX = minimum value of contour. Contours are given at even decades and at 3 times the even decade values (eg, 10,30,100).

IXL = number of latitudes used to define grid

KK = number of longitudes used to define grid

Y1(I),X1(J,I) = coordinates (in terms of ordinate and abscissa scales) of points showing the location of longitude traces. The points are given for each 10 degrees in latitude and longitude.

The second record describes the contours as follows:

NTEST, NOCON1, MAXPTS, ((X2(I,J),Y2(IJ),
I=1,MAXPTS),J=1,NOCON1)

where

NTEST = flag to determine if two sets of contours will be prepared.*

NCONI = number of contours

MAXPTS = number of points defining contour

X2(I,J),Y2(I,J) = coordinates (in terms of ordinate and absscissa scales) of points defining contours.

Note that if NTEST=1, the next data on the file are the data for the second set of contours (same format as for the first set of contours.) If NTEST=0, the next data on the file are for the next plot.

*As described in Volume 1 (section 3.2.3.4), the contour plots can be complicated when the projection of the longitudinal axis doubles back on itself (two points on the projection having the same latitude or longitude). For these cases two separate plots are prepared for the external plot file that should be plotted on the same grid. The actual contours would be continuous, but the separate contours illustrate the extent of effects and are relatively simple to prepare. If two sets of contours are prepared NTEST is set to 1 for the first set and to 0 for the second set.

SUBROUTINE GWPLME

This routine determines the motion of a high-altitude fireball after reaching apogee due to gravity and atmospheric wind forces. A simplified flow chart for the routine is shown in Figure 16.

The fireball motion is controlled by gravity and wind forces acting near the altitude of peak ionization. While this altitude is calculated in routine FBEN, it is simply chosen as 350 km for purposes of estimating fireball motion. The location of the point along the central field line in the fireball that is at 350 km altitude is found by calling routine MAGFLD. The number of time steps to be used is established by dividing the interval between the starting time and the final time into the minimum number of intervals that are not over 1 hour each. The date (year, month, day) and local time at the starting location and time are determined from routines ZTTOUT and DATE. Routine DATE is called to determine the UT time at the time of interest and then routine ZTTOUT is called to determine the local time at the location of peak ionization.

For each time step the local time at the location of peak ionization is found and the east-west and north-south velocities due to winds found from routine UVWD. Then the velocities due to gravity are computed and added to the wind velocities. The effects of atmospheric winds will not be included if the wind option (given as input to the WESCOM code) is exercised.

After the velocities are determined, the location of the peak ionization point at the end of the time step is found by assuming a constant velocity during the time interval. If the parameter MODE given in the call statement is zero, the location of the peak ionization at the end of the last time step is used to find the location of the point at altitude HSETL (chosen as 150 km) that is on the same field line as the peak ionization. This location is used as the debris location.

If the parameter MODE is greater than zero, the location and velocity of the peak ionization point is found at the end of the last time step. The reference altitude of the fireball is then found so that it moves from the apogee altitude specified in routine FBMHT to the altitude of peak ionization

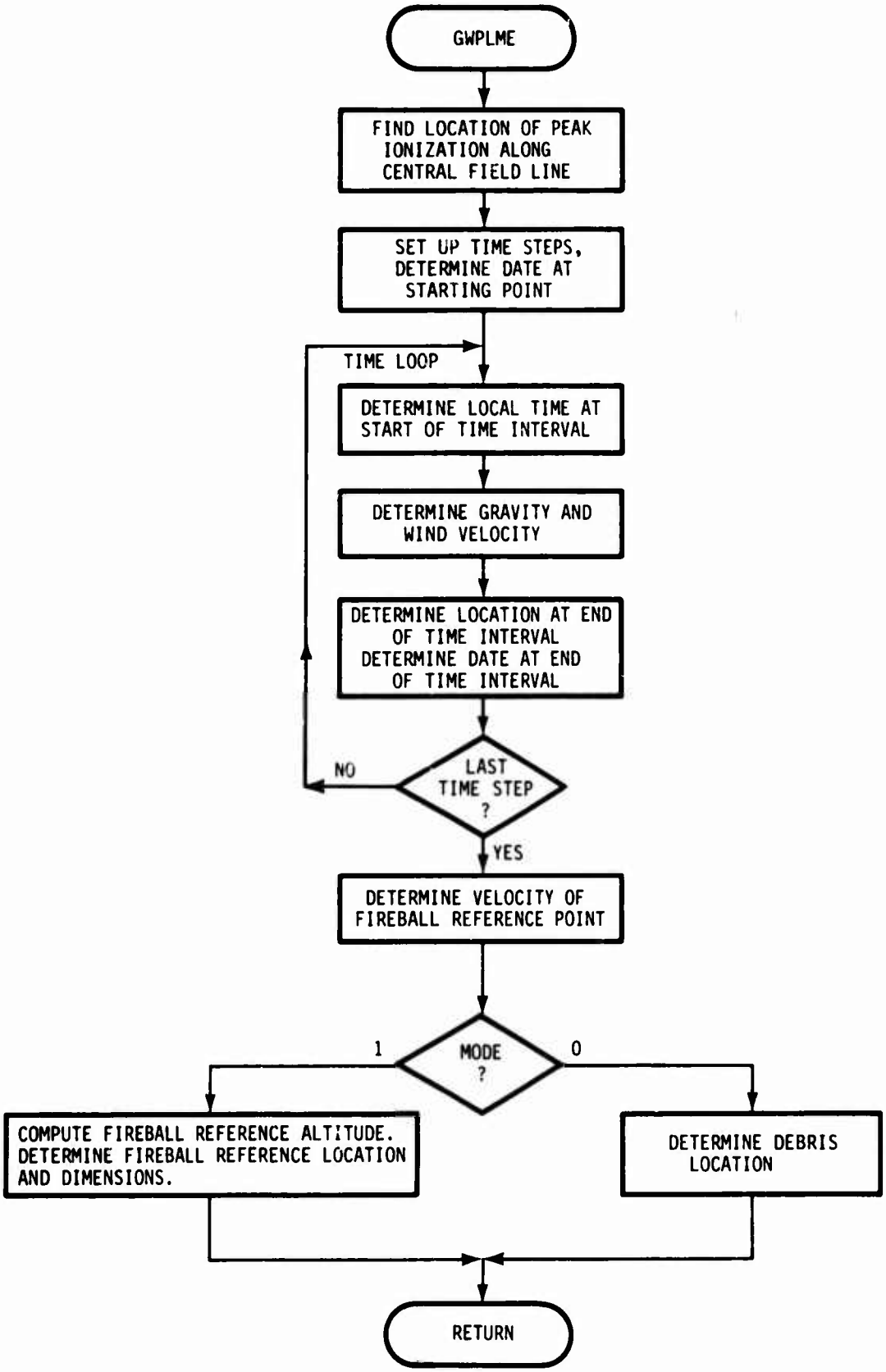

Figure 16. Flowchart for subroutine GWPLME.

by the time TMAX. The fireball transverse radius and tilt angle are also modified as the fireball moves across field lines.

SUBROUTINE HPCHEM

This routine partitions the total energy lost by loss cone, ion leak, and charge exchange particles undergoing inelastic and elastic collisions. The energy is partitioned into heavy particle thermal, electron thermal, dissociation, ionization, excitation, and radiation. A model of heavy particle prompt chemistry is also used to compute the change in number densities of N_2, O_2, $N(^4S)$, $N(^2D)$, N_2^+, O_2^+, N^+, O^+ and electrons. The routine is essentially the same as routine HPCHEM developed for ROSCOE.

SUBROUTINE INITAL

This routine determines the neutral species concentration at the end of phase 2 following a burst. The routine is similar to routine INITAL developed for ROSCOE.

First, the species concentrations after the prompt energy deposition are obtained. Then a test is made to see if the energy deposited by the burst increases the gas temperature. The temperature is computed from

$$T = \frac{p}{kn}$$

where

p = pressure (dynes cm^{-2})

k = Boltzmann's constant (1.38044×10^{-16} ergs deg^{-1})

n = total particle density including charged particles.

If the temperature has changed by more than 10 percent, routine DRATE is called to recompute the reaction rate coefficients.

SUBROUTINE INPUT

This routine reads and checks input data.

On the first call to routine INPUT routines BLKDTA and IDEFLT are called to obtain constants, parameters, and default input data. Input data to be read in for the current problem case are obtained by calling routine CARDIN which stores the data in AFILE when the ENCODE/DECODE statements are used. If these statements cannot be used, the input data can be stored in file LFIDO as indicated by comment statements in routines CARDIN and INPUT.

For each numbered input block the input data read in on the numbered input card are stored in common. If additional input data are to be read in as part of the input block, routine CARDIN is called and data obtained from input cards with a letter in column 1 as described in Volume 1 (Section 3.1.1). Tests are made to insure that sufficient data are given and that the data are in the proper order. In some cases routine TEST is called to check the magnitude of an input quantity. If errors are found, error messages are prepared.

If an orbiting satellite is specified in Input Block 3, routine ORBIT is called to obtain orbit parameters that can be used to determine the satellite position at each calculation time. In processing Input Block 6 data, routine SPCTRM is called to obtain weapon device data and radiation spectrums. Routines WOG1, WON1, and WOX1 are called to determine parametric energy deposition data for later use in computing energy deposition at specific locations.

If, after reading the input data for a problem case, there are no errors detected, routine INPUTP is called to perform preliminary processing of the data. Calculations are stopped by calling library routine EXIT when an input card with a twelve in columns 1 and 2 is given. If errors are detected in the input data for a problem case, the rest of the input cards for that and subsequent problem cases are checked for additional errors and library routine EXIT called when the input card with a twelve in columns 1 and 2 is read.

Additional control options can be read in as part of Input Block 1 and stored as one of the dummy variables in OPTION common (see Table 5). This may be useful, for example, to control preparation of user plot file.

SUBROUTINE INPUTP

This routine performs preliminary processing of input data and prepares summary output describing input data.

The major data processing performed is geometry coordinate conversion. Routine CORDTF is called to convert input coordinates to an earth-centered vector coordinate system. Tangent plane coordinates and geographic coordinates are also determined for summary output.

Data processing is performed when FM modulation is specified. Routines BB and RRMSTP are called to obtain the maximum baseband frequency and rms and peak frequency deviations. Calculations are also made to convert system noise figure to noise temperature.

SUBROUTINE MANPTS

This routine determines mandatory integration points related to beta tubes, low-altitude ionization sources, and heavy particle ionization sources.

The low-altitude ionization source points are located near the closest point of approach of the path and the ionization source. The beta particle mandatory points are located at the points where the ray path intersects the beta ionization region where the region is taken as large or larger than the actual region. If detailed propagation output is requested (input option) the beta region intersection altitudes are written out on a detailed output file (file LFDO). Note that because the beta ionization region used to determine the mandatory points is chosen conservatively (larger than the actual region) the actual beta particle ionization may occur over a smaller altitude interval along the ray path than indicated by the mandatory altitudes.

The ion-leak, loss-cone, and charge-exchange heavy particles produce ionization within geomagnetic tubes similar to the beta tube. It would be desirable to calculate mandatory points for the heavy particle ionization regions to insure calculations where effects are large and to eliminate calculations in regions where effects would be minimal. A special problem arises with the heavy particle mandatory points since they refer to the time when the energy is deposited (burst times) and not to the calculation time. Thus, the location of the air ionized by ion-leak, loss-cone, and charge-exchange particles can move due to heave such that it is not between mandatory points determined at burst time. However, since only vertical air motion is allowed in the current heave model, heavy particle ionization calculations can be minimized by only making calculations for propagation paths which are in or above the initial ionization tubes. The location of the propagation path relative to the heavy particle ionization tubes is determined by comparing their geomagnetic coordinates (latitude and longitude). If the portion of the propagation path above 100 km is in or above the ionization tubes, logical calculation flags are set to unity (ionization calculations to be performed).

SUBROUTINE NINT

This routine determines a normalized integral over the antenna pattern used in computing the receiver antenna noise temperature due to fireball thermal radiation.

The noise temperature is computed assuming that the radiation is independent of position within the antenna beam. Then the integral of receiver antenna gain over the fireball can be computed separately from fireball temperature and emissivity calculations.

The method of evaluation depends upon the location and size of the fireball with respect to the antenna pattern. If the fireball is entirely in the sidelobe, or if it is very small relative to the main lobe, the integral is approximated as

$$\int \frac{G_R}{4\pi} d\Omega \approx \frac{G_R(\phi_C)}{4\pi} \Omega_{FB}$$

where

ϕ_C = angle off beam maximum to fireball center

Ω_{FB} = solid angle subtended by fireball

G_R = receiver gain.

If the fireball extends into the main lobe and is not small relative to the main lobe,* a numerical integration procedure is employed. The main lobe is partitioned into zones by dividing the angular extent off the beam maximum into four equal rings and cutting the 360-degree extent of each ring around the beam maximum into six equal sections, except the zone which is circular. This yields a total of 19 zones. A ray through the center of each zone is checked to

*The main lobe is considered to extend one receiver antenna beamwidth off the beam maximum, at which point the $(\sin x/x)^2$ function is down about 18 dB for a mechanically steerable or phased array type antenna.

determine if it intersects the fireball. If it does, the fireball is assumed to fill the zone. The resulting numerical approximation to the desired integrals may be written as

$$\frac{G_R}{4\pi}\, d\Omega \approx \sum_j \frac{G_R(\phi_J)}{4\pi}\ \Omega_J$$

where

ϕ_J = angle off beam maximum to the ray through the center of the jth zone which intersects the fireball

Ω_J = solid angle covered by the jth zone.

In performing the integration, tests are performed to make sure that the integrals do not exceed their theoretical upper limits and that the total solid angle included in the integration does not exceed the solid angle subtended by the fireball. Once all zones have been checked, the contribution of the remaining portion of the fireball, if any, is computed by assuming that the remaining portion is in the side lobe. This integration procedure allows the several fireball geometries defined by the phenomenology model to be handled in the same basic manner, with the only major differences occurring in the relations needed to determine whether a ray through the center of a zone intersects the fireball. This determination is performed by the intersection subroutine RINTER.

SUBROUTINE PHENOM

This routine is a driver routine for the phenomenology models. A simplified flow diagram for the routine is shown in Figure 17.

The PHENOM routine is called for a specified time at which fireball, debris, and dust region parameters are desired. A test is made to determine whether any burst times are between the current calculation time and the last calculation time for which routine PHENOM was called. If there are bursts in the last time interval, time-independent scaling for each such burst is performed.

The first step in the time-independent block is to determine the atmospheric properties including those of a dipole geomagnetic field at the burst point. If the modeling option parameter MAMB is zero, the atmospheric properties are determined for conditions applicable at the origin. If MAMB is greater than zero, atmospheric quantities are determined for the particular burst location and time. Next, the time independent fireball quantities are found. For burst altitudes less than or equal to 75 km the low-altitude time-independent fireball model (routine FBMLI), the radiation output model (routine RADOUT), and the dust model (routine DUSTMI) are called. Routine RADOUT provides the total photon emission (assumed to occur instantaneously) causing photodissociation of ozone. For burst altitudes above 75-km routine FBMHI is called to determine the high-altitude time independent quantities. However, if the fireball does not rise above 250 km, a logical flag LMCF is set to 1 and the low-altitude model is used. Thus, the "low-altitude" model is used for all bursts below 75 km and for bursts above 75 km where the fireball does not rise above 250 km.

Three labeled common blocks are used to store quantities calculated in the time-independent section of routine PHENOM. Quantities used only by routines called from routine PHENOM are stored in the labeled common block PHEN. Quantities used by routines other than those called by routine PHENOM are stored in labeled common blocks BREG and DCREG. The quantities stored in block DCREG describe dust clouds.

After the time-independent quantities have been calculated for bursts occurring since the last calculation time, the time-independent test on LMCF is

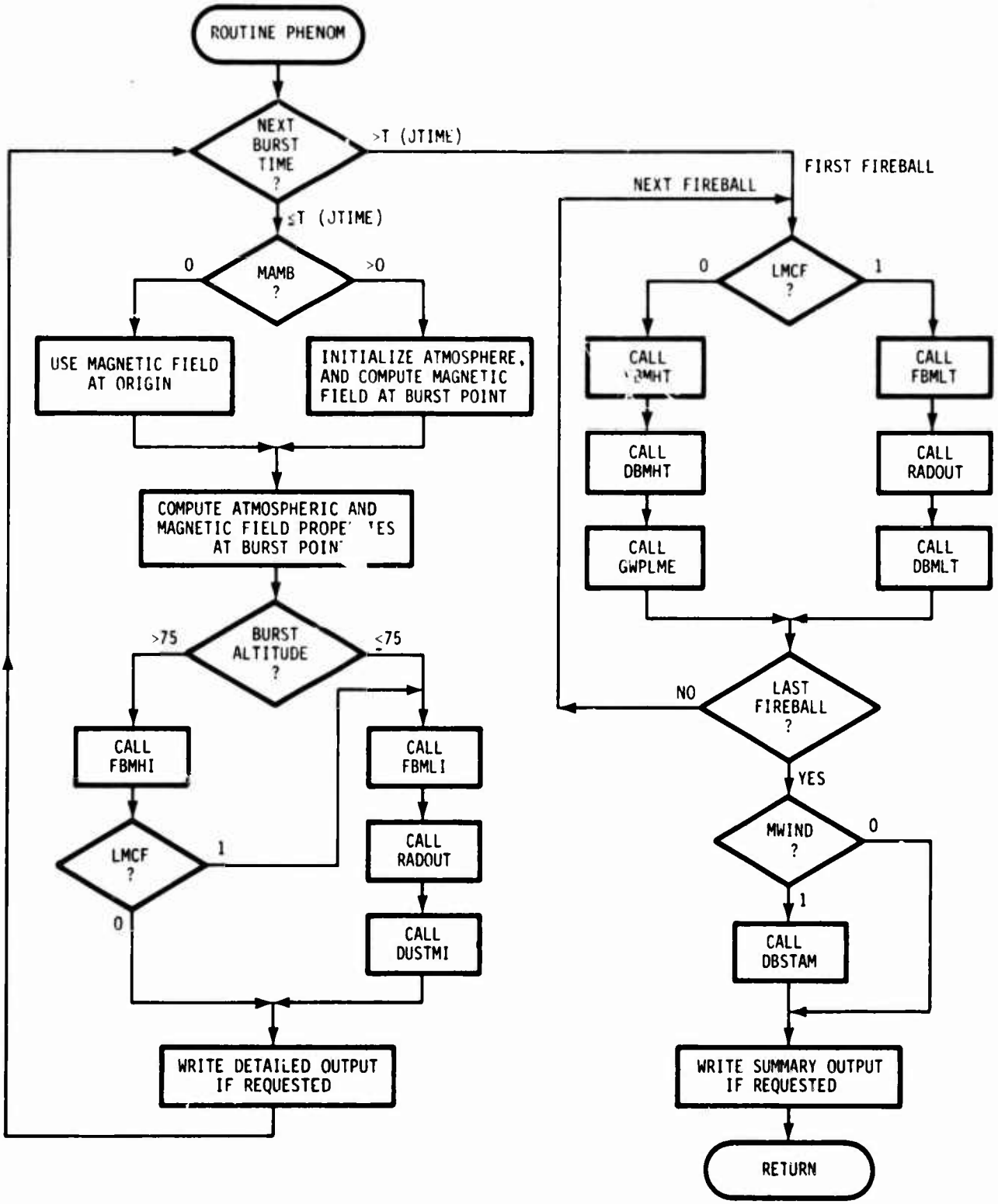

Figure 17. Flowchart for subroutine PHENOM.

made and either the low- or high-altitude models used. Routine RADOUT is called in the time-dependent section to determine the time-dependent photon emission causing photodetachment and photodissociation of negative ions. Routines DBMLT and DBMHT provide time-dependent debris region scaling for low- and high-altitude bursts respectively. Routine GWPLME determines the effects of gravity and atmospheric winds on the late-time fireball plume.

Time-independent data are stored in two labeled common blocks: block FBREG for fireball quantities and block DBREG for debris quantities. The fireball quantities are stored in terms of the fireball index (NFB) which is the same as the burst index (one fireball per burst). The debris region properties are indexed with a separate debris index (NDB). Up to four debris regions can be used to represent the debris distributions for a burst. The number of debris regions is redetermined at each calculation time and may change for a given burst. Logical indexes are stored that define the fireball, burst, and weapon device type for each debris region.

After the time-independent quantities have been computed for each fireball and debris region, the input parameter MWIND is checked. If MWIND = 1, routine DBSTAM is called to determine the effect of atmospheric winds on the late-time debris region location and geometry.

SUBROUTINE PIONF

This routine determines the species densities, pressure, and temperature at a specified location above 100 km following the energy deposition due to radiation from a specified burst. A flowchart for the routine is shown in Figure 18.

The effective slant range from the burst to the deposition point is computed first. If the specified deposition point is within the initial fireball, its effective location is assumed to be at the edge of the fireball in the same direction from the burst point.

Next, the UV source strength for each energy group is computed in the direction of the deposition point. Parameters describing the extent of the UV "burnout" region are obtained from BREG common. The location and atmospheric properties of the edge of the burnout region in the direction of the deposition point are obtained for use in the air mass-penetrated calculation for attenuation of the UV flux.

Next the properties of the air at the fireball edge are found from subroutine ATMOSU or ATMOSF, and the calculation of mass penetrated and number-density line integrals from the fireball edge to the deposition point is begun. If any point on the path is at or below 100 km, the effects of heave on the air density along the path are neglected and the mass penetrated is determined with function PMASS. If the path is entirely above 100 km, the mass penetrated is obtained by dividing the path into segments, assuming the mass density varies exponentially with slant range. In addition, neutral-particle composition terms are determined to convert mass penetrated to the line integrals of individual neutral particles.

For computing the mass penetrated in the heaved air, the path is divided into N segments, where N is defined as follows:

$$N = \text{Minimum}[K, \text{Int}(S/DMAX) + 1]$$

where

K = maximum number of path segments

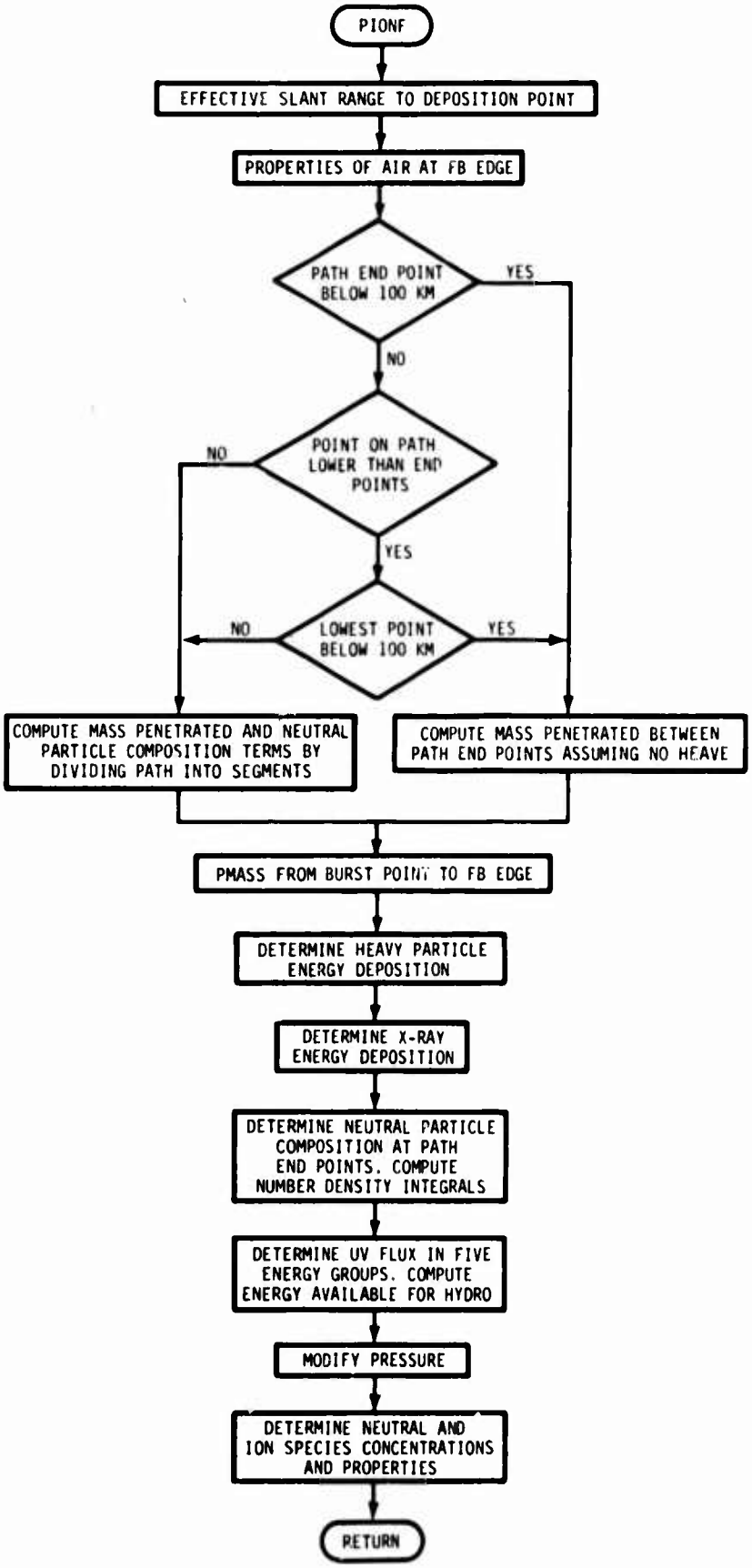

Figure 18. Flowchart for subroutine PIONF.

= N1 if lowest point is end point

= N2 if lowest point is between end points

Int(X) = largest integer smaller than X

S = path length (km)

DMAX = minimum length of path segments that can be further divided (km).

The parameter values used are N1 = 3, N2 = 3, and DMAX = 100 km. The properties of the air at the end points of each path segment are obtained from subroutine ATMOSF, and the mass penetrated along each segment is determined assuming the mass density varies exponentially with slant range. If the initial path from the fireball edge to the deposition point has a lowest point, then each segment may be further subdivided as described above.

The energy deposited by heavy particles is found by calling routine DEBRIS. Routine HPCHEM is called to determine the change in species concentrations and air properties caused by the heavy particle energy deposition. The X-ray energy deposition coefficient is found by calling routine WOXP and used to determine the energy depositied by X-rays.

The UV flux in five energy groups is determined. The species line integrals are scaled from the mass penetrated and the composition terms. The UV energy available for hydro is added to the energy deposition due to X-rays to compute a modified pressure. Then routine PCHEM is called to determine the species densities and air properties at the end of the prompt energy deposition phase.

SUBROUTINE PKOPEN

This routine is the driver routine for the propagation module. The module determines environmental quantities and propagation effects along a straight-line path (ray path) between two specified locations. A flowchart for the routine is shown in Figure 19.

The propagation module can be called with one of two calculation options determined by the logical option MODE. For MODE = 1 only absorption between the terminals is calculated. This option is used when calling routine PROPEN from the noise module. For MODE = 2 all of the propagation effects requested as part of the input specification are calculated. This option is used for the main ray path specified as input.

First, preliminary geometry calculations are made and integral quantities initialized. The geometry calculations include determination of minimum and maximum mandatory slant ranges from the transmitter terminal. These are chosen as 50 and 101 km for MODE = 1 and as 50 and 250 km for MODE = 2 if the ray path extends over these altitudes. If not, the ray path terminals are used for the mandatory points. An F-region altitude (HFTEST) is chosen for use in editing bursts as F-region ionization sources. This altitude is chosen as 200 km or the minimum altitude on the path if the ray path is above 200 km. If the ray path is entirely below 200 km, HFTEST is chosen as the highest point on the ray path.

Next, routine AMBABS is called to determine the attenuation due to water vapor and molecular oxygen in the ambient atmosphere. This calculation is not made for MODE = 1.

Next, mandatory altitudes (altitudes at which environment calculations must be made) for beta tubes, low-altitude ionization sources, and heavy particle ionization sources are obtained by calling routine MANPTS.

After the mandatory points are determined a test is made on HFTEST. If HFTEST is greater than 100 km, routine CMFEDT is called to select bursts to be used as F-region ionization sources. Routine FBINT is called to determine fireball intersections and propagation effects and routine DSTINT is called to

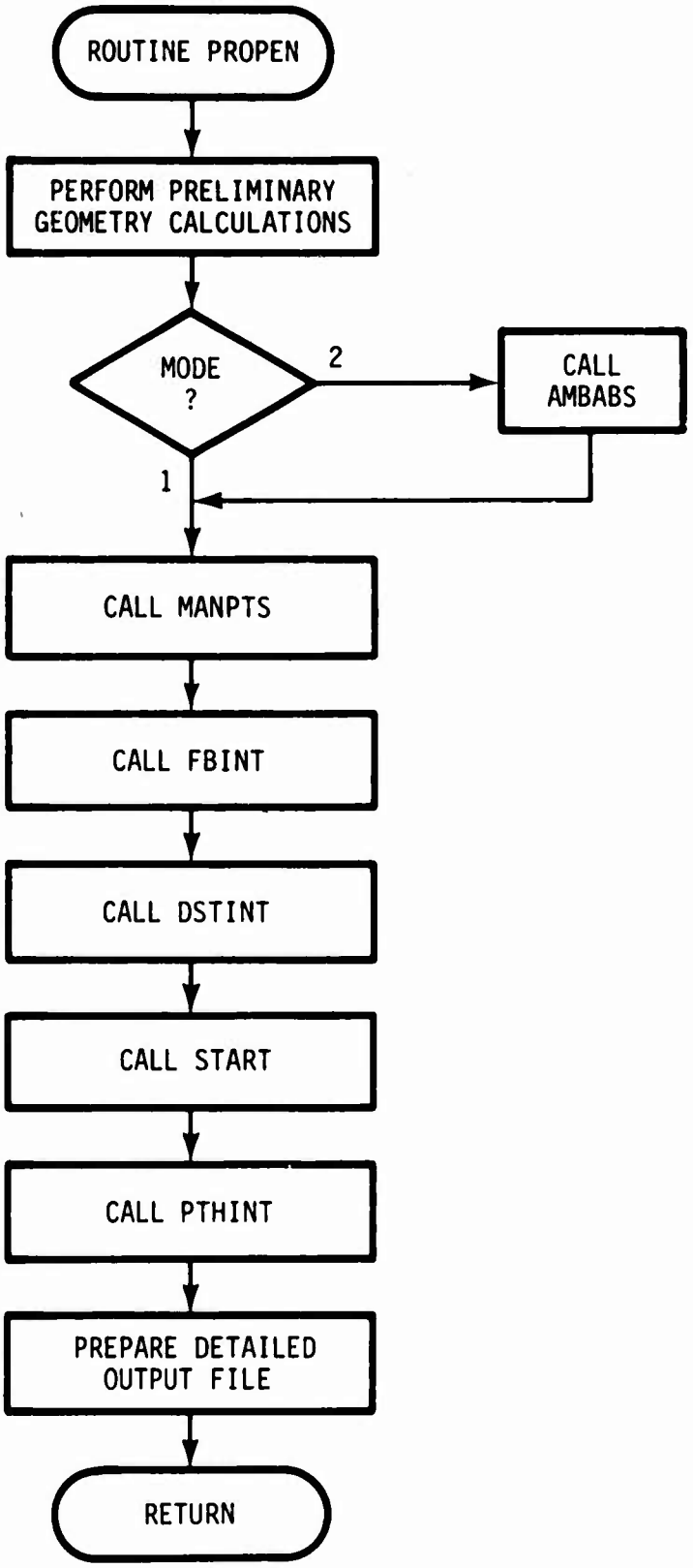

Figure 19. Flowchart for subroutine PROPEN.

determine dust cloud intersections and propagation effects.

Routine START prepares an ordered set of mandatory points from those determined above. The mandatory points are used in routine PTHINT called to obtain propagation effects along the path between terminal points. If detailed output was temporarily stored in file LFIDO, the output is transferred to file LFDO.

SUBROUTINE PSDM

This routine is the driver routine for the post-stabilization debris module for a specified debris region. Figure 20 shows a flowchart for the routine.

First the number and location of marker particle altitudes and the number and times of evaluation times are determined. The initial location of the marker particles are established. The initial location is taken as the latitude and longitude of the debris center at stabilization time and the altitudes determined above.

Next, a time loop and an altitude loop are started. For each particle the particle velocity is determined by calling routine UVWD.

After the marker particle velocities have been determined, the velocities are averaged over a mixing length by calling routine UVWAV. Then the velocities are used to determine the location of the marker particles at the end of the time interval.

At the end of the last time interval (time equal to input calculation time), routine ARRLIM is called to determine the debris location and geometry from the marker particle locations.

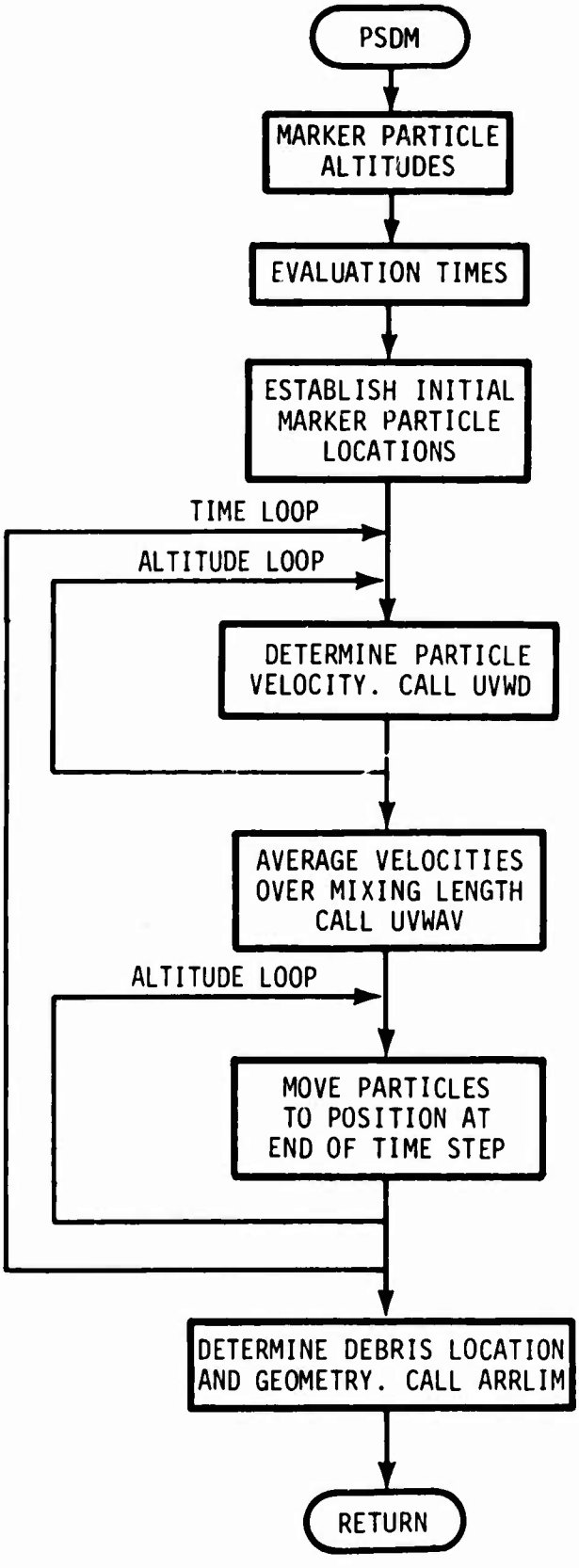

Figure 20. Flowchart for subroutine PSDM.

SUBROUTINE PTHINT

This routine determines ionization and propagation effects along a specified ray path. A flowchart for the routine is shown in Figure 21.

Calculations are started at the first mandatory point (mandatory point closest to transmitter terminal) and integral quantities are determined for the region between the first mandatory point and the transmitter. At each calculation point routine ELDEN is called to determine ionization and collision frequency terms. Then the incremental absorption and incremental phase term N_{er} where

$$N_{er} = \frac{N_e}{1 + \frac{\nu^2}{\omega^2}}$$

are calculated. For altitudes below 100 km, a nominal step size ΔS corresponding to a 2-1/2-km altitude increment is chosen (but not more than 10 km), with a minimum step size ΔS_{min} equal to half that value and a maximum step size ΔS_{max} equal to twice that value. For altitudes above 100 km, the minimum step size is increased to 2 ΔS and the maximum step size is increased to 8 ΔS. The step size starts out at ΔS_{min} and is doubled (subject to ΔS_{max}) each time the phase effects term and incremental absorption vary by less than a factor or two. If the electron density is decreasing with position, the maximum step size is allowed to continue to increase.

The phase effects term and the incremental absorption are assumed to vary linearly between two field points if the change in magnitude is less than a factor of 2; otherwise an exponential variation is assumed.

The integration from the first mandatory point to the transmitter is stopped when all of the following checks are satisfied: (1) the incremental absorption is decreasing; (2) the incremental absorption multiplied by the remaining path length is less than 0.1 dB; and, for MODE = 2 only, (3) the phase effect term is decreasing; (4) the phase effect term multiplied by the remaining path length is less than 0.1 times the current phase integral.

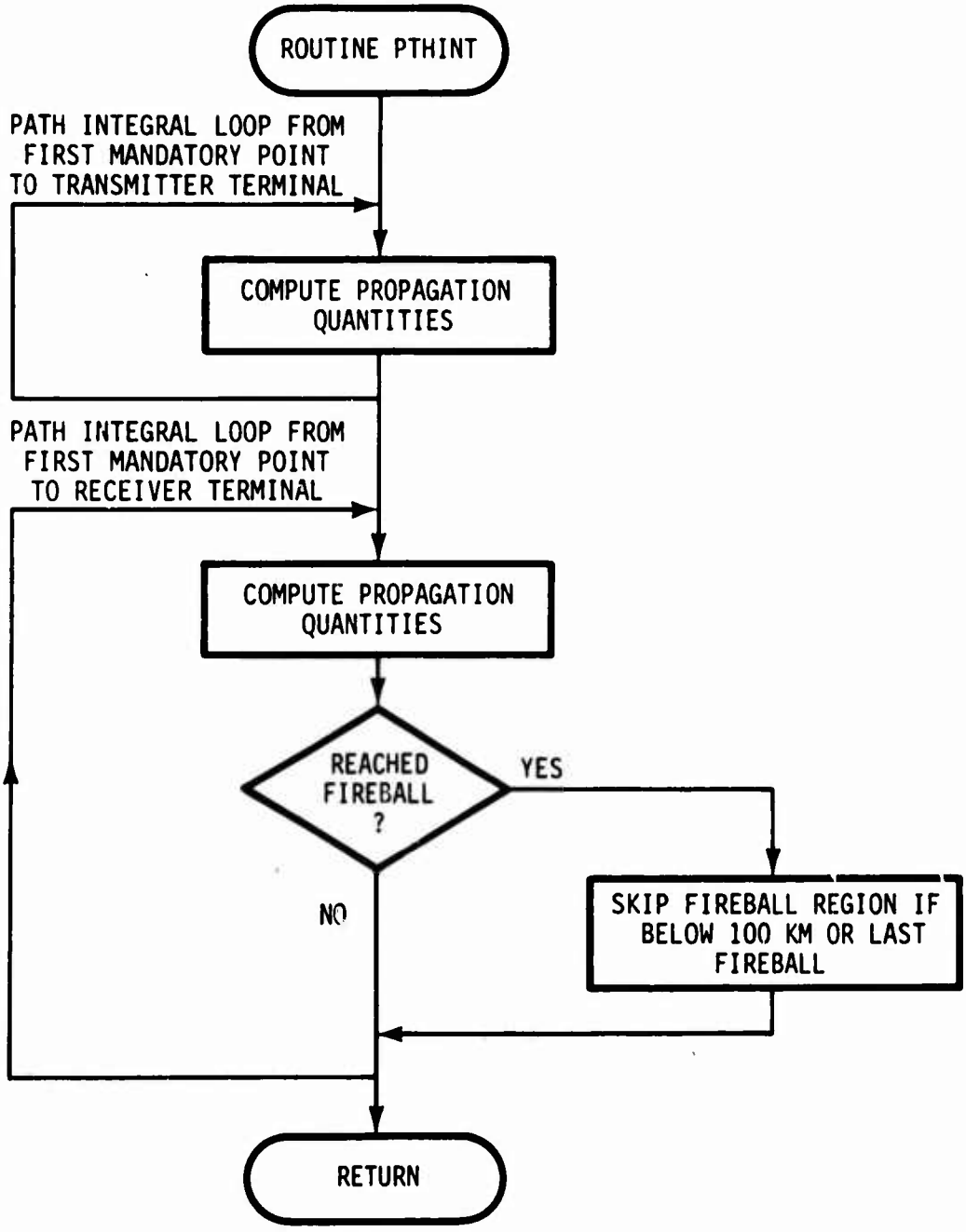

Figure 21. Flowchart for subroutine PTHINT.

The remaining path length in the above is computed as the minimum of the remaining path length and the exponential absorption and phase effect scale lengths

After the integral quantities between the first mandatory point and the transmitter have been calculated the integration between the first mandatory point and the receiver terminal is started. The procedure is the same as previously described except that the integration is not allowed to stop as long as there are any mandatory points left. At each mandatory point the step size is set to the minimum step size. Tests are made at each mandatory point to see if the mandatory point is associated with a fireball. For low-altitude fireballs and the fireball from the last high-altitude burst, the region along the path occupied by the fireball is skipped since all ionization sources are included in the fireball calculation. If there is more than one high-altitude burst, the ionization and propagation effects for the region occupied by all but the last fireball are calculated as if the earlier fireballs were not there since prompt and delayed radiation sources are not included in the region calculations.

SUBROUTINE RADOUT

This routine calculates either of two types of output for a specified burst. The first type of output approximates the radiated power in each of six frequency bands covering IR through far UV at a specified calculation time. The second type of output approximates the radiated energy resulting from the integration of power in the sixth frequency band over a time span from 10^{-6} s to approximately ten times thermal maximum. The routine is a modified version of routine RADOUT developed for ROSCOE.

Calculations are made for bursts below 100 km; however, bursts between 50 and 100 km are treated as if they were detonated at 50 km. The power and energy outputs are determined from empirical fits to RADFLO data. The power-time curve is divided into six time segments and empirical fits used for each time segment. The radiated power and [illegible]v are modified if there has been a radiation merge to account for the effect of reduced air density caused by the first fireball.

SUBROUTINE RINTER

This routine computes the intersection points between a ray path and a fireball, debris, or beta tube region. The region shapes included are the right-circular or skewed spheroid, cones, magnetically defined tubes, and the torus. The routine is a modified version of routines INTERS developed for WOE code.

The intersection with the spheroid or cone is obtained analytically. Let $\vec{S}$ be the vector from the transmitter to a point a distance s up the ray path:

$$\vec{S} = s\hat{S} \tag{1}$$

where $\hat{S}$ is the unit vector in the direction of $\vec{S}$. Let $\vec{F}$ be a vector from the transmitter to the center of the spheroid or cone and let $\vec{T}$ be a vector from the center of the spheroid or cone to a point on its symmetry axis a distance t from the center:

$$\vec{T} = t\hat{T} \tag{2}$$

where $\hat{T}$ is again a unit vector.

The vector from point s to point t is

$$\vec{D}(s,t) = \vec{F} + \vec{T}(t) - \vec{S}(s) \quad . \tag{3}$$

The distance from the point s to point t is the absolute value of $\vec{D}$:

$$\begin{aligned} D^2(s,t) &= |\vec{D}(s,t)|^2 \\ &= |\vec{F}|^2 + t^2 + s^2 + 2t(\vec{F} \cdot \hat{T}) \\ &\quad - 2s(\vec{F} \cdot \hat{S}) - 2ts(\hat{T} \cdot \hat{S}) \quad . \end{aligned} \tag{4}$$

For any distance s up the ray path, the distance from s to the closest point on the symmetry axis of the spheroid or cone can be found by minimizing $D^2(s,t)$ with respect to t:

$$0 = \frac{\partial}{\partial t} D^2(s,t)$$

$$= 2t + 2(\vec{F} \cdot \hat{T}) - 2s(\hat{T} \cdot \hat{S}) \quad .$$

Thus

$$t = (\hat{T} \cdot \hat{S})s - \vec{F} \cdot \hat{T} = as + b \quad . \tag{5}$$

Substituting t back into Equation 4 gives the shortest distance from s to the axis:

$$D_{\perp}^2 = As^2 + Bs + C \quad , \tag{6}$$

where

$$A = 1 + a^2 - 2a(\hat{T} \cdot \hat{S}) \quad ,$$

$$B = 2\left[ab - \vec{F} \cdot \hat{S} + a(\vec{F} \cdot \hat{T}) - b(\hat{T} \cdot \hat{S})\right] \quad ,$$

$$C = |\vec{F}|^2 + b^2 + 2b(\vec{F} \cdot \hat{T}) \quad .$$

The distance R from the surface to the axis of a right-circular spheroid or cone is just:

$$R^2 = A_q t^2 + B_q t + C_q \quad , \tag{7}$$

where for the spheroid

$$A_q = -R_T^2/R_L^2 \quad ,$$

$$B_q = 0 \quad ,$$

$$C_q = R_T^2 \quad ,$$

R_L = semi-axis along symmetry axis,

R_T = semi-axis transverse to symmetry axis,

and for the cone

$$A_q = \tan^2 \theta \quad ,$$

$$B_q = 2 R_o \tan \theta \quad ,$$

$$C_q = R_o^2 \quad ,$$

$$R_o = \text{cone radius at center} \quad ,$$

$$\theta = \text{cone half-angle} \quad .$$

Writing R as a function of s through Equation 5 and subtracting it from $D_\perp^2$ gives a quadratic equation in s:

$$D_\perp^2 - R^2 + A's^2 + B's + C' = 0 \quad , \tag{8}$$

where

$$A' = A - a^2 A_q \quad ,$$

$$B' = B - 2\,abA_q - aB_q \quad ,$$

$$C' = C - b^2 A_q - bB_q - C_q \quad .$$

The solutions for the intersection points are then

$$S = -(B'/2A') \pm \sqrt{(B'/2A')^2 - C'/A'} \quad , \tag{9}$$

where an intersection exists only if the radical is real. Two special cases may arise. If $A' = 0$, which corresponds to the ray path being parallel to part of a cone surface, then there is only one intersection given by

$$S = -C'/B' \tag{10}$$

If B' is positive the intersection is an exit point, and if B' is negative, the intersection is an entry point. If B' and A' are zero, the ray path is parallel to a cylinder and is wholly within or without depending on whether C' is negative or positive, respectively.

To calculate the intersection of the ray path with a skewed spheroid or cone, Equation 5 must be replaced with a relation between s and t such that point s is horizontal to t. This is given by

$$s = s_p + \frac{\cos \tau}{\sin E_s} t \quad , \tag{11}$$

where

s_p = slant range up path to horizontal plane through region center

τ = region symmetry axis tilt angle from vertical

E_s = angle between ray path and horizontal plane through region center.

Thus a and b in Equation 5 are replaced by

$$a = \frac{\sin E_s}{\cos \tau} \quad , \tag{12}$$

$$b = -s_p \frac{\sin E_s}{\cos \tau} \quad ,$$

and the rest of the calculations are the same except that Equation 7 represents the corresponding skew figures (R is horizontal).

The equation for the intersection of a ray path and a torus is a quartic expression in the path variable and is tedious to solve. It is simple, however, to determine whether or not a given point is inside the torus. This allows a fast numerical procedure for finding the intersection points. The numerical iteration for the torus intersection points is carried out in subroutine TOROID which is called from RINTER.

Intersections with magnetic field line defined tubes are also obtained numerically via iteration techniques. The function TUBE calculates the intersection points. If any of the regions are truncated, the routine calculates the intersection of the ray path with the bottom and top altitudes and adjusts the previously obtained intersection points if necessary.

Intersections with beta tubes are found by first determining the closest point of approach of the ray path vector and a vector located at 80 km on the geomagnetic field line through the center of the debris region having the direction of the geomagnetic field. The closest point of approach is used as the starting point in routine TUBE to determine intersection points. First, routine TUBE is called with a single point calculation option to determine whether the closest point of approach is within the tube. If it is within the tube in either the debris region or the conjugate of the debris region, routine TUBE is called again with an option to allow iterating to find the ray path and tube boundary intersections.

Use of the closest point of approach of the ray path with a straight line approximation to the geomagnetic field to obtain the starting point and initial test of whether any intersection exists is a reasonable approximation for beta particle ionization where the interest is in a relatively small altitude region. However, for field-aligned fireballs the intersection of interest can occur over a large altitude region. For this case, the region (field-aligned fireball region) is broken up into five altitude segments and tests made for intersections (in both the local and conjugate region) for each segment.

SUBROUTINE SATC

This routine is the driver routine for satellite communication calculations. A simplified flowchart for the routine is shown in Figure 22.

First, the ground terminal locations are determined from either locations given as input or from routine TORBIT if ground terminal motion is specified. For KALCS=1 or 2 (multiple link circuits) routine SLINK is called to determine whether propagation and noise calculations have been previously made for the link. If they have, the calculation flags LFLAG and NFLAG are set to 1. For KALCS=2 (down link broadcast option) each link is different and circuit calculations are made for each link.

Next path geometry quantities are defined for the link and if MAMB (input option) is 1 atmospheric and magnetic field routines are initialized at the location of the path.

Propagation and noise quantities are calculated and stored for up to 41 links. Link indexes LLINK and LNINK are used to store and retrieve propagation and noise data. If LFLAG=1, propagation quantities for the link have been previously calculated and the call to routine PROPEN is skipped. If NFLAG=1, noise calculations have been made. However, if NFLAG=0 further tests (not shown in Figure 22) are required to determine if noise calculations are required. If they are, routine ANTND is called. If the receiver is being jammed, routine JAMND is called to determine the jamming noise density. Then, routine SATLNK is called to define link performance and prepare summary output.

After calculations for all the links in a particular circuit have been performed, routine SATCIR is called to determine circuit performance quantities.

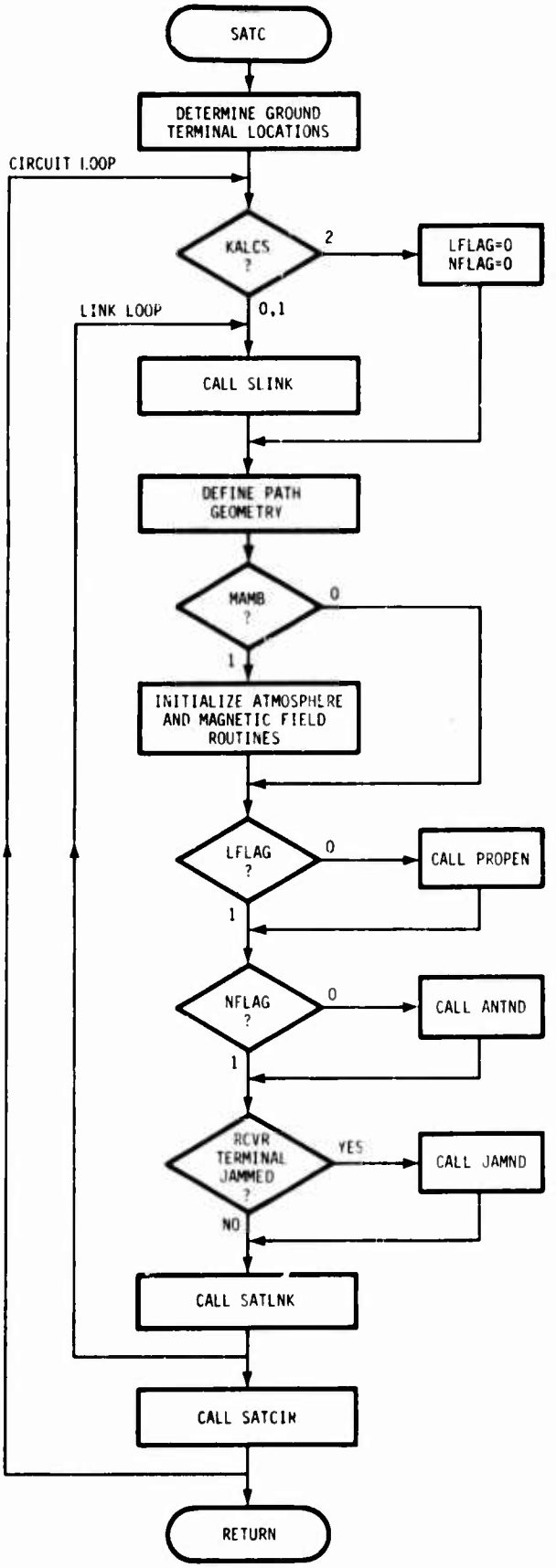

Figure 22. Flowchart for subroutine SATC.

SUBROUTINE SATCIR

This routine determines performance quantities for satellite communication circuits. A simplified flow diagram for the routine is shown in Figure 23.

Circuit performance for free space conditions is calculated at the first calculation time. At subsequent calculation times circuit performance is only calculated for disturbed conditions. For either free space (KAMBF=1) or disturbed (KAMBF=0) conditions a link loop is established and the signal-to-noise ratio calculated. If there is no signal processing, the ratio is an effective ratio for the links in the circuit. If there is signal processing, the signal-to-noise ratio and bit energy-to-noise ratio are computed for each link. For FM systems an FM improvement factor is computed and for disturbed conditions the intermodulation noise due to dispersion is determined.

Next, the bit error rate (analytic models) or message error rate (data base models) are calculated for digital modulation system (see Figure 24). If there is signal processing, the error rates are computed for each link and then combined into an effective error rate for the circuit. After the error rates are computed for disturbed conditions summary output is prepared and written on file LFNO.

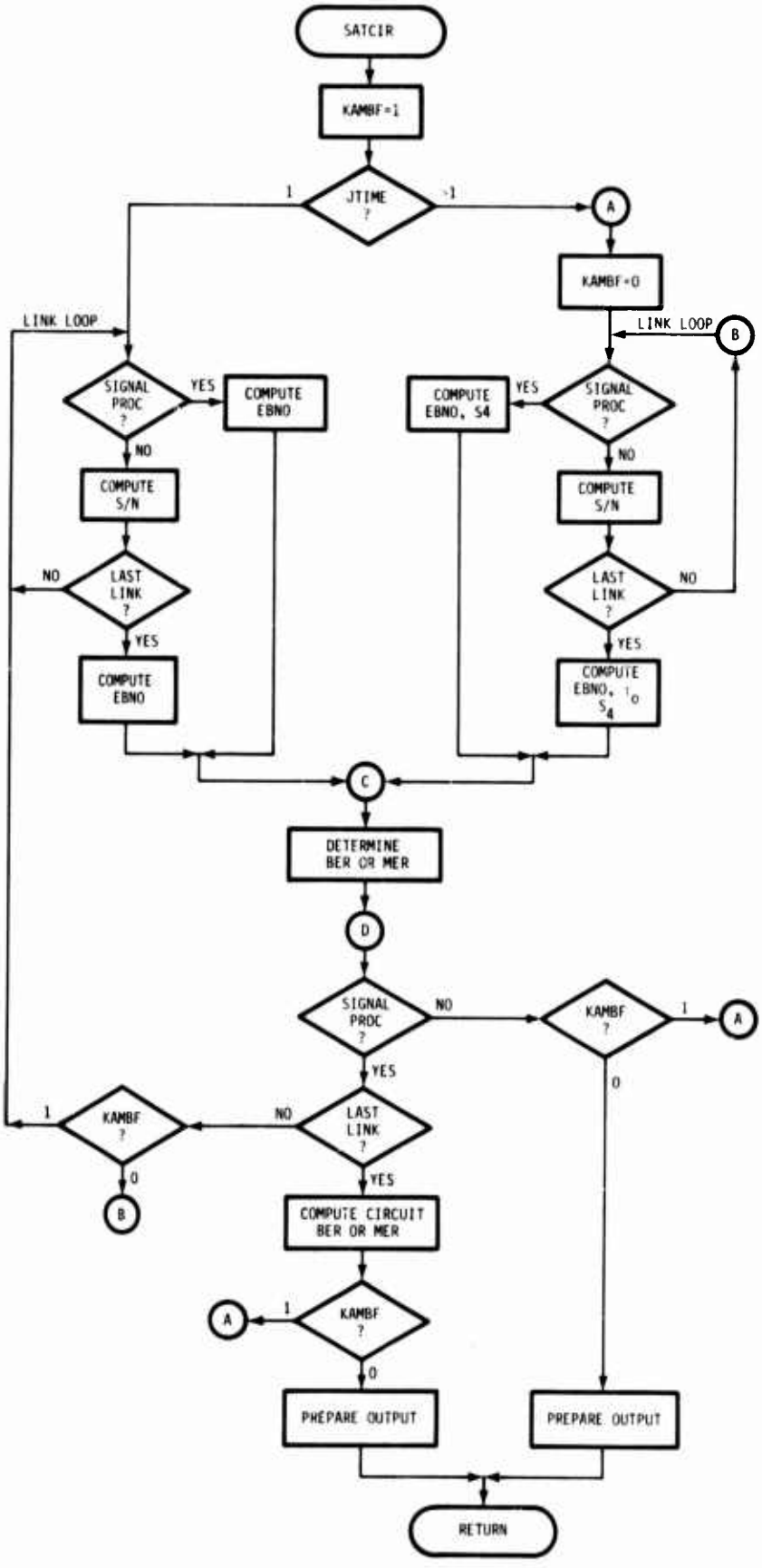

Figure 23. Flowchart for subroutine SATCIR.

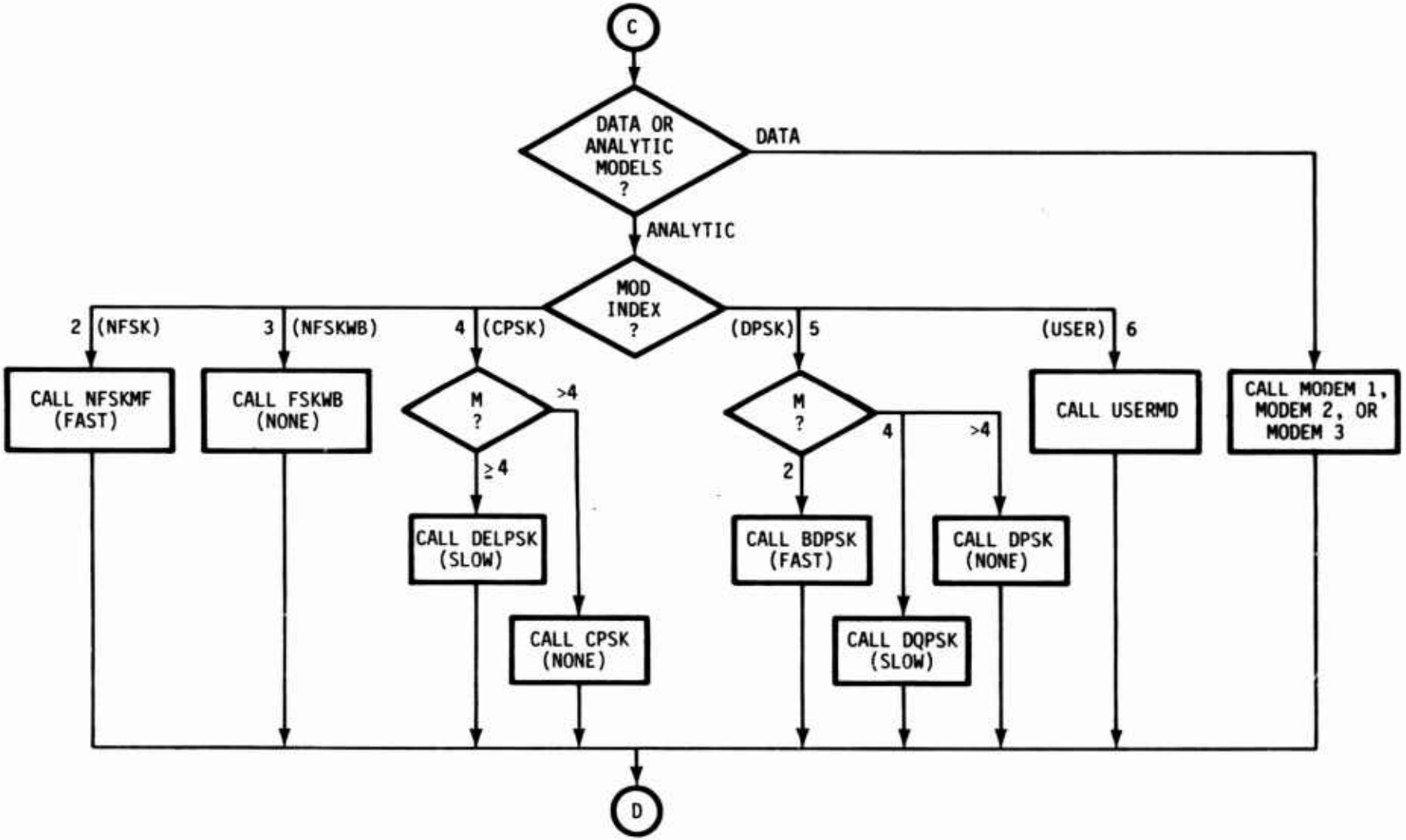

Figure 24. Detail of error rate calculation in Figure 23.

SUBROUTINE SATLNK

This routine determines link propagation quantities for satellite communication circuits.

First, the transmitter, receiver, and antenna parameters are obtained for the link and quantities required to compute received signal and noise are determined. Routines GAIN and SLOBE are used to determine the antenna main beam and side lobe gains.

Next, the received signal and noise for free space and disturbed conditions are determined and stored in common block SIGCOM. Scintillation quantities for the link are also defined and stored. If there is beam spread loss due to scintillation, the received signal for disturbed conditions is reduced.

Output describing propagation quantities for the link is prepared and written on file LFNO if level 1 summary output is requested.

ROUTINE SPECDP

This routine determines effects of prompt radiation on neutral species concentrations at a specified altitude below 100 km at a specified calculation time. The routine is essentially the same as routine SPECDP developed for ROSCOE.

First mean values for O_3 and α are computed. Then the neutral species concentrations are computed.

Next, the species concentrations are limited by the ambient neutral species values. For nighttime conditions this only involves limiting the values of O, NO, and $O_2(^1\Delta)$. For daytime a new ambient model consistent with the amount of odd nitrogen produced is first determined. This requires an iterative procedure which has been chosen to minimize the number of iterations. Then the value of odd oxygen ($O+O_3$) is allowed to decay from the burst produced value toward the new, modified ambient value. The value of odd oxygen at the time of interest is used to determine the other species by assuming photochemical equilibrium. An iterative procedure is required to determine the photoequilibrium distribution of species consistent with the values of odd oxygen and odd nitrogen. The decay or build up of species is not allowed to surpass the modified ambient values.

SUBROUTINE SLINK

This routine determines whether propagation or noise calculations have been previously made for a link.

The matrix INDEX stores indexes used to identify propagation quantities. Propagation quantities for up to 41 links can be stored. If propagation quantities have not been calculated, the link index is incremented and a propagation calculation flag (LFLAG) is set to require propagation calculations. If propagation calculations for the link have been made, the link index is stored in INDEX. Tests are also made to see if noise calculations have been made and a noise calculation flag is set. Additional noise tests and a noise index are calculated in routine SATC.

If L=1 (first circuit), propagation and noise calculations are required. For L>1 propagation calculations are not required for JLINK=2 (satellite-to-satellite link), since there is only one such link. For all other links, tests are made to see if propagation and noise calculations have been made. First, tests are made to see if a previous link has the same terminal locations. If it does and the propagation frequencies are the same, propagation calculations are the same for both links. If the propagation frequencies are the same and the receiver antennas are the same, noise calculations are the same for both links unless one link is an up link and the other is a down link.

SUBROUTINE START

This routine prepares an array of mandatory points, ordered in increasing slant range from the transmitter, which must be considered when integrating propagation quantities along a path.

Mandatory points are placed at the minimum and maximum slant range as computed in routine PROPEN. Mandatory points are placed at the entrance and exit points of the ray path with beta tubes and fireballs and near low-altitude gamma sources. In preparing the mandatory points for fireballs, all fireballs from high-altitude bursts except the most recent burst are skipped. The mandatory points are contained in the mandatory point array SMP(I). For each mandatory point SMP(I) there are two integer tags in the array INDMP (2,100). The code for INDMP is

INDMP(1,I)	=	0	Not used.
	=	J	Fireball index associated with the intersection points
INDMP(2,I)	=	1000	Beta tube, low-altitude gamma points
	=	2000	Fireball entry point
	=	2002	Fireball exit point

SUBROUTINE WOG1

This routine determines energy deposition coefficient for prompt and delayed gamma rays. The routine is essentially the same as routine WOG1 developed for ROSCOE.

The effective normalized energy deposition coefficient for the spectrum UBARGP(I,K) is calculated and stored for each of 15 different mass depths, PMG(K). Note that index I specifies device type, index J specifies spectral energy group, and index K specifies mass depth. The double-dimensional array UG(K,J) stores energy deposition coefficient data from the ATR code for monochromatic energy sources at photon energy corresponding to spectral group J and at mass depths PMG(K). The calculation of UBARGP is a convolution of this monochromatic data with the energy spectrum. The effective normalized energy deposition coefficient for the delayed spectrum, UBARGD(I,K), is calculated and stored for each of the 15 mass depths in the same manner as for the prompt energy deposition coefficient.

The parameters FEDG(I) and FTHERM(I) for device type I are made available to the other phenomenology models through labeled common block DEVICE. The tabular data UBARGP(I,K), UBARGD(I,K), and PMG(K) are transmitted to subroutines WOGP and WOGD through labeled common block WOG.

SUBROUTINE WON1

This routine determines energy deposition coefficients for neutron energy deposition. The routine is essentially the same as routine WON1 developed for ROSCOE.

First the energy deposited by each spectral group, the total energy deposited, and a mean neutron cross section are computed. Then the yield fraction in deposited neutron energy is calculated as the total neutron energy deposited divided by the total weapon yield. Note that this differs from the kinetic energy yield fraction given as input in that it includes both the kinetic and capture energies.

The folded energy deposition coefficients for prompt, UBARNP, elastic scatter, UBARNE, and capture, UBARNC, phases of the energy deposition are computed for each mass depth PMN(K). This would form a complete set of data to determine the prompt and delayed energy deposition. However, since the computation of the power law exponent for the elastic scatter deposition phase requires a time-consuming iterative solution, we make that calculation here for each mass depth PMN(K). The value of the exponent for any mass depth is found later by interpolation. The parameters UBARNP, UBARNC, and the exponent EXPQNE then form a complete set and are passed to subroutines WONP and WOND through WON common, along with the mass penetrated array PMN. The yield fraction FEDN(I) is made available to the other phenomenology models through DEVICE common.

SUBROUTINE WOX1

This routine determines energy deposition coefficients for X-rays. The routine is essentially the same as routine WOX1 developed for ROSCOE.

In addition to the effective energy deposition coefficient, $\bar{\mu}_x$, an X-ray containment factor, f_{cx}, is also computed for use in the fireball phenomenology model as

$$f_{cx}(M) = \int_0^M \bar{\mu}_x(m)\, dm \quad , \tag{1}$$

where M is the air mass penetrated (gm/cm^3). The function $f_{cx}(M)$ is the fraction of the X-ray flux that would be absorbed within a mass depth M.

Because the X-ray transport may vary significantly from one spectrum to another, the deposition coefficient, URARX, and the containment factor, FCONTX, are precomputed and stored for a different set of air masses for each device type. The set of air masses for device type I are given by PMXBAR(I)*PMXR(K), K = 1,15. The normalizing mass PMXBAR(I) is defined by

$$\text{PMXBAR(I)} = \sum_{j=1}^{18} (F_x)_j M_{oj} \quad gm\ cm^{-3} \tag{2}$$

where $(F_x)_j$ is the energy in spectral group j for device type I and M_{oj} is the mass normalization for spectral group j. The 15 values of PMXR(K) are defined as follows:

K	PMXR	K	PMXR	K	PMXR
1	0.001	6	0.4	11	2.0
2	0.01	7	0.6	12	3.0
3	0.05	8	0.8	13	4.0
4	0.1	9	1.0	14	5.0
5	0.2	10	1.5	15	10.0

The integral of the X-ray spectrum, ETOTAL, and the normalizing mass PMXBAR(I) are computed for each normalized mass depth. Then X-ray energy deposition coefficient, UBARX, and the containment factor FCONTX, are computed. (An exponential algorithm is employed to perform the integral in Equation 1.) The normalizing mass PMXBAR, and the tabulated values for PMXR, UBARX, and FCONTX are placed in WOX common for later interpolation by routines WOXP and WOXC. The yield fraction, FEDX, is made available to the other phenomenology routines through labeled common DEVICE.

DISTRIBUTION LIST

DEPARTMENT OF DEFENSE

Assistant Secretary of Defense
Comm, Cmd, Cont & Intell
ATTN: Dir of Intelligence Sys, J. Babcock

Assistant to the Secretary of Defense
Atomic Energy
ATTN: Executive Assistant

Command & Control Technical Center
ATTN: C-312, R. Mason
ATTN: C-650, G. Jones
ATTN: C-650
3 cy ATTN: C-650, W. Heidig

Defense Communications Agency
ATTN: Code 205
ATTN: Code 480
ATTN: Code 810, J. Barna
ATTN: Code 101B
ATTN: Code 480, F. Dieter

Defense Communications Engineer Center
ATTN: Code R820
ATTN: Code R410, N. Jones
ATTN: Code R410, R. Craighill
ATTN: Code R410, J. McLean
ATTN: Code R123

Defense Intelligence Agency
ATTN: DC-7D, W. Wittig
ATTN: DB-4C, E. O'Farrell
ATTN: HQ-TR, J. Stewart
ATTN: DB, A. Wise
ATTN: DT-5
ATTN: DT-1B

Defense Nuclear Agency
ATTN: NATD
ATTN: RAEE
ATTN: STNA
ATTN: NAFD
3 cy ATTN: RAAE
4 cy ATTN: TITL

Defense Technical Information Center
12 cy ATTN: DD

Field Command
Defense Nuclear Agency
ATTN: FCPR

Field Command
Defense Nuclear Agency
Livrmore Branch
ATTN: FCPRL

Interservice Nuclear Weapons School
ATTN: TTV

Joint Chiefs of Staff
ATTN: C3S
ATTN: C3S, Evaluation Office

DEPARTMENT OF DEFENSE (Continued)

Joint Strategic Target Planning Staff
ATTN: JLA
ATTN: JLTW-2

National Security Agency
ATTN: R-52, J. Skillman
ATTN: W-32, O. Bartlett
ATTN: B-3, F. Leonard

NATO School (SHAPE)
ATTN: U.S. Documents Officer

Under Secretary of Defense for Rsch & Engrg
ATTN: Stratetic & Space Sys (OS)

WWMCCS System Engineering Org
ATTN: J. Hoff

DEPARTMENT OF THE ARMY

Assistant Chief of Staff for Automation & Comm
Department of the Army
ATTN: DAAC-ZT, P. Kenny

Atmospheric Sciences Laboratory
U.S. Army Electronics R&D Command
ATTN: DELAS-EO, F. Niles

BMD Advanced Technology Center
Department of the Army
ATTN: ATC-T, M. Capps
ATTN: ATC-O, W. Davies

BMD Systems Command
Department of the Army
2 cy ATTN: BMDSC-HW

Deputy Chief of Staff for Operations & Plans
Department of the Army
ATTN: DAMO-RQC

Electronics Tech & Devices Lab
U.S. Army Electronics R&D Command
ATTN: DELET-ER, H. Bomke

Harry Diamond Laboratories
Department of the Army
ATTN: DELHD-N-RB, R. Williams
ATTN: DELHD-N-P, F. Wimenitz
ATTN: DELHD-I-TL, M. Weiner
ATTN: DELHD-N-P

U.S. Army Comm-Elec Engrg Instal Agency
ATTN: CCC-CED-CCO, W. Neuendorf
ATTN: CCC-EMEO-PED, G. Lane

U.S. Army Communications Command
ATTN: CC-OPS-WR, H. Wilson
ATTN: CC-OPS-W

U.S. Army Communications R&D Command
ATTN: DRDCO-COM-RY, W. Kesselman

DEPARTMENT OF THE ARMY (Continued)

U.S. Army Foreign Science & Tech Ctr
ATTN: DRXST-SD

U.S. Army Material Dev & Readiness Cmd
ATTN: DRCLDC, J. Bender

U.S. Army Missile Intelligence Agency
ATTN: J. Gamble

U.S. Army Nuclear & Chemical Agency
ATTN: Library

U.S. Army Satellite Comm Agency
ATTN: Document Control

U.S. Army TRADOC System Analysis Actvy
ATTN: ATAA-PL
ATTN: ATAA-TCC, F. Payan, Jr
ATTN: ATAA-TDC

DEPARTMENT OF THE NAVY

Joint Cruise Missiles Project Ofc
Department of the Navy
ATTN: JCMG-707

Naval Air Development Center
ATTN: Code 6091, M. Setz

Naval Air Systems Command
ATTN: PMA 271

Naval Electronic Systems Command
ATTN: PME 117-20
ATTN: PME 117-211, B. Kruger
ATTN: PME 106-13, T. Griffin
ATTN: Code 3101, T. Hughes
ATTN: PME-117-2013, G. Burnhart
ATTN: PME 106-4, S. Kearney
ATTN: Code 501A

Naval Intelligence Support Ctr
ATTN: NISC-50

Naval Ocean Systems Center
ATTN: Code 5322, M. Paulson
ATTN: Code 532
ATTN: Code 532, J. Bickel
3 cy ATTN: Code 5324, W. Moler
3 cy ATTN: Code 5323, J. Ferguson

Naval Research Laboratory
ATTN: Code 7500, B. Wald
ATTN: Code 4187
ATTN: Code 7950, J. Goodman
ATTN: Code 4780, S. Ossakow
ATTN: Code 7550, J. Davis
ATTN: Code 4700, T. Coffey

Naval Space Surveillance System
ATTN: J. Burton

Naval Surface Weapons Center
ATTN: Code F31

Naval Telecommunications Command
ATTN: Code 341

DEPARTMENT OF THE NAVY (Continued)

Office of Naval Research
ATTN: Code 420
ATTN: Code 421
ATTN: Code 465

Office of the Chief of Naval Operations
ATTN: OP 981N
ATTN: OP 65
ATTN: OP 941D

Strategic Systems Project Office
Department of the Navy
ATTN: NSP-2722, F. Wimberly
ATTN: NSP-2141
ATTN: NSP-43

DEPARTMENT OF THE AIR FORCE

Aerospace Defense Command
Department of the Air Force
ATTN: DC, T. Long

Air Force Geophysics Laboratory
ATTN: OPR, H. Gardiner
ATTN: OPR-1
ATTN: LKB, K. Champion
ATTN: OPR, A. Stair
ATTN: S. Basu
ATTN: PHP
ATTN: PHI, J. Buchau
ATTN: R. Thompson

Air Force Technical Applications Ctr
ATTN: TN

Air Force Weapons Laboratory
Air Force Systems Command
ATTN: NTYC
ATTN: SUL
ATTN: NTN

Air Force Wright Aeronautical Lab
ATTN: A. Johnson
ATTN: W. Hunt

Air Logistics Command
Department of the Air Force
ATTN: OO-ALC/MM, R. Blackburn

Air University Library
Department of the Air Force
ATTN: AUL-LSE

Air Weather Service, MAC
Department of the Air Force
ATTN: DNXP, R. Babcock

Assistant Chief of Staff
Intelligence
Department of the Air Force
ATTN: INED

Assistant Chief of Staff
Studies & Analyses
Department of the Air Force
ATTN: AF/SASC, C. Rightmeyer
ATTN: AF/SASC, W. Keaus

DEPARTMENT OF THE AIR FORCE (Continued)

Ballistic Missile Office
Air Force Systems Command
ATTN: MNNXH, J. Allen
ATTN: MNNL, S. Kennedy

Deputy Chief of Staff
Operations Plans and Readiness
Department of the Air Force
ATTN: AFXOKT
ATTN: AFXOXFD
ATTN: AFXOKCD
ATTN: AFXOKS

Deputy Chief of Staff
Research, Development, & Acq
Department of the Air Force
ATTN: AFRDSP
ATTN: AFRDS
ATTN: AFRDSS

Electronic Systems Division
ATTN: DCKC, J. Clark

Electronic Systems Division
ATTN: XRW, J. Deas

Electronic Systems Division
ATTN: YSM, J. Kobelski
ATTN: YSEA

Foreign Technology Division
Air Force Systems Command
ATTN: NIIS Library
ATTN: TQTD, B. Ballard

Headquarters Space Division
Air Force Systems Command
ATTN: SKA, D. Bolin
ATTN: SKY, C. Kennedy

Headquarters Space Division
Air Force Systems Command
ATTN: YZJ, W. Mercer

Headquarters Space Division
Air Force Systems Command
ATTN: E. Butt

Rome Air Development Center
Air Force Systems Command
ATTN: TSLD
ATTN: OCS, V. Coyne

Rome Air Development Center
Air Force Systems Command
ATTN: EEP

Strategic Air Command
Department of the Air Force
ATTN: ADWATE, B. Bauer
ATTN: DCX
ATTN: DCXT
ATTN: NRT
ATTN: DCXR, T. Jorgensen
ATTN: XPFS
ATTN: XPFS, B. Stephan

OTHER GOVERNMENT AGENCIES

Central Intelligence Agency
ATTN: OSWR/NED

Department of Commerce
National Bureau of Standards
ATTN: Sec Ofc for R. Moore

Department of Commerce
National Oceanic & Atmospheric Admin
ATTN: R. Grubb

Institute for Telecommunications Sciences
ATTN: W. Utlaut
ATTN: A. Jean
ATTN: L. Berry

U.S. Coast Guard
Department of Transportation
ATTN: G-DOE-3/TP54, B. Romine

DEPARTMENT OF ENERGY CONTRACTORS

EG&G, Inc
ATTN: D. Wright
ATTN: J. Colvin

Lawrence Livermore National Lab
ATTN: Tech Info Dept Library
ATTN: L-389, R. Ott
ATTN: L-31, R. Hager

Los Alamos National Scientific Lab
ATTN: MS 664, J. Zinn
ATTN: J. Wolcott
ATTN: E. Jones
ATTN: D. Westervelt
ATTN: R. Taschek
ATTN: D. Simons
ATTN: R. Jeffries
ATTN: P. Keaton
ATTN: MS 670, J. Hopkins

Sandia Laboratories
Livermore Laboratory
ATTN: B. Murphey
ATTN: T. Cook

Sandia National Lab
ATTN: D. Thornbrough
ATTN: 3141
ATTN: D. Dahlgren
ATTN: Space Project Div
ATTN: Org 1250, W. Brown
ATTN: Org 4241, T. Wright

DEPARTMENT OF DEFENSE CONTRACTORS

Aerospace Corp
ATTN: J. Straus
ATTN: S. Bower
ATTN: T. Salmi
ATTN: D. Olsen
ATTN: V. Josephson
ATTN: R. Slaughter
ATTN: I. Garfunkel
ATTN: N. Stockwell

DEPARTMENT OF DEFENSE CONTRACTORS (Continued)

University of Alaska
ATTN: Technical Library
ATTN: N. Brown
ATTN: T. Davis

Analytical Systems Engineering Corp
ATTN: Radio Sciences

Analytical Systems Engineering Corp
ATTN: Security

Barry Research Corporation
ATTN: J. McLaughlin

BDM Corp
ATTN: T. Neighbors
ATTN: L. Jacobs

Berkeley Research Associates, Inc
ATTN: C. Prettie
ATTN: J. Workman

BETAC
ATTN: J. Hirsch

Boeing Co
ATTN: G. Hall
ATTN: S. Tashird
ATTN: M/S 42-33, J. Kennedy

Boeing Co
ATTN: D. Clauson

Booz-Allen & Hamilton, Inc
ATTN: B. Wilkinson

University of California at San Diego
ATTN: H. Booker

Charles Stark Draper Lab, Inc
ATTN. J. Gilmore
ATTN: D. Cox

Communications Satellite Corp
ATTN: D. Fang

Comsat Labs
ATTN: R. Taur
ATTN: G. Hyde

Cornell University
ATTN: D. Farley, Jr
ATTN: M. Keily

Electrospace Systems, Inc
ATTN: H. Logston
ATTN: P. Phillips

ESL, Inc
ATTN: J. Marshall

General Electric Co
ATTN: A. Harcar
ATTN: M. Bortner

General Electric Co
ATTN: A. Steinmayer
ATTN: C. Zierdt

DEPARTMENT OF DEFENSE CONTRACTORS (Continued)

General Electric Co
ATTN: F. Reibert

General Electric Tech Services Co, Inc
ATTN: G. Millman

General Research Corp
ATTN: J. Ise, Jr
ATTN: J. Garbarino

Horizons Technology, Inc
ATTN: R. Kruger

HSS, Inc
ATTN: D. Hansen

IBM Corp
ATTN: F. Ricci

University of Illinois
ATTN: Security Supervisor for K. Yen

Institute for Defense Analyses
ATTN: H. Wolfhard
ATTN: E. Bauer
ATTN: J. Bengston
ATTN: J. Aein

International Tel & Telegraph Corp
ATTN: Technical Library
ATTN: G. Wetmore

JAYCOR
ATTN: J. Sperling

JAYCOR
ATTN: J. Doncarlos

Johns Hopkins University
ATTN: J. Phillips
ATTN: P. Komiske
ATTN: T. Potemra
ATTN: T. Evans
ATTN: J. Newland

Kaman TEMPO
ATTN: T. Stephens
ATTN: M. Stanton
ATTN: DASIAC
ATTN: W. Knapp
ATTN: W. McNamara

Linkabit Corp
ATTN: I. Jacobs

Litton Systems, Inc
ATTN: R. Grasty

Lockheed Missiles & Space Co, Inc
ATTN: M. Walt
ATTN: R. Johnson
ATTN: W. Imhof

Lockheed Missiles & Space Co, Inc
ATTN: D. Churchill
ATTN: Dept 60-12

DEPARTMENT OF DEFENSE CONTRACTORS (Continued)

M.I.T. Lincoln Lab
ATTN: D. Towle
ATTN: L. Loughlin

Martin Marietta Corp
ATTN: R. Heffner

McDonnell Douglas Corp
ATTN: Tech Library Services
ATTN: W. Olson
ATTN: G. Mroz
ATTN: R. Halprin
ATTN: N. Harris
ATTN: J. Moule

Meteor Communications Consultants
ATTN: R. Leader

Mission Research Corp
ATTN: R. Bogusch
ATTN: R. Hendrick
ATTN: R. Kilb
ATTN: S. Gutsche
ATTN: F. Fajen
ATTN: Tech Library
ATTN: D. Sappenfield

Mitre Corp
ATTN: A. Kymmel
ATTN: C. Callhan
ATTN: B. Adams
ATTN: G. Harding

Mitre Corp
ATTN: M. Horrocks
ATTN: J. Wheeler
ATTN: W Foster
ATTN: W. Hall

Pacific-Sierra Research Corp
ATTN: E. Field, Jr
ATTN: H. Brode
ATTN: F. Thomas

Pennsylvania State University
ATTN: Ionospheric Research Lab

Photometrics, Inc
ATTN: I. Kofsky

Physical Dynamics, Inc
ATTN: E. Fremouw

R & D Associates
ATTN: R. Lelevier
ATTN: W. Wright
ATTN: W. Karzas
ATTN: F. Gilmore
ATTN: G. Gabbard
ATTN: C. Greifinger
ATTN: H. Ory
ATTN: R. Turco
ATTN: M. Gantsweg
ATTN: P. Haas

R & D Associates
ATTN: L. Delaney
ATTN: B. Yoon

DEPARTMENT OF DEFENSE CONTRACTORS (Continued)

Rand Corp
ATTN: E. Bedrozian
ATTN: C. Crain

Riverside Research Institute
ATTN: V. Trapani

Rockwell International Corp
ATTN: R. Buckner

Rockwell International Corp
ATTN: S. Quilici

Santa Fe Corp
ATTN: D. Paolucci

Science Applications, Inc
ATTN: C. Smith
ATTN: D. Hamlin
ATTN: L. Linson
ATTN: E. Straker

Science Applications, Inc
ATTN: SZ

Science Applications, Inc
ATTN: J. Cockayne

SRI International
ATTN: W. Jaye
ATTN: W. Chesnut
ATTN: R. Leadabrand
ATTN: R. Hake, Jr
ATTN: R. Tsunoda
ATTN: A. Burns
ATTN: G. Price
ATTN: G. Smith
ATTN: V. Gonzales
ATTN: D. Neilson
ATTN: M. Baron
ATTN: J. Petrickes
ATTN: R. Livingston
ATTN: C. Rino
ATTN: D. McDaniels

Sylvania Systems Group
ATTN: M. Cross

Technology International Corp
ATTN: W. Boquist

Tri-Com, Inc
ATTN: D. Murray

TRW Defense & Space Sys Group
ATTN: R. Plebuch
ATTN: D. Dee

Utah State University
ATTN: J. Dupnik
ATTN: L. Jensen
ATTN: K. Baker

VisiDyne, Inc
ATTN: C. Humphrey
ATTN: J. Carpenter

BLANK PAGE